

# **Design of New Multifunctional Materials**

Thesis by

Ryan K. Zeidan

In Partial Fulfillment of the Requirements for  
the Degree of Doctor of Philosophy



California Institute of Technology

Pasadena, California

2007

(Defended February 16<sup>th</sup>, 2007)

© 2007

Ryan K. Zeidan

All Rights Reserved

## Acknowledgments

I must begin by thanking all the people who have contributed to my work and life. First of all, I must express my sincerest appreciation to my advisor Prof. Mark Davis. I will always be grateful for his kindness in taking me into his lab at the end of my second year, and for the constant intellectual and personal support he provided. I have been privileged to work with him and will always be grateful for the opportunity I had to work on so many different scientific challenges and to learn how to approach problems in the most direct and efficient manner.

I am also deeply indebted to many others in the world of chemistry. First of all, Prof. Brian Stoltz for supporting me during my first two years at Caltech and teaching me effective techniques for doing synthesis as well as a mentality necessary to success in the lab. Second, Prof. Tim Jamison served as my undergraduate advisor in the lab and has been a friend and advisor in all aspects of life to this day. I am very grateful for all that he has done for me and would not be writing this thesis today were it not for his support through thick and thin. I am also thankful to my committee, Prof. Bob Grubbs, Prof. Harry Gray, and Prof. Jonas Peters for their time and commitment to seeing me through this process and their advice and guidance.

Almost every project I have worked on has been done in collaboration with exceptional co-workers. I would like to thank all of them for their ideas, support, hard work, and friendship. Much of our catalysis work has been done in collaboration with Veronique Dufaud, who has been a continued source of ideas and support in pushing this project forward. Prof. Alex Katz was also involved in many thoughtful discussions, and I am grateful for his advice and suggestions. Sonjong Hwang in the solid state NMR

facility has also proved invaluable in obtaining solid state NMR data on many of our catalysts. I had the pleasure of working with J. J. Cheng and Swaroop Mishra on the synthesis of chloroquine analogs and always enjoyed working with and getting to know both of them. Labeling work on cyclodextrin compounds was done in collaboration with Stacey Kalovidouris who, likewise, was a pleasure to work with. My co-workers in the Davis lab were always good company, and I am particularly grateful to Chris Alabi and John McKeen for making it a pleasure to come in every morning and talk with them about everything from science ideas to plans for getting rich. They were not only fantastic co-workers, but also good friends, and for that I will always be thankful.

Caltech was filled with many enjoyable people who helped me get through such a long process with their friendship, there are too many people to thank. I had the pleasure of making some great friends in the Stoltz lab, particularly Dr. Uttam Tambar and Ernie Cruz, whom I look forward to remaining close friends with for years to come.

Last, I would like to thank my family for all their support through the years. My father has always supported me in pursuing education, and my mother's untimely passing 9 years ago has motivated me to push myself everyday in her memory. And finally, I would like to thank Katie McMenimen for helping me get through every day and giving me something to look forward to going home to at the end of the day, with the help of H.G.B.

## Abstract

Research in areas of science and technology critical to society, such as energy, medicine, electronics, protective equipment, and consumer goods relies on the ability to create new materials with desirable properties. The diversity in the properties of these materials is enormous. An important factor in the quest for developing exciting new materials is the ability to use synthetic chemistry to prepare new materials starting from a molecular point of view. It is this approach that I use in this work.

I have used principles of synthetic organic chemistry to guide the molecular design of materials that contain a variety of functionalities. This thesis describes three types of designed functional materials. First, new heterogeneous catalysts have been prepared that incorporate two organic functional groups in a manner that allows for cooperativity between them in catalyzing organic reactions, giving increases in reaction rates and selectivities. In particular, thiol/sulfonic acid bi-functional mesoporous materials have been prepared that give significant enhancements in reactivity and selectivity towards bisphenol A synthesis. These enhancements arise from interactions between thiol and sulfonic acid sites due to their proximity on the surface of the catalyst. Acid-base bi-functional materials have also been synthesized that exhibit excellent reactivity in the aldol condensation between acetone and 4-nitrobenzaldehyde. These catalysts are particularly important as the acid and base groups are mutually incompatible in solution and provide reactivity not achievable without immobilization on the surface of solids. Second, a method for incorporating traceable and quantifiable labels onto cyclodextrins and cyclodextrin containing polymers has been designed that utilizes the reactivity between the primary alcohols on cyclodextrins and ethylene oxide gas, and

allows the cyclodextrins to be labeled for use in animal biodistribution studies. Third, polymers bearing aromatic disulfide groups have been prepared that can be degraded through a dual-trigger mechanism requiring simultaneous photochemical and hydrogen peroxide activation.

**Table of Contents**

<b>Acknowledgments.....</b>	<b>iii</b>
<b>Abstract.....</b>	<b>v</b>
<b>List of Figures.....</b>	<b>ix</b>
<b>List of Tables.....</b>	<b>xiii</b>
 Chapter 1: Introduction.....	 1
 Chapter 2: Design of Thiol/Sulfonic Acid Functionalized Catalysts.....	 4
2.1 Abstract.....	5
2.2 Introduction.....	6
2.3 Background.....	11
2.4 Results and Discussion.....	14
2.5 Experimental Section.....	36
2.6 References.....	60
 Chapter 3: Acid-Base Bifunctional Heterogeneous Catalyst Design.....	 62
3.1 Abstract.....	63
3.2 Introduction.....	64
3.3 Results and Discussion.....	65
3.4 Experimental Section.....	78
3.5 Acid pKa Effect.....	79
3.6 Catalyst Characterization.....	84
3.7 Experimental Section.....	91
3.8 References.....	93

Chapter 4: Labeling Method for Cyclodextrins.....	95
4.1 Abstract.....	96
4.2 Introduction.....	97
4.3 Results and Discussion.....	97
4.4 Experimental Section.....	105
4.5 References.....	107
Chapter 5: Design of a Polymer with Dual-fold Mechanism of Degradation.....	108
5.1 Abstract.....	109
5.2 Introduction.....	110
5.3 Results and Discussion.....	113
5.4 Experimental Section.....	120
5.5 References.....	131
Chapter 6: Conclusions.....	132
6.1 Conclusions.....	133
Appendix A: Progress toward the Total Synthesis of Nomofungin.....	135
A.1 Abstract.....	136
A.2 Introduction.....	137
A.3 Results.....	138
A.4 Conclusions and Future Work.....	164
A.5 Experimental Section.....	166
A.6 References.....	169



## List of Figures

Figure 2.1	Formation of MCM-41 mesoporous material.....	7
Figure 2.2	Methods for incorporating organic functional groups into mesoporous materials.....	9
Figure 2.3	Bisphenol A synthesis.....	10
Figure 2.4	Mechanism of bisphenol A production.....	10
Figure 2.5	Synthesis of neighboring sulfonic acid functionalized SBA-15.....	12
Figure 2.6	Incomplete thiol oxidation.....	15
Figure 2.7	Synthesis of thiol/sulfonic acid functionalized SBA-15.....	20
Figure 2.8	$^{13}\text{C}$ solid state NMR of the dual functionalized SBA-15 solids after EtOH extraction.....	21
Figure 2.9	$^{29}\text{Si}$ NMR of dual functionalized SBA-15 solids.....	22
Figure 2.10	XRD patterns of functionalized SBA-15 materials.....	23
Figure 2.11	Typical $\text{N}_2$ adsorption isotherm.....	24
Figure 2.12	Possible mechanism for thiol involvement in the condensation reaction of phenol and acetone.....	30
Figure 2.13	Positioning of thiol/sulfonic acid sites.....	31
Figure 2.14	Sultone appended olefin synthesis.....	32
Figure 2.15	Direct immobilization of sultone.....	33
Figure 2.16	Simple sultone preparation.....	34
Figure 2.17	Alternate surface coupling strategy.....	35
Figure 2.18	Approach to thiol/sulfonic acid positioning.....	35
Figure 2.19	Typical HPLC trace of bisphenol A condensation reaction.....	39
Figure 2.20	Conversion vs. selectivity for homogeneous and SBA-15-DF (1:1) catalyzed reactions.....	40
Figure 2.21	Conversion vs. selectivity for heterogeneous reaction.....	40

Figure 2.22 Ally sulfonate <b>8</b> $^1\text{H}$ NMR.....	45
Figure 2.23 Sulfonyl chloride <b>9</b> $^1\text{H}$ NMR.....	46
Figure 2.24 Sulfonyl chloride <b>9</b> $^{13}\text{C}$ NMR.....	47
Figure 2.25 Sulfonate ester <b>12</b> $^1\text{H}$ NMR.....	48
Figure 2.26 Sultone <b>13</b> $^1\text{H}$ NMR.....	49
Figure 2.27 Sultone <b>13</b> $^{13}\text{C}$ NMR.....	50
Figure 2.28 Sulfonate ester <b>10</b> $^1\text{H}$ NMR.....	51
Figure 2.29 Sulfonate ester <b>10</b> $^{13}\text{C}$ NMR.....	52
Figure 2.30 Sultone <b>1</b> $^1\text{H}$ NMR.....	53
Figure 2.31 Sultone <b>1</b> $^{13}\text{C}$ NMR.....	54
Figure 2.32 Olefin functionalized SBA-15 <b>4</b> $^{13}\text{C}$ NMR.....	55
Figure 2.33 Olefin functionalized SBA-15 <b>4</b> $^{29}\text{Si}$ NMR.....	56
Figure 2.34 Allyl sultone <b>20</b> $^1\text{H}$ NMR.....	57
Figure 2.35 Allyl sultone <b>20</b> $^{13}\text{C}$ NMR.....	58
Figure 2.36 Olefin reduction side product of hydrosilylation reactions.....	59
Figure 3.1 Synthesis of acid-base bifunctional catalyst.....	66
Figure 3.2 $^{13}\text{C}$ CP/MAS solid state NMR of organically functionalized materials.....	67
Figure 3.3 $^{29}\text{Si}$ CP/MAS solid state NMR of organically functionalized materials.....	68
Figure 3.4 XRD analysis of solid state catalysts.....	69
Figure 3.5 Aldol reaction between acetone and 4-nitrobenzaldehyde.....	70
Figure 3.6 Mechanism of aldol reaction.....	71
Figure 3.7 Solvent effect on $^1\text{H}$ MAS NMR lineshape.....	75
Figure 3.8 Proposed cooperative mechanism of acid and base in aldol condensation....	77
Figure 3.9 Catalyst syntheses with different acid groups.....	79
Figure 3.10 Reaction kinetics and selectivity plot for aldol reaction with SBA-15-C.A.....	82

Figure 3.11 XRD diffraction pattern of heterogeneous catalysts.....	84
Figure 3.12 TGA analysis of SBA-15-C.A.....	85
Figure 3.13 $^{29}\text{Si}$ solid state CP/MAS NMR of SBA-15-C.A.....	85
Figure 3.14 $^{13}\text{C}$ solid state CP/MAS NMR of SBA-15-C.A.....	86
Figure 3.15 $\text{N}_2$ adsorption isotherm of SBA-15-C.A.....	87
Figure 3.16 TGA analysis of SBA-15-P.A.....	88
Figure 3.17 $^{29}\text{Si}$ solid state CP/MAS NMR of SBA-15-P.A.....	88
Figure 3.18 $^{13}\text{C}$ solid state CP/MAS NMR of SBA-15-P.A.....	89
Figure 3.19 $\text{N}_2$ adsorption isotherm of SBA-15-P.A.....	90
Figure 4.1 Schematic of reaction of $\beta$ -cyclodextrin with ethylene oxide-d4.....	98
Figure 4.2 ESI/MS analysis of $\beta$ -CD that was not dried and treated with EO-d4.....	99
Figure 4.3 ESI/MS analysis of labeled $\beta$ -CD.....	100
Figure 4.4 Schematic of radioactively labeled EO reaction with IT-101.....	101
Figure 4.5 TLC analysis of labeled polymer.....	102
Figure 4.6 Radioscan of TLC plate with $^{14}\text{C}$ ethylene oxide reacted IT-101.....	103
Figure 4.7 Radioscan of TLC plate with $^{14}\text{C}$ ethylene glycol.....	104
Figure 5.1 Design of a dual trigger degradable polymer.....	112
Figure 5.2 Disulfide cleavage and possible oxidation.....	113
Figure 5.3 Model system for degradation.....	114
Figure 5.4 Acetate protected monomer degradation.....	115
Figure 5.5 Polyamide preparation.....	116
Figure 5.6 $^1\text{H}$ NMR analysis of polyamide.....	117
Figure 5.7 $^1\text{H}$ NMR and IR analysis of polymer 2.....	118
Figure 5.8 $^1\text{H}$ and IR analysis of polymer 3. ....	119

Figure 5.9 $^1\text{H}$ NMR of carboxylic acid monomer.....	124
Figure 5.10 $^1\text{H}$ NMR of olefin appended monomer.....	125
Figure 5.11 $^1\text{H}$ NMR of acrolein modified monomer.....	126
Figure 5.12 $^1\text{H}$ NMR of carboxyl appended monomer.....	127
Figure 5.13 $^1\text{H}$ NMR of polymer <b>1</b> .....	128
Figure 5.14 $^1\text{H}$ NMR of acetate protected monomer.....	129
Figure 5.15 $^{13}\text{C}$ NMR of acetate protected monomer.....	130

**List of Tables**

Table 2.1 Cooperative sulfonic acid catalysis results.....	14
Table 2.2 Effect of thiol on homogeneous synthesis of bisphenol A.....	16
Table 2.3 Effect of thiol on heterogeneous catalysts.....	18
Table 2.4 Structural and textural characterization of solid SBA-15 catalysts.....	24
Table 2.5 Quantitative analysis of the solid materials containing both thiol and sulfonic acid functional groups.....	26
Table 2.6 Catalysis using dual-functionalized catalysts.....	28
Table 2.7 Steric effects of thiol.....	31
Table 3.1 Catalyst characterization data.....	69
Table 3.2 Acid-base bifunctional catalysis data.....	72
Table 3.3 Solvent effect on catalysis.....	74
Table 3.4 Catalyst quenching experiments.....	76
Table 3.5 Acid-base variations catalysis data.....	81
Table 3.6 Substrate scope.....	83

## **Chapter 1**

### **Introduction**

The design of materials with new functional properties is a central theme of research to many disciplines ranging from chemistry, chemical engineering, polymer science to materials science. A common goal in these fields is to use chemical reactions to build new small molecules, macromolecules, and polymers on distance scales ranging from nanometers to millimeters. From pharmaceutical chemists synthesizing natural products as drugs to engineers making new polymeric materials as plastics for consumer goods, the unifying theme is the ability to carry out chemical reactions and incorporate chemical functionalities to impart unique and desirable properties (solubility, reactivity, stability, hardness, etc.) into materials.

The general focus of the work reported herein has been the utilization of synthetic organic chemistry principles to design new materials bearing practical functionality for a wide range of purposes. The next two chapters are aimed at preparing heterogeneous catalysts through the incorporation of organic functionalities into mesoporous materials in order to create new reactivity properties through the cooperative catalysis between these groups immobilized together on a surface. Chapter four presents a method for using the chemical reactivity inherent in cyclodextrin containing materials to prepare polymeric drug delivery systems that incorporate new chemical functionalities serving as isotopic or radioactive labels. These labels impart the ability to minimally alter the chemical reactivity of the polymers while incorporating a quantifiable group, but also the ability to carry out bio-distribution studies using these polymers and accurately monitor and quantify the passage of the polymer through an animal. The final chapter presents new polymer materials bearing organic functional groups that give rise to a mechanism for degradation of the polymers precisely using a dual-trigger mechanism. These type of

polymers could have applications in a variety of areas such as adhesives, fibers, and protective coatings.

The general theme through these very different projects has been the rational synthesis of new materials through synthetic chemistry to incorporate desirable reactivity and physical properties into the material. We have worked with a number of different functionalities to impart unique properties into these materials. Catalysis work was mainly focused on acidic, basic and nucleophilic functionalities in terms of reactive properties in order to emulate the types of catalytic properties observed in enzymes. These included sulfonic acids, carboxylic acids, phosphoric acids, amines, and thiol sites. Ethylene oxide's reactivity with primary alcohol functionalities was utilized to incorporate deuterium and  $^{14}\text{C}$  labeled ethylene oxide into cyclodextrin compounds. Aromatic disulfide groups with para-amino functionalities were incorporated into polymers due to their unique ability to be homolytically photolyzed into sulfur radicals and be trapped in situ with peroxide to irreversibly cleave the linkage. The ability to synthesize organically functionalized materials with a variety of groups, such as the ones listed above, have led to a number of interesting materials with practical applications in a catalysis, polymer synthesis and drug delivery.



## Chapter 2

### Design of Thiol/Sulfonic Acid Functionalized Catalysts

This chapter was reproduced in part with permission from Zeidan, et al., *Journal of Catalysis* 239, 299-305 (2006). Copyright 2006 Elsevier.

This chapter was reproduced in part with permission from Dufaud, et al., *Journal of the American Chemical Society* 125, 9403-9413 (2003). Copyright 2003 A.C.S.

## 2.1 Abstract

Enzymes have earned the distinction as nature's greatest catalysts due to their ability to carry out a wide variety of reactions with remarkable selectivity and reaction rates. This feat is achieved through very precise positioning of reactive functional groups immobilized in the active site region by the peptide backbone. By taking a clue from how nature performs catalytic reactions, we have designed new heterogeneous catalysts that are immobilized combinations of organic functional groups on mesoporous silica SBA-15 supports. Through a "one-pot" preparation using organosilanes, direct synthesis allows for incorporation of the functional groups into structures that can then be used to carry out heterogeneous catalysis. Immobilization of thiols and sulfonic acids allow for cooperative catalysis to occur in the synthesis of bisphenol A leading to dramatic rate and selectivity enhancements.

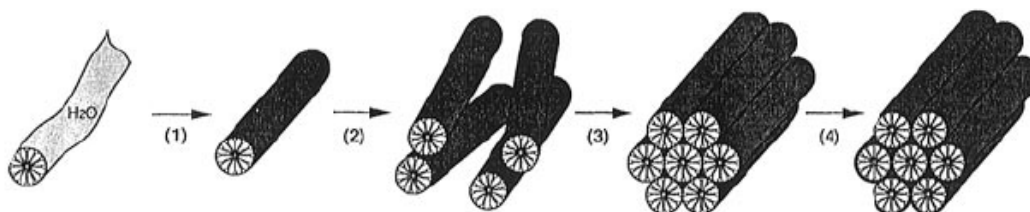
## 2.2 Introduction

Heterogeneous catalysis has become a very important area of research in the catalysis field driven by the industrial utility of such catalysts. These catalysts offer significant advantages from a practical standpoint, such as ease of separation and recyclability. In particular, zeolite materials have been broadly used in the petroleum industry as heterogeneous catalysts for carrying out shape selective chemical reactions. Zeolites have a number of interesting properties that make them ideal heterogeneous catalysts, such as rigid and highly ordered pore structures capable of discriminating very small size differences, on the order of 1 Å. However, one limitation with zeolite catalysts is that the pores are typically 20 Å wide at most, greatly limiting the utility of zeolites for catalyzing reactions with larger reactants. More recently, the advent of larger pore mesoporous materials and simple methods for functionalization of these materials with organic groups has drawn much interest.

There are a number of classes of mesoporous materials ranging in pore size from 20 to 100 Å in the largest cases. The ability for small molecules (larger than small chain alkanes) to enter the pores has the advantage of being more robust in terms of what reactions these materials can be used to catalyze and has the disadvantage of losing the precise shape selectivity properties of small pore zeolites. However, the ease of functionalization of these materials with organic groups gives them significant advantages over traditional zeolite catalysts. It is difficult to incorporate large organic functional groups with high loadings into zeolites without disrupting the rigidly ordered framework. Mesoporous materials, while being hexagonally ordered pores, are disordered and non-crystalline in the walls which form these pores. This feature greatly

simplifies the incorporation of organic groups into mesoporous materials without impacting the ability to form ordered structures.

Mesoporous materials were first reported in the 1980s with the discovery of the MCM family of materials at Mobil.<sup>1</sup> These materials were generated using hydrophobic surfactants with cationic ammonium head groups, which form micelles under aqueous conditions, that guide the formation of the ordered structure. The surfactant first orders into rod-like micelles in aqueous solution and begins to form the template for pore formation (Figure 2.1). A silica source, typically tetraethylorthosilicate (TEOS), is in solution and is hydrolyzed either by acid or base and begins to condense around the rod-like micelles. Once these tubes have formed, condensation continues as the tubes become merged and form the stacked, hexagonal pore structure.



**Figure 2.1** Formation of MCM-41 mesoporous material.

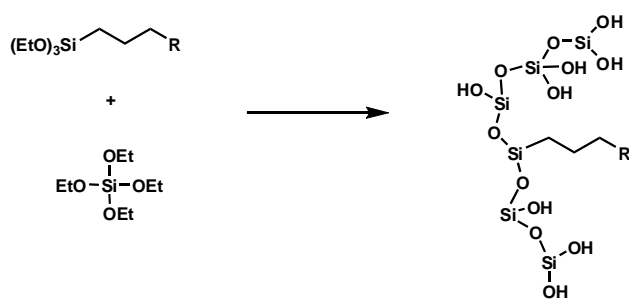
A number of different materials have been used to direct formation of mesoporous materials ranging from cationic ammonium species with long aliphatic chain tails to block co-polymers such as Pluronic 123. The different structure directing agent (SDA) dictates the general size of the pores obtained as well as the packing order of the tubes (hexagonal, cubic, etc.). In order to remove the surfactants that are trapped in the pore structure after synthesis, calcination at high temperatures is usually carried out to

thermally degrade the organic SDA and leave behind the silica pore structure. However, chemical methods have also been used (such as extraction with acid) to remove the SDA without calcination in order to allow for organic groups to remain in the mesoporous material.

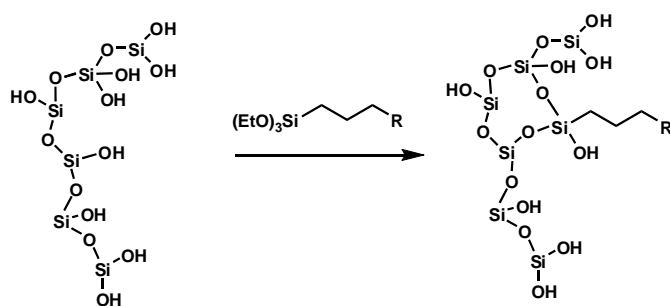
Two general methods have been developed that specifically allow for incorporation of organic functional groups into mesoporous silica materials.<sup>2</sup> The first of which, termed “co-condensation,” involves including an organic functional group with a silane head group directly into the synthesis pot with the silica source (Figure 2.2). The silica head group is hydrolyzed analogous to the TEOS and is randomly dispersed throughout the resulting silica framework, directly incorporating the organic into the material. In this method, non-calcination based methods of template removal (such as acid extraction) are required so as to avoid burning out the incorporated functional group with the template at high temperatures. The second method, termed “post-synthetic grafting” or simply “grafting,” involves treating an already synthesized and calcined mesoporous material with an organosilane. The organosilane reacts with the surface silanols of the mesoporous material, and the organic group becomes anchored and attached to the surface of the material. This method allows for the mesoporous material to be calcined in order to remove the template completely before incorporating the organic group, ensuring the only residual organic is the desired functional group being incorporated into the material. There are advantages and disadvantages to both methods. For “co-condensation,” the organic is randomly dispersed consistently throughout the entire material, and higher organic loadings can be achieved, but calcination is not possible, and residual template may remain in the extracted material. The “grafting”

method has the advantage of allowing for calcination of the structure before incorporation of the organic, but lower loadings are typically achieved through this method and the organic does not necessarily incorporate evenly and randomly throughout the material (i.e. grafts occur more easily at the readily accessible pore entrances and more exposed areas of the material). A number of organic functional groups have been incorporated into mesoporous materials through these methods, including sulfonic acids, amines, thiols, ligands, metals, and many other organosilane derivatives.

**Co-Condensation:**



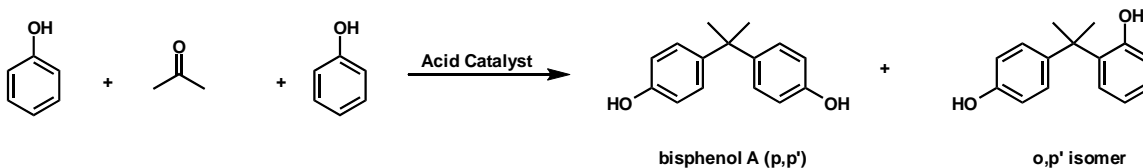
**Post-Synthetic Modification:**



**Figure 2.2** Methods for incorporating organic functional groups into mesoporous materials.

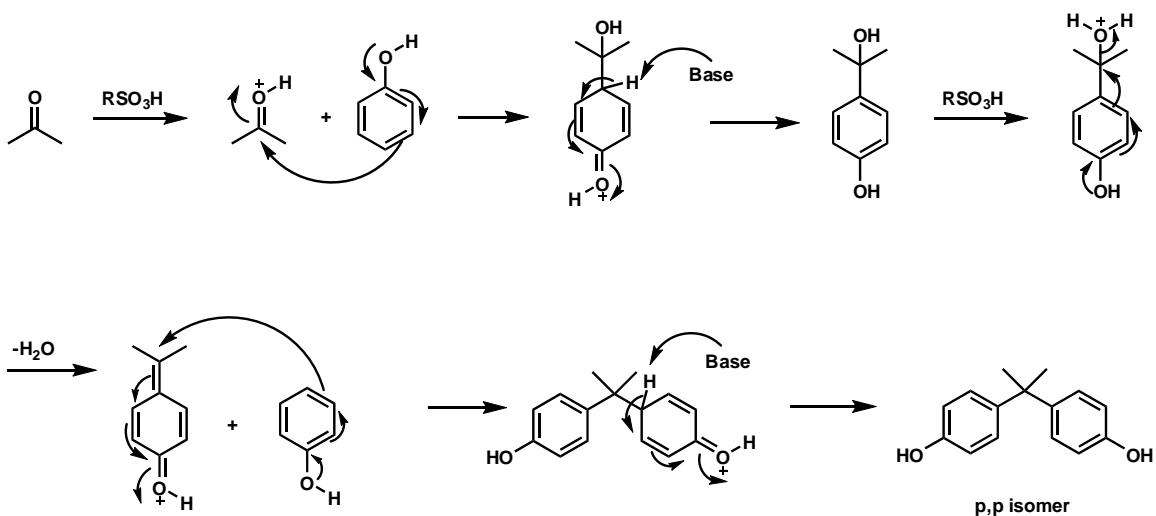
A reaction that has been extensively studied for heterogeneous catalysis systems due to its industrial importance is the condensation between two equivalents of phenol and one equivalent of acetone to produce bisphenol A.<sup>3</sup> Bisphenol A is produced

annually on multiple million ton scale and is used in polycarbonate synthesis as well as in plastics and epoxy resins. In this reaction, which is typically catalyzed homogeneously by acid catalysis, phenol reacts with acetone to give bisphenol A and a regiomeric o,p' side product (Figure 2.3) which is typically an undesirable side product in this reaction.



**Figure 2.3** Bisphenol A synthesis.

In order to design better catalysts for such a reaction, it is necessary to examine the reaction mechanism that occurs in forming bisphenol A and the undesired regioisomer. This reaction is acid catalyzed and in the first step the acid catalyst protonates acetone to activate the carbonyl to electrophilic attack (Figure 2.4).



**Figure 2.4** Mechanism of bisphenol A production.

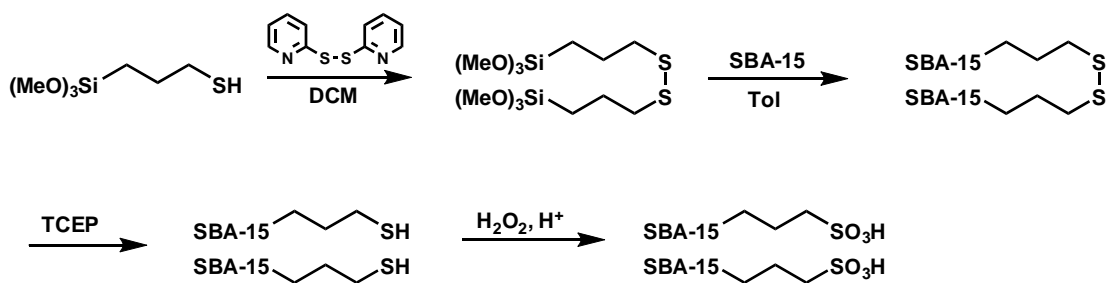
In the second step, one equivalent of phenol adds into the electrophilic carbonyl assisted by the phenolic oxygen electron pair, followed by a rapid re-aromatization of the addition adduct by the conjugate base of the acid catalyst. The resulting tertiary alcohol is rapidly protonated under acidic conditions, and water is expelled as a leaving group, again through assistance by the phenol oxygen electron pairs. The resulting pseudo-oxocarbenium ion is then attacked by a second equivalent of phenol, generating bisphenol A after rapid re-aromatization. The orientation of the second phenol equivalent upon addition to the carbocation intermediate determines the final regiochemistry of the product, if addition occurs in an ortho sense the o,p' product is obtained.

### 2.3 Background

Previous work in the group had been done towards preparing improved heterogeneous catalysts for synthesizing bisphenol A.<sup>4</sup> Sulfonic acid functionalized mesoporous materials were prepared for use as catalysts for this reaction. In order to observe if cooperative catalysis was possible by neighboring sulfonic acid sites, SBA-15 was prepared that contained neighboring sulfonic acid catalytic sites. SBA-15 is a silica mesoporous material that is synthesized using Pluronic 123 as an SDA and was chosen due to its high surface area, large pore diameter (60-80 Å) and acidic synthesis conditions allowing for functionalization with acidic groups. This catalyst was prepared through the route outlined below in Figure 2.5 beginning with trimethoxypropyl thiol. This thiol is first dimerized in a sulfide exchange reaction using Aldrithiol 2. The resulting disulfide was then “grafted” onto previously synthesized and calcined SBA-15, followed by a reductive cleavage of the disulfide using TCEP. Due to the nature of the molecular



templating method used for placement of these thiol sites by covalently linking them in a disulfide prior to grafting, these thiol sites are neighboring to one another on the surface in one-to-one pairs. This material with adjacent thiol sites was then oxidized using peroxide and sulfuric acid to convert the thiols to sulfonic acid sites that were neighboring to one another.

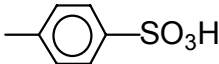
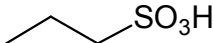
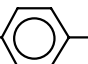


**Figure 2.5** Synthesis of neighboring sulfonic acid functionalized SBA-15.

Catalysis experiments were then carried out using this material with neighboring sulfonic acid sites and the appropriate control catalysts. Entry 1 (Table 2.1) is carried out using p-toluenesulfonic acid as a homogeneous catalyst for a control as well as entry 2 which uses propanesulfonic acid homogeneously as another control. In both of these cases, a selectivity of 2:1 was observed for bisphenol A over the o,p' isomer, typical of homogeneous acid catalysis conditions. The aromatic sulfonic acid (entry 1) exhibited a rate approximately three times greater than the aliphatic sulfonic acid (entry 2) due to the difference in acid strength, the aromatic sulfonic acid being significantly more acidic than the aliphatic. Entry 3 (Table 2.1) was carried out using p-toluenesulfonic acid immobilized on SBA-15 support (prepared by hydrolysis of an immobilized sulfonic

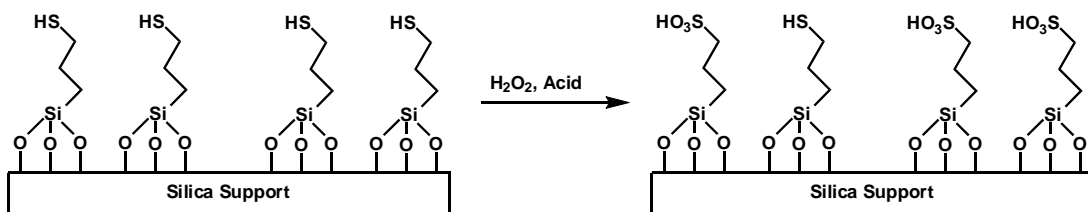
ester) as another control, and similar selectivities were observed as in entries 1 and 2. However, the reaction rate decrease by approximately a factor of 3 compared to the homogeneous p-toluenesulfonic acid due to surface diffusion limitations as is typical of heterogeneous systems. Entry 4 (Table 2.1) was carried out using an immobilized propanesulfonic acid immobilized on SBA-15 (prepared from simple oxidation of immobilized propyl thiol). Entry 5 (Table 2.1) was done using the SBA-15 prepared with neighboring sulfonic acid sites and shows significant improvements in selectivity and reaction rate when compared to the control experiments, indicating a cooperative effect between neighboring sulfonic acid sites. The selectivity in entry 4 was unexpectedly high for a simple sulfonic acid, and the reaction rate did not decrease as much in moving from aromatic to aliphatic (entry 3 vs. entry 4) as was observed homogeneously (entry 1 vs. entry 2). In examining the entries prepared through oxidation (entries 4 and 5), it was observed that the sulfur balance showed discrepancies between acid titration and elemental analysis results. The nature of the cooperative catalytic effect was not clear based on the data, and it was necessary to examine this effect further.

**Table 2.1** Cooperative sulfonic acid catalysis results.

<u>Entry</u>	<u>Catalyst</u>	<u>mmol/g SiO<sub>2</sub></u>		<u>p,p/p,o</u>	<u>STY (hr<sup>-1</sup>)</u>
		<u>S anal.</u>	<u>titration</u>		
1		—	—	2	1.50
2		—	—	2	0.50
3	SBA-15- 	0.3	0.3	3	0.50
4	SBA-15-(CH <sub>2</sub> ) <sub>3</sub> -SO <sub>3</sub> H	0.5	0.3	10	0.36
5	SBA-15-[(CH <sub>2</sub> ) <sub>3</sub> -SO <sub>3</sub> H] <sub>2</sub>	0.6	0.4	12	0.75

## 2.4 Results and Discussion

In order to further investigate the nature of the cooperativity observed in the work described above, it was necessary to examine the procedures used to prepare each material. The materials prepared from thiol precursors that were oxidized into sulfonic acids exhibited significantly higher selectivities for bisphenol A than sulfonic acids generated through other strategies. The possibility of small amounts of unoxidized thiol remaining on the surface was considered, even though there was no evidence in the <sup>13</sup>C NMR of residual thiol (Figure 2.6). However, solid state <sup>13</sup>C NMR has very low resolution, and it remained a possibility that small amounts of thiol existed on the surface. This would indicate that these sites with sulfonic acid paired with unreacted thiols might exhibit remarkable selectivity and reactivity to affect the results so dramatically when only in trace amounts.



**Figure 2.6** Incomplete thiol oxidation.

There is a precedent in the literature for thiols<sup>5-11</sup> being used in combination with sulfonic acid residues to alter the selectivity in the bisphenol A reaction, but the role of thiol was unclear. This is where we began experiments, focusing on investigating the role of thiol in this reaction to determine if the cooperativity was indeed caused by residual thiol sites on the surface.

In order to examine the effect of thiols on the reaction, homogeneous control experiments were carried out using combinations of thiols and sulfonic acids. The reaction was run at 100 °C for 24 hours with 0.01 equivalents of sulfonic acid relative to acetone and 3.5 equivalents of phenol relative to acetone. Reactions were monitored and conversions calculated by HPLC analysis at 272 nm on an Agilent 1100 Series HPLC using a Prevail C18 5  $\mu\text{m}$  column. Conversions are reported on a per site yield (PSY) basis relative to sulfonic acid.

**Table 2.2** Effect of thiol on homogeneous synthesis of bisphenol A.

BPA (p,p')                      o,p' isomer

Entry	Catalyst (eq)	Additive (eq)	Conv. BPA (%)	Conv. o,p' (%)	p,p' : o,p'	PSY
1	(0.01)	—	10.7	7.5	1.4:1	18.2
2	(0.01)	(0.01)	44.0	6.6	6.6:1	50.6
3	(0.01)	(0.005)	40.9	8.4	4.9:1	49.3
4	(0.01)	—	54.7	6.9	7.9:1	61.6
5	(0.01)	—	57.8	7.7	7.5:1	65.5
6	(0.01)	—	33.6	7.7	4.4:1	20.0
7	(0.005)	—	14.1	6.0	2.3:1	20.1
8	(0.01)	(0.005)	53.9	9.4	5.7:1	31.7
9	(0.005)	(0.005)	40.5	6.6	6.1:1	47.1
10	(0.005)	—	15.7	6.8	2.3:1	22.5
11	—	(0.01)	0.0	0.0	—	0.0

Reaction conditions: 3.5 eq phenol, 1.0 eq acetone, 0.01 eq sulfonic acid, 100°C, 24 hours.  
 Yields determined by HPLC quantification of BPA and o,p' isomer production. Conversion calculated based on acetone as limiting reagent. Per site yield calculated per sulfonic acid site.

Entry 1 (Table 2.2) was carried out using propane sulfonic acid homogeneously as a catalyst for a control, and a selectivity of 1.5:1 was observed for bisphenol A with 18% conversion obtained after 24 hours. The second entry (Table 2.2) was carried out as per entry 1 except with 0.01 equivalents of propane thiol added (1:1 ratio of sulfonic acid to thiol), and significant enhancements in reactivity were observed, as the selectivity improved to 6.6:1 for bisphenol A, and 50% conversion was obtained. Entry 3 (Table 2.2) was carried out analogous to entry 1 but with an added 0.005 equivalents of propane thiol relative to acetone (2:1 ratio of sulfonic acid to thiol) to examine the effect of a sub-stoichiometric amount of thiol on conversion and selectivity. The effect on the reaction

of the thiol was dramatic as the selectivity increased to 4.9:1, and 49% conversion was obtained, clearly indicating the dramatic effect thiols have on this reaction. Entry 4 (Table 2.2) was carried out using a tethered thiol/sulfonic acid catalyst with the two sites bound intramolecularly, and the effect on reactivity is even more dramatic in this case. The selectivity improved to 6.8:1, and nearly 62% conversion was obtained in this case when the two groups were bound together covalently. Entry 5 is similar to entry 4 except the tether is extended by 1 methylene group, and similar reactivity is observed with a 7.5:1 selectivity and 65% conversion, the added flexibility of a longer tether leading to small improvements in selectivity and conversion.

A similar series of experiments were carried out using two sulfonic acid sites intramolecularly tethered for comparison, as well as to further examine the likelihood of sulfonic acid cooperativity being responsible for the previously observed cooperative effect. Entry 6 (Table 2.2) illustrates clearly diminished reactivity when using adjacent sulfonic acid sites homogeneously as the selectivity decreases to 4.4:1 for bisphenol A and the per site yield decreases to 20%. Entry 6 was carried out using 0.01 equivalents of the di-acid, which corresponds to 0.02 equivalents of sulfonic acid. Entry 7 (Table 2.2) was carried out using 0.005 equivalents of the di-acid, corresponding to 0.01 equivalents of sulfonic acid for consistency. In this case, the selectivity further decreases to 2.2:1, and the per site yield remains consistent at 20%. Entries 8 and 9 (Table 2.2) are analogous to entries 6 and 7 except that in these entries 0.005 equivalents of propane thiol are added to the reaction mixture to examine the effect of thiol on these di-acid catalysts. From these two entries, the dramatic effect of thiols on reactivity is again clearly demonstrated as the selectivity improves to approximately 6:1 in both cases, and per site

yield approaches 47% in entry 9, corresponding to 94% conversion of acetone. Entry 10 (Table 2.2) was carried out using a di-sulfonic acid catalyst tethered with an extra methylene group to impart added flexibility, and the selectivity remained near 2.2:1 and a per site yield of 23% was observed. These catalysts with neighboring sulfonic acids, when used homogeneously, are indistinguishable in terms of reactivity from singly functionalized sulfonic acid catalysts, further illustrating the lack of cooperativity between sulfonic acid sites. Entry 11 (Table 2.2) was another control using only 0.01 equivalents of propane thiol as a catalyst with no sulfonic acid to ensure the thiols alone were not responsible for changes in reactivity, and no conversion was observed in this case as expected. Having demonstrated the significant impact of thiol homogeneously on this reaction, the role of thiol with heterogeneous catalysts was now of importance to understanding the observed cooperative catalysis.

Experiments were then carried out using heterogeneous catalysts of immobilized sulfonic acid sites on SBA-15 support<sup>12</sup> in combination with homogeneous propyl thiol.

**Table 2.3** Effect of thiol on heterogeneous catalysts.

Reaction scheme: Phenol + Acetone → BPA (p,p') + o,p' isomer

Entry	Catalyst (eq)	Additive (eq)	Conv. BPA (%)	Conv o,p' (%)	p,p' : o,p'	Per site yield
1	SBA-15-CH <sub>2</sub> CH <sub>2</sub> CH <sub>2</sub> SO <sub>3</sub> H (0.01)	—	3.3	1.6	2.1:1	4.9
2	SBA-15-CH <sub>2</sub> CH <sub>2</sub> CH <sub>2</sub> SO <sub>3</sub> H (0.01)	CH <sub>3</sub> CH <sub>2</sub> CH <sub>2</sub> SH (0.01)	13.2	1.8	7.5:1	15.0
3	SBA-15-CH <sub>2</sub> CH <sub>2</sub> CH <sub>2</sub> SO <sub>3</sub> H (0.01)	CH <sub>3</sub> CH <sub>2</sub> CH <sub>2</sub> SH (0.0025)	12.2	1.9	6.2:1	14.1

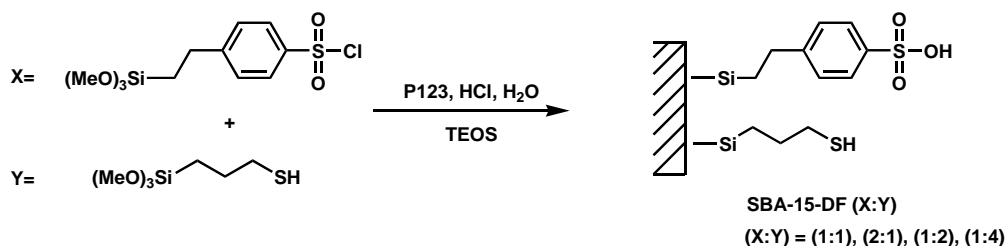
Reaction conditions: 3.5 eq phenol, 1.0 eq acetone, 0.01 eq sulfonic acid, 100°C, 24 hours  
 Yields determined by HPLC quantification of BPA and o,p' isomer production. Conversion calculated based on acetone as limiting reagent. Per site yield calculated per sulfonic acid site.

Entry 1 (Table 2.3) is a control experiment with the sulfonic acid functionalized SBA-15 catalyst alone used at a catalyst loading of 0.01 equivalents of sulfonic acid relative to acetone, analogous to the homogeneous experiments above. Consistent with homogeneous reactions with sulfonic acids, selectivity of 2.1:1 was observed, and a per site yield of 4.9% was obtained, much lower than the homogeneous cases due to the surface diffusion necessary with immobilized catalysts as well as the weaker acidity of aliphatic sulfonic acids. Entry 2 (Table 2.3) again clearly demonstrates the dramatic improvements in reactivity when thiols are present in the reaction mixture, even with heterogeneous sulfonic acid catalysts. In entry 2, 0.01 equivalents of propane thiol (1:1 ratio of sulfonic acid to thiol) was added to the reaction mixture, and the selectivity improved significantly to 7.5:1 and the per site yield nearly tripled to 15.0%. These levels of selectivity were beginning to approach the increases observed when neighboring sulfonic acid sites were positioned. Entry 3 (Table 2.3) illustrates the effect of even small amounts of thiol on the reaction. In this case only 0.0025 equivalents of propane thiol were added (4:1 acid to thiol ratio), and selectivity remained high at 6.2:1 and the conversion only dropped slightly to 14%. These results clearly demonstrated significant effects on reactivity in a heterogeneous sense in the presence of homogeneous thiols in the reaction mixture.

Having identified the presence of small amounts of thiol on the surface as the likely cause of the enhanced selectivity and reactivity observed, it was of interest to prepare a heterogeneous catalyst containing both sulfonic acid and thiol functional groups on the surface. Initial experiments were conducted using the “co-condensation” method to incorporate both functional groups simultaneously into SBA-15 materials. The

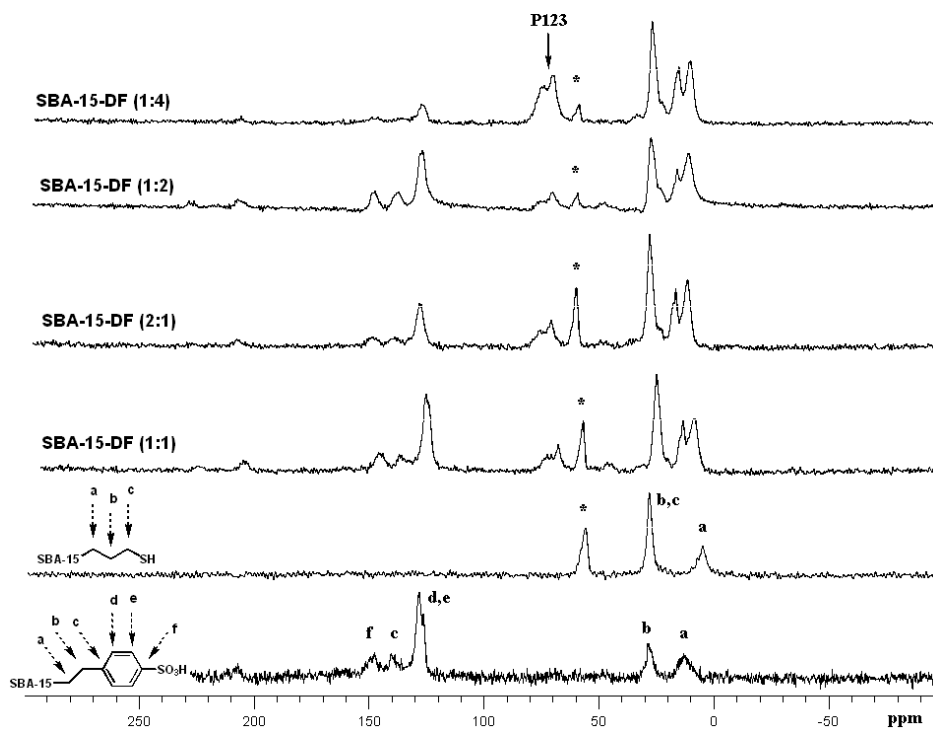


sulfonyl chloride of p-toluenesulfonic acid bearing a trimethoxysilane is commercially available as well as trimethoxypropyl thiol. By first adding the sulfonyl chloride component to the pH 1 synthesis conditions and allowing 5 minutes hydrolysis time, the sulfonyl chloride is rapidly hydrolyzed to the sulfonic acid. In a second addition, the thiol component was then added in the desired amount relative to the sulfonic acid and the synthesis allowed to stir at 40 °C for 20 hours and then aged at 100 °C for 24 hours as per typical SBA-15 syntheses (Figure 2.7). Through this method, mesoporous materials functionalized with differing ratios of thiols and sulfonic acids immobilized on the surface were prepared. The advantage of using “co-condensation” to incorporate both functionalities is that both functional groups are presumably randomly distributed equally throughout the material, with some combinations of thiol-thiol pairs, sulfonic acid-sulfonic acid pairs, and in some cases thiol-sulfonic acid sites adjacent to one another through a random distribution. The appropriate control materials were also synthesized through this method to make materials bearing only sulfonic acids on the surface or only thiols. The numbers in parenthesis in each material indicates the ratio of sulfonic acid to thiol in that catalyst, for example SBA-15-DF(1:2) corresponds to the catalyst with a 1:2 ratio of sulfonic acid to thiol.



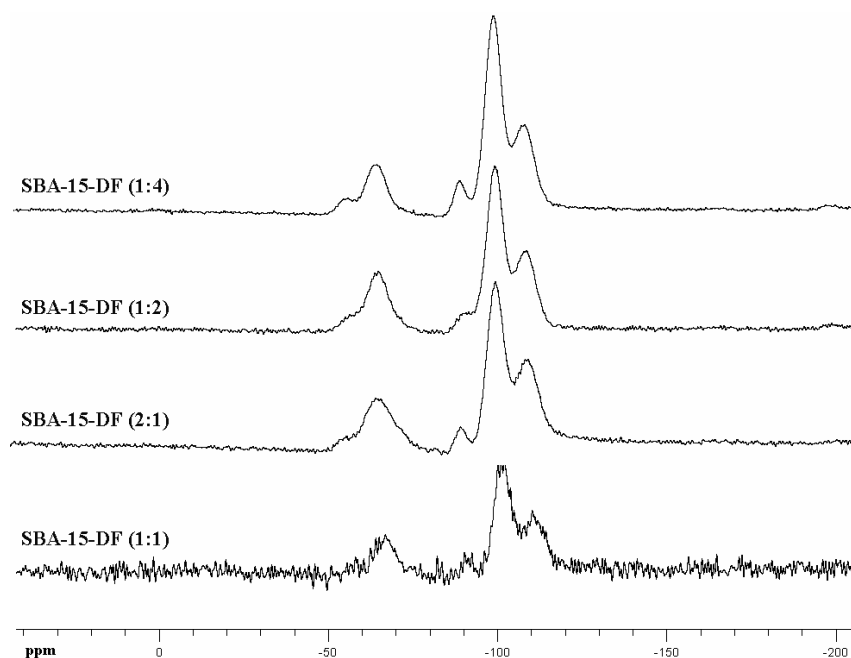
**Figure 2.7** Synthesis of thiol/sulfonic acid functionalized SBA-15.

These dual functionalized SBA-15 catalysts were then characterized by a number of solid state techniques including solid state CP/MAS NMR, XRD, TGA, N<sub>2</sub> adsorption, and functional group titrations. Figure 2.8 shows the solid state <sup>13</sup>C CP/MAS NMR spectra of the dual functionalized catalysts as well as the control materials bearing thiol and sulfonic acid groups alone. The <sup>13</sup>C NMR clearly shows incorporation of the desired functional groups into each material, and the relative ratio of each group appears reasonable, although it is difficult to quantify by <sup>13</sup>C solid state NMR, the qualitative appearance of each spectrum is as expected based on the synthesis ratios employed. The aromatic peaks of the sulfonic acid as well as the peaks due to the aliphatic chain of the propyl thiol groups are clearly distinguished.



**Figure 2.8** <sup>13</sup>C solid state NMR of the dual functionalized SBA-15 solids after EtOH extraction. Residual methoxy (Si(OMe)) denoted with a \*.

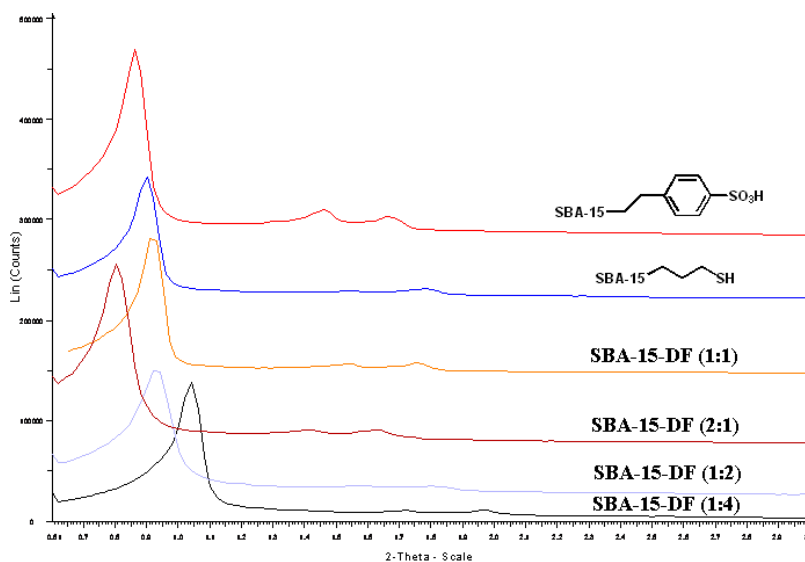
The  $^{29}\text{Si}$  CP/MAS NMR (Figure 2.9) was also recorded for each catalyst to examine the state of the silicon atoms in the catalyst. T type sites ( -65 ppm) are distinguished in all catalysts indicating incorporation of the organically functionalized tertiary silica atoms bearing three oxygens and one carbon substituent into the structure. The Q type sites ( -100 ppm) are due to the SBA-15 support and are characteristic of the quaternary silica atoms bearing four oxygens composing the SBA-15 scaffold.



**Figure 2.9**  $^{29}\text{Si}$  NMR of dual functionalized SBA-15 solids.

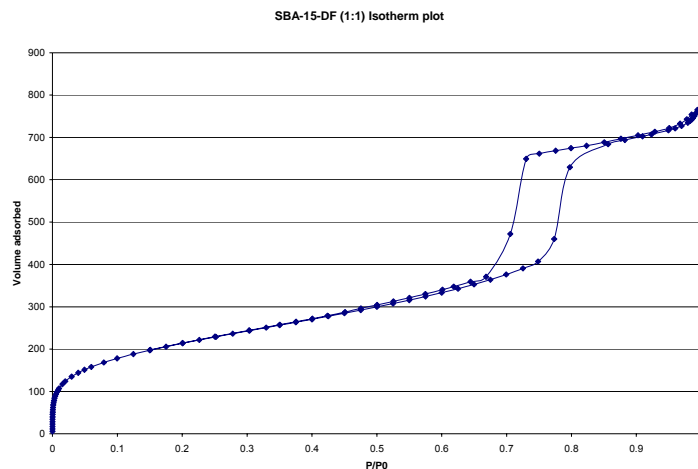
X-ray powder diffraction was also carried out on the dual-functionalized SBA-15 catalysts and the singly functionalized control materials in order to investigate the ordering of the materials after synthesis. In all cases very distinct (100) peaks at  $2\theta$  of  $0.8^\circ$  are observed indicating formation of pores and in most cases (110) and (200) peaks

at higher angles are also distinguishable, indicating long range structural ordering (Figure 2.10). In the cases with higher organic loading, the degree of long range ordering is decreased in the XRD patterns as is typically observed with higher organic loadings and is apparent from the decreased (110) and (200) peaks.



**Figure 2.10** XRD patterns of functionalized SBA-15 materials.

Nitrogen adsorption measurements were also carried out in order to determine the surface area and pore diameters in these materials. A typical  $N_2$  adsorption trace is presented (Figure 2.11) and exhibits a type IV isotherm typical of the SBA-15 family of materials, and very similar traces were obtained for all samples analyzed. In all cases, mean pore diameters were calculated to be in the range of 53-75 Å calculated using the desorption branch of the BJH method of analysis. BET surface areas were calculated in the range of 670-830  $m^2/g$  for all catalysts.



**Figure 2.11** Typical N<sub>2</sub> adsorption isotherm.

The structural and textural properties of all materials are summarized in Table 2.4. All catalysts exhibit similar physical characteristics and dimensions within reason for such complex and ordered materials. The data indicate relatively large pores, high surface areas and some degree of long range ordering in all samples.

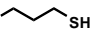
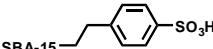
**Table 2.4** Structural and textural characterization of solid SBA-15 catalysts.

Entry	Sample	XRD		N <sub>2</sub> Adsorption	
		d <sub>100</sub> (Å) <sup>a</sup>	wall thickness (Å) <sup>b</sup>	D <sub>p</sub> (Å) <sup>c</sup>	S <sub>BET</sub> (m <sup>2</sup> /g)
1	SBA-15-DF (1:1)	96.4	49.1	62.2	827
2	SBA-15-DF (2:1)	110.7	65.1	62.7	753
3	SBA-15-DF (1:2)	95.3	56.8	53.2	783
4	SBA-15-DF (1:4)	84.9	50.6	47.4	666
5	SBA-15- <chem>CCCCSH</chem>	98.1	59.2	54.1	838
6	SBA-15- <chem>c1ccc(cc1)CC(S(=O)(=O)O)C</chem>	103.1	43.9	75.1	782

a. d(100) spacing b. Calculated by ( $a_0$  - pore size) where  $a_0 = 2d_{100} / \sqrt{3}$  c. Pore size determined from desorption branch using the BJH method of analysis.

Extensive characterization was also carried out to determine the organic loading of each functional group in the dual functionalized catalyst. In order to precisely determine the accessible organic loading of thiols and sulfonic acids in each material, chemical titrations were carried out on each group independently. In order to examine the sulfonic acid loading, an acid-base titration<sup>13</sup> was carried out by exchanging samples with NaCl to produce HCl (after exchange between R-SO<sub>3</sub>H and NaCl) which was then quantified by acid-base titration with NaOH using Phenol Red as an indicator. The thiol content was examined using a very sensitive technique from biology:<sup>14</sup> titration with Ellman's reagent. Using these two methods, precise calculation of the independent functional group loading for sulfonic acid and thiol sites was determined. As can be seen in Table 2.5, the values for the four dual-functionalized catalysts from titration analysis were in reasonable agreement with the ratios used in the synthesis. Elemental analysis was carried out on all of these samples as well, and the titration data and elemental analysis data likewise were in reasonable agreement taking into account the error (+/- 0.3%) in the elemental analysis values. These data confirm the incorporation of each functional group into the synthesized materials and are representative of the readily accessible amounts of each functional group, i.e., functional groups buried in the disordered walls are inaccessible and not accounted for by titration. For this reason, the titration values are used in all subsequent calculations for catalyst loading, as these values are representative of the amount of functional group the reactants would be exposed to on the surface of the heterogeneous catalyst.

**Table 2.5** Quantitative analysis of the solid materials containing both thiol and sulfonic acid functional groups.

Entry	Catalyst	Theoretical SO <sub>3</sub> H:SH	SO <sub>3</sub> H Titration <sup>1</sup> mmole/g	SH Titration <sup>2</sup> mmole/g	Obs. Ratio	% S from titrations	% S from E.A. <sup>3</sup>
1	SBA-15-DF (1:1)	1:1	0.33	0.34	1:1	2.2	2.5
2	SBA-15-DF (2:1)	2:1	0.47	0.35	1.4:1	2.6	3.3
3	SBA-15-DF (1:2)	1:2	0.32	0.64	1:2	3.1	4.1
4	SBA-15-DF (1:4)	1:4	0.16	0.83	1:5.3	3.2	3.3
5	SBA-15 	—	—	0.90	—	2.9	3.2
6	SBA-15 	—	0.59	—	—	1.6	1.6

1. Acid titration done by exchanging with NaCl and then titrating resulting solution with NaOH.

2. SH titration done with Ellman's reagent and measured absorbance at 412 nm.

3. Elemental Analysis done by QTI of N. J. Values reported are +/- 0.3%.

With these precise values of organic loading for the functionalized SBA-15 materials, it was then possible to examine the performance of these catalysts toward bisphenol A synthesis and compare accurately with homogeneous reactions. Experiments were run under the same conditions as the homogeneous experiments with 0.01 equivalents of sulfonic acid relative to acetone in all cases. Entry 1 (Table 2.6) was carried out using the SBA-15 catalyst functionalized with a 1:1 ratio of sulfonic acid to thiol immobilized on the surface. In this first example, the effect of immobilizing these functional groups in a manner that they can interact together in a cooperative fashion is clear. The selectivity achieved with this catalyst was 17.3:1 for bisphenol A, a dramatic improvement over the best case homogeneous examples. The per site yield also increased to 74.6%, as this dual-functionalized catalyst outperforms the best case homogeneous cases (Table 2.2) in terms of reactivity as well. This increase in reactivity and selectivity presumably is due to interactions between thiol and sulfonic acid sites. If

interactions were taking place between adjacent sulfonic acid sites or adjacent thiol sites, the upper limit on conversion and selectivity would be that obtained with catalysts bearing sulfonic acids alone and thiols alone. Increases in selectivity and reactivity beyond those values would indicate some interaction between thiols and sulfonic acids interacting due to proximity. This will be discussed further when entry 5 is examined. Entry 2 (Table 2.6) was obtained using the dual-functionalized catalyst bearing a 2:1 ratio of sulfonic acid to thiol sites and the selectivity decreased to 12:1 and a per site yield of 65% was observed, a slight decrease from entry 1. This entry illustrates two important points. The first is that as the relative ratio of acid sites to thiol sites is increased, hence decreasing thiol/sulfonic acid interactions, the selectivity and reactivity decrease significantly. The second is that increasing sulfonic acid/sulfonic acid interactions, by decreasing the amount of thiol immobilized on the surface, causes a decrease in selectivity and reactivity, further illustrating that neighboring sulfonic acid sites are likely not responsible for improved reactivity. Entry 3 (Table 2.6) was carried out with the dual-functionalized catalyst bearing a 1:2 ratio of sulfonic acid sites to thiol sites. In this case, selectivity of nearly 20:1 was observed with 82% per site yield, the most reactive catalyst used in this study. By increasing the thiol content, the likelihood of sulfonic acid/thiol interactions is increased and a respective increase in selectivity and rate was observed. Entry 4 (Table 2.6) is an extension of this example with a 1:4 ratio of sulfonic acid to thiol sites. In this case the excess thiol begins to dilute sulfonic acid/thiol interactions and selectivity decreases to 16.3:1 with a per site yield of 75.7%. Entry 5 is critical in examining the nature of the cooperative effect occurring between adjacent sulfonic acid and thiol sites. Entry 5 (Table 2.6) was carried out with a physical mixture



of SBA-15 functionalized with sulfonic acid alone and SBA-15 functionalized with thiol alone mixed in a 1:1 ratio based on organic loading, making the composition of the reaction identical to entry 1 except that the thiol and sulfonic acid are physically separated on different supports. In this case, the selectivity decreases to 3.0:1 and the per site yield plummets to 19.5%. By simply isolating these groups from one another physically, the enhancements in reactivity and selectivity are completely lost and the system behaves as a sulfonic acid catalyst alone. This experiment highlights the effect of the thiol and sulfonic acid groups being on the surface adjacent to each other and the enhancements in reactivity observed through interactions between these groups.

**Table 2.6** Catalysis using dual-functionalized catalysts.

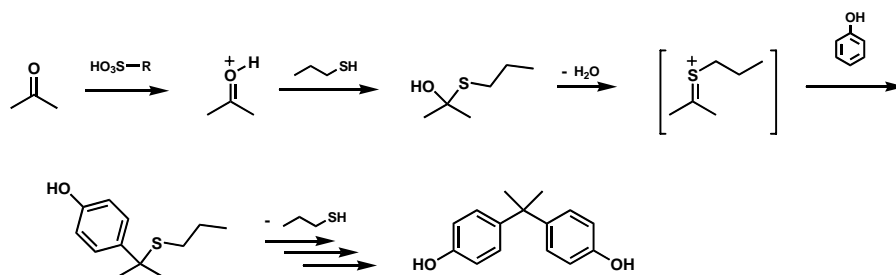
BPA (p,p')                      o,p' isomer

Entry	Catalyst (eq)	Ratio (acid:SH)	% BPA	% o,p'	p,p' : o,p'	PSY
1	SBA-15-DF (1:1)	1:1	70.6	4.0	17.3:1	74.6
2	SBA-15-DF (2:1)	2:1	60.0	5.0	12.0:1	65.0
3	SBA-15-DF (1:2)	1:2	78.0	3.9	19.8:1	81.9
4	SBA-15-DF (1:4)	1:4	71.3	4.4	16.3:1	75.7
5	Phys. Mix.	1:1	14.6	4.9	3.0:1	19.5
6	pTSA	—	20.5	5.1	4.0:1	25.6
7	1:1	1:1	25.6	5.7	4.5:1	31.3
8	pTSA +  SBA-15-CH <sub>2</sub> CH <sub>2</sub> CH <sub>2</sub> SH	1:1	29.5	7.2	4.1:1	36.7

Reaction conditions: 3.5 eq phenol, 1.0 eq acetone, 0.01 eq sulfonic acid, 100°C, 24 hours  
 Yields determined by HPLC quantification of BPA and o,p' isomer production. Conversion calculated based on acetone as limiting reagent. Per site yield calculated per sulfonic acid site. pTSA = para-toluenesulfonic acid. Entry 5 is a physical mixture of SBA-propyl-SH and SBA-SO<sub>3</sub>H in a 1:1 ratio.

The remaining entries were carried out as control experiments. Entry 6 (Table 2.6) was carried out homogeneously with p-toluenesulfonic acid and shows a 4.0:1 selectivity and 25% conversion. Entries 7 and 8 (Table 2.6) were carried out with SBA-15 functionalized with thiol sites alone and sulfonic acid was added homogeneously. Both entries illustrate the importance of the thiol and sulfonic acid sites being immobilized neighboring to one another, as in these cases where the acid is not immobilized the selectivities and yields remain low. The enhancements in reactivity achievable by immobilization of thiols and sulfonic acids together on SBA-15 in the formation of bisphenol A are clearly illustrated by these catalysis results.

In order to rationalize the cooperativity between thiol and sulfonic acid sites, it was necessary to examine the reaction mechanism. A mechanistic explanation for the cooperative effect must account for interactions between the reagents, thiols, and sulfonic acids and must explain the increased reaction rate as well as improved selectivity. As shown in Figure 2.12, after protonation of the carbonyl, a nearby nucleophilic thiol group may add into the carbonyl and generate a charged sulfur intermediate bearing a full positive charge, hence activating the carbonyl further. This would accelerate the reaction and explain the rate enhancement observed. The phenol would then add into this charged intermediate and the mechanism would proceed as before. The side chain of the thiol is adjacent to the site of phenol attack and may affect the geometry of phenol approach due to steric hindrance of the carbonyl.



**Figure 2.12** Possible mechanism for thiol involvement in the condensation reaction of phenol and acetone.

In order to examine the affect of the sterics of the thiol group, experiments were carried out using different thiol additives. Entry 1 (Table 2.7) was carried out homogeneously using propanesulfonic acid as a catalyst with 0.01 equivalents of t-butyl thiol. In this case the selectivity decreases to 1.5:1 and the per site yield drops to 14.5%, as the thiol substituent is so large that the proposed reaction mechanism involving thiol is significantly hindered and simple acid catalyzed reactivity is observed. However, when benzyl thiol (Entry 2, Table 2.7) was used as an additive, the selectivity improves to 7.1:1 and a per site yield of 51% was observed as the effect of thiol is restored upon using a less sterically hindered thiol. Entries 3 and 4 (Table 2.7) show the same trend when the thiol is added homogeneously to a reaction with immobilized sulfonic acid used as a catalyst. There is a clear balance of sterics and reaction rate that is influenced by the size of the substituent on the thiol additive.

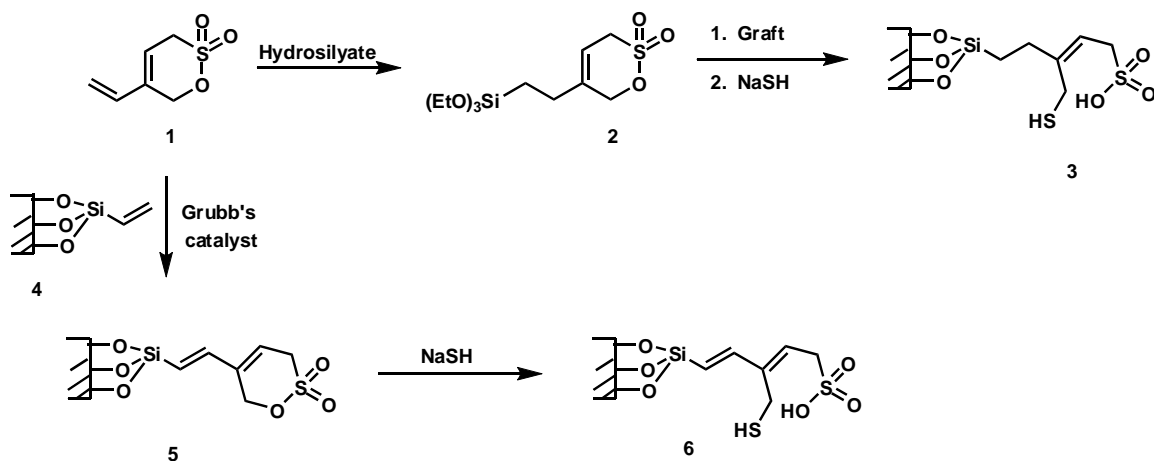
**Table 2.7** Steric effects of thiol.

BPA (p,p')                      o,p' isomer

Entry	Catalyst (eq)	Additive (eq)	Conv. BPA (%)	Conv o,p (%)	p,p' : o,p'	PSY
1	SO <sub>3</sub> H (0.01)	(0.01)	8.8	5.7	1.5:1	14.5
2	SO <sub>3</sub> H (0.01)	(0.01)	45.3	6.4	7.1:1	51.7
3	SBA-15 SO <sub>3</sub> H (0.01)	(0.01)	2.9	1.0	2.8:1	3.9
4	SBA-15 SO <sub>3</sub> H (0.01)	(0.01)	12.7	1.1	11.1:1	13.8

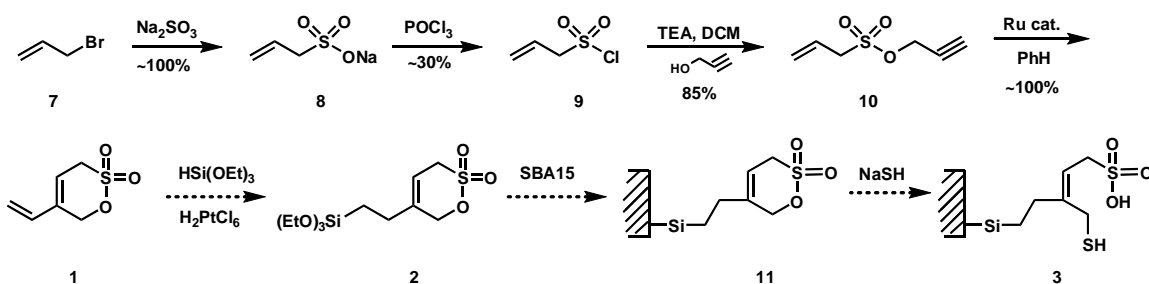
Reaction conditions: 3.5 eq phenol, 1.0 eq acetone, 0.01 eq sulfonic acid, 100 °C, 24 hours  
 Yields determined by HPLC quantification of BPA and o,p isomer production. Conversion calculated based on acetone as limiting reagent. Per site yield calculated per sulfonic acid site.

In order to examine the effect of distance between thiol and sulfonic acid sites, an approach toward precisely positioning the sites at a fixed distance was designed (Figure 2.13).

**Figure 2.13** Positioning of thiol/sulfonic acid sites.

In this approach, an olefin appended sultone could be hydrosilylated and then grafted onto the surface of SBA-15 followed by a ring opening with NaSH to afford immobilized neighboring sulfonic acid and thiol sites. Alternatively, this olefin could be used in a cross-metathesis reaction with SBA-15 that is modified with mono-substituted olefins on the surface to afford the immobilized sultone, which could then similarly be ring opened to afford neighboring sites.

In order to examine this approach, the olefin appended sultone synthesis below was carried out (Figure 2.14).

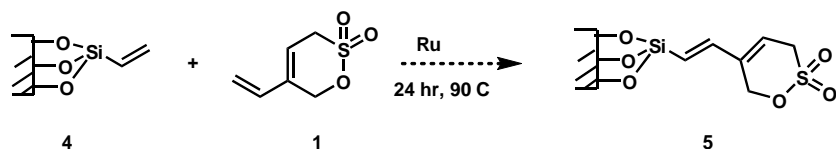


**Figure 2.14** Sultone appended olefin synthesis.

Allyl bromide was first sulfonated<sup>15</sup> with sodium sulfite to produce the sodium sulfonate **8** in good yield. This product could then be chlorinated<sup>16</sup> with phosphorous oxychloride to generate the sulfonyl chloride **9**. Coupling this sulfonyl chloride with propargyl alcohol in dichloromethane with triethylamine<sup>17</sup> afforded the sulfonate ester **10** in 85% yield. This sulfonate ester could then be cyclized in an ene-yne metathesis reaction<sup>18</sup> with Grubb's second generation catalyst to afford the olefin appended sultone **1** in quantitative yield. A number of conditions were attempted to afford hydrosilylation product **2** of this olefin in order to install a silane to allow for immobilization on SBA-15. However, in all

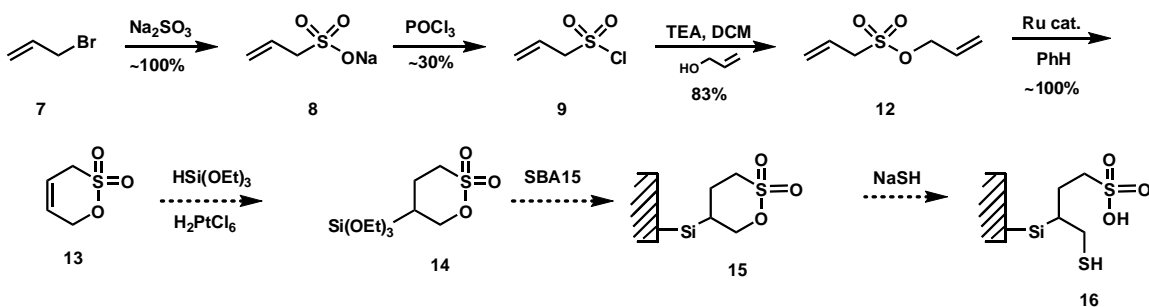
cases either no reaction or complete reduction of both olefins occurred, affording no hydrosilylated product.

In order to avoid a dead end synthetically for this material, the alternative approach outlined above (Figure 2.13) was examined in which the olefin appended sultone was attempted to be immobilized on olefin functionalized SBA-15 directly (Figure 2.15). In this approach, SBA-15 was surface modified with simple mono-substituted olefin functional groups and then treated with the olefin appended sultone under a number of cross-metathesis conditions. No cross metathesis was observed under standard conditions, and typically the only reaction product observed was decomposition in addition to blackening of the SBA-15. This approach had limited screening capabilities due to the lengthy solid state NMR experiments required to observe reactivity, so a second approach was envisioned.



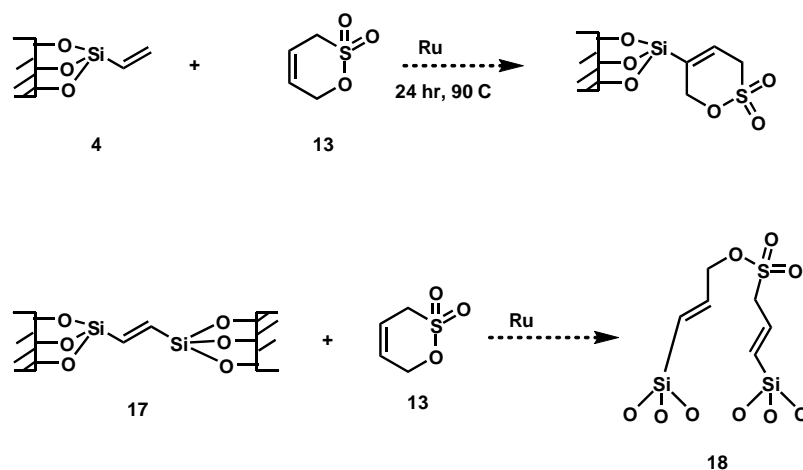
**Figure 2.15** Direct immobilization of sultone.

In the next synthetic approach, the sultone precursor was simplified in order to aid in the hydrosilylation reaction. The simple sultone incorporating the olefin directly into the sultone was prepared as in Figure 2.16.



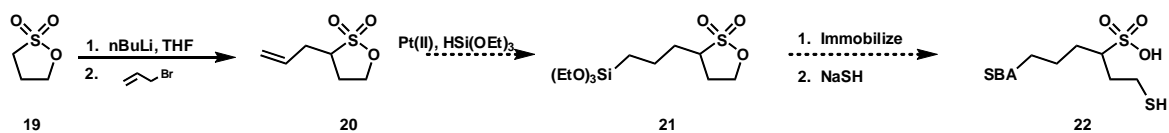
**Figure 2.16** Simple sultone preparation.

As shown above in Figure 2.16, allyl bromide was first sulfonated with sodium sulfite and the sulfonyl chloride formed as in the former strategy. This sulfonyl chloride was then reacted with vinyl alcohol in dichloromethane with triethylamine<sup>17</sup> to afford the olefin appended sulfonate ester. This substrate was then treated with Grubb's second generation catalyst to form the cross-metathesis product<sup>18</sup> sultone in quantitative yield. Similar attempts to hydrosilylate this olefin containing sultone under a variety of platinum catalyzed conditions proved unsuccessful. In an attempt to avoid hydrosilylation, cross-metathesis was also attempted directly with this sultone and SBA-15 functionalized with mono- and di-substituted olefins. In both cases, no cross product was obtained and only decomposition was observed (Figure 2.17).



**Figure 2.17** Alternate surface coupling strategy.

An alternative strategy in which a sultone is immobilized and then ring-opened with nucleophilic NaSH was envisioned (Figure 2.18). Toward this goal, 1,3-propane sultone was first alkylated<sup>19</sup> with allyl bromide using *n*BuLi. This allyl sultone was then treated with a number of different hydrosilylation conditions in order to install a silane group to allow for immobilization onto SBA-15. In all conditions tested, either no reaction was observed or a simple reduction of the olefin was observed; no hydrosilylated product was obtained using typical hydrosilylation conditions. Interactions between the sultone and the Pt(II) catalyst may inhibit reactivity and prevent hydrosilylation from occurring.



**Figure 2.18** Approach to thiol/sulfonic acid positioning.



## 2.5 Experimental Section

All reactions were run under an inert argon atmosphere. Silane reagents were purchased from Gelest and used as obtained. P123 was purchased from Aldrich (MW 5,800). Sulfonic acids were purchased from Aldrich as sodium salts and acidified with concentrated HCl before use. HPLC analysis was done on a HP 1100 series instrument with a C18 Prevail reverse phase column and measuring UV-Vis absorption at 272 nm. A representative HPLC trace is shown in Figure 2.19.

**“One-pot” oxidation synthesis.** To a teflon bottle was added P123 (1.99 g, 0.344 mmole) and then 2.0 M HCl (60.0 mL, 120 mmole) and water (3.0 mL, 166.5 mmole) were added. This mixture was stirred at 40 °C until P123 fully dissolved. Tetraethoxysilane (4.1 mL, 18.9 mmole) was then added and the resulting cloudy white solution was stirred for 45 minutes at 40 °C. Hydrogen peroxide (2.1 mL, 30 wt% solution) was then added followed by mercaptopropyltrimethoxysilane (0.38 mL, 2.0 mmole). The solution was then stirred at 40 °C for 20 hours and then aged under static conditions at 100°C for 24 hours. The solid white product was then isolated by filtering under aspirator and rinsing with copious amounts of water (3 x 300 mL). The product was dried under aspirator overnight. The as-synthesized material was then refluxed in EtOH (400 mL EtOH / g solid catalyst) for 24 hours to remove P123. The extracted product was then filtered, rinsed with copious amounts of EtOH (3 x 300 mL) and dried under aspirator overnight. The solid was then further dried under vacuum at 80 °C and stored under Ar.

**One-pot synthesis.** Outlined below is a general procedure for the one-pot method of producing the organically functionalized SBA-15-DF catalysts. P123 (4.0 g,

0.688 mmole) was weighed into a teflon bottle. Then 2.0 M HCl (120.0 mL, 240.0 mmole) and H<sub>2</sub>O (6.0 mL, 333.0 mmole) were added and stirred at 40°C until P123 fully dissolved. TEOS (8.2 mL, 37.8 mmole) was then added to the reaction and allowed to stir at 40°C for 45 minutes pre-hydrolysis time. The two silanes were then added in the desired amounts and relative ratios. For catalyst with a 1:1 ratio, 2-(4-chlorosulfonylphenyl)-ethyltrimethoxysilane (0.65 g, 50/50 w/w solution in dichloromethane, 1.0 mmole) was added first to allow for hydrolysis of the sulfonyl chloride followed by 3-mercaptoptrimethoxysilane (0.19 mL, 1.0 mmole). The remaining catalysts were done in the same manner by changing the relative ratio of these two precursors. The mixture was then allowed to stir at 40°C for 20 hours. It was then aged at 100°C for 24 hours. The mixture was then cooled to RT and the resulting solid was filtered and rinsed with excess H<sub>2</sub>O repeatedly (4 x 500 mL). The solid was then allowed to dry overnight on an aspirating filter. The dried solid was then extracted with EtOH (400 mL per gram) by refluxing in EtOH for 24 hours to remove P123. The solid was again filtered and rinsed repeatedly with EtOH (4 x 500 mL), and then dried overnight on the aspirator to obtain a dry white solid. The solid was then further dried at 80°C under vacuum for 24 hours and stored under Ar.

**Characterization.** Solid state NMR spectra were recorded using a Bruker Avance 200 MHz spectrometer with spinning at 4 KHz (Bruker 7 mm CP MAS probe). A 2 ms cross polarization contact time was used to acquire <sup>29</sup>Si and <sup>13</sup>C spectra with a repetition delay of 1.5 s and 32,000 scans. X-ray powder diffraction (XRD) data were acquired on a Bruker D5005 Diffractometer using Cu K<sub>α</sub> radiation. Nitrogen adsorption and desorption isotherms were measured at 77 K. Samples were dried at 100°C for 12 hours

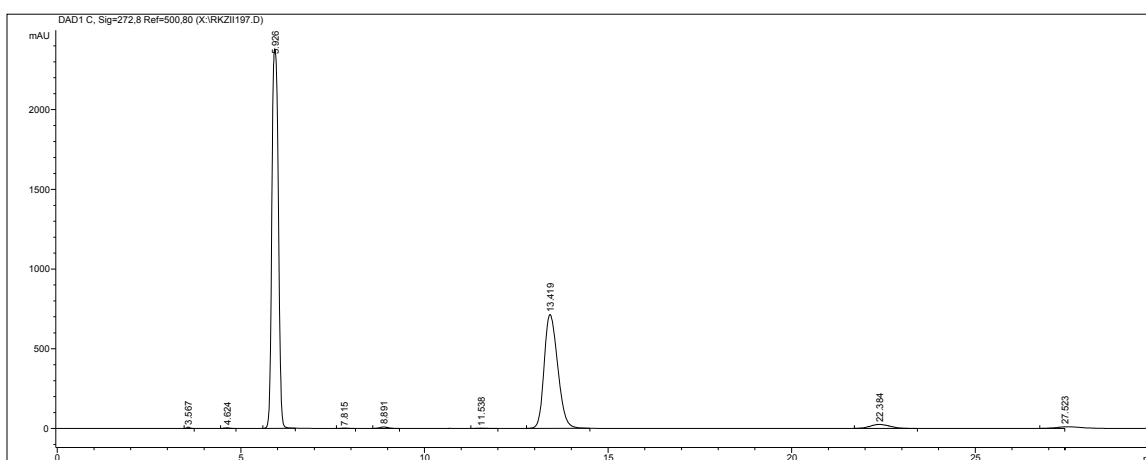
before analysis. Surface areas were calculated using the BET procedure. Pore size distribution was calculated using the BJH pore analysis applied to the desorption branch of the isotherm. XRD and N<sub>2</sub> adsorption were carried out at the Institute of Research on Catalysis, Lyon, France. Elemental analysis was carried out by QTI technologies, NJ.

The acid capacities of the sulfonic acid functionalized mesoporous materials were determined by ion-exchange with an aqueous solution of sodium chloride (2M) during 24 hours. The resulting suspension was then filtered, rinsed with water, and the filtrate was titrated with 0.01 N NaOH (aq) with phenol red as an indicator.

Thiol content was determined by the Ellman's titration assay.<sup>11</sup> Sodium phosphate dibasic buffer was prepared in water (0.1 M). The thiol containing mesoporous material (1-3 mg) was suspended in sodium phosphate buffer (4.0 mL) and then a solution of Ellman's reagent in sodium phosphate buffer (1.0 mL, 4 mg/mL) was added to this solution. The resulting solution was incubated at room temperature over 4 hours to allow for complete exchange. After four hours, the solution was diluted (1:3 dilution) with sodium phosphate buffer and the absorption at 412 nm was recorded. The concentration of thiol was then determined using an experimentally determined extinction coefficient of 13,600 M<sup>-1</sup> cm<sup>-1</sup>.

**Catalytic Experiments.** Catalytic reactions were carried out in sealed vials under an Ar atmosphere. Catalyst was tared into an oven dried vial (typically 100-300 mg, 0.01 eq) and the catalyst was then dried under vacuum at 80°C for 12 hours before use. Phenol (typically ~1.6 g, 3.5 eq) was then added to the reaction, followed by acetone (typically ~350  $\mu$ L, 1.0 eq). The reaction was then sealed under Ar and heated at 100°C for 24 hours. The reaction was then quenched by addition of a carefully measured

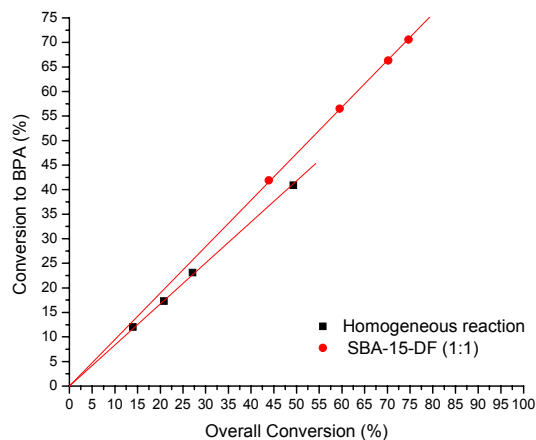
amount of acetonitrile (~10 mL). This diluted reaction was then further diluted for HPLC analysis (typically 100  $\mu$ L reaction + 700  $\mu$ L acetonitrile). This was done with an isocratic method of 60:40 H<sub>2</sub>O:ACN (0.01% TFA). Phenol elutes at 5.9 minutes, BPA at 13.1 minutes, and o,p isomer at 22.0 minutes using this method. Conversion was then quantified using a diode array detector based on a standardized calibration curve for BPA.



**Figure 2.19** Typical HPLC trace of bisphenol A condensation reaction.

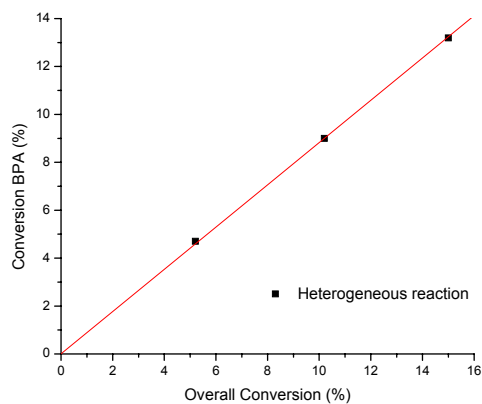
In order to compare the catalysis results at different levels of conversion, it was necessary to investigate how selectivity varied with conversion. This was done by preparing multiple reactions under identical conditions and then analyzing the reaction mixture by HPLC at varying time intervals (every 4 hours over 24 hours). Figure 2.20 illustrates the results for the case where the reaction was run homogeneously with 1:2 propane sulfonic acid:propane thiol (homogeneous reaction) as well as where the reaction was carried out with SBA-15-DF (1:1) as a catalyst. It is clear from Figure 2.20 that the

selectivity is constant over the course of the reaction, and that the selectivity is constant at all levels of conversion.



**Figure 2.20** Conversion vs. selectivity for homogeneous and SBA-15-DF (1:1) catalyzed reactions.

This analysis was also carried out for the heterogeneous catalysis case, where sulfonic acid bound to SBA-15 was used as a catalyst with an equimolar amount of propane thiol in solution (heterogeneous reaction). Figure 2.21 shows that the selectivity is also constant at all levels of conversion in this case as well.



**Figure 2.21** Conversion vs. selectivity for heterogeneous reaction (Table 2.3, entry 2).

Synthesis of allyl sulfonate **8**. To 33.3 g (264.5 mmole) sodium sulfite at 50°C in 100 mL water was added 35 g (264.5 mmole) of allyl bromide. Reaction was stirred at 50°C for 4 hours until homogeneous. Reaction was then cooled to RT, extracted with Et<sub>2</sub>O (3x50 mL) to remove excess allyl bromide, the aqueous phase was collected and concentrated in vacuo. The crude white solid was then recrystallized in hot EtOH to afford the allyl sulfonate **8** (37.6 g) in nearly quantitative yield. <sup>1</sup>H NMR (300 MHz, DMSO-d<sub>6</sub>): 5.80 (m, 1H), 5.06 (m, 2H), 3.17 (d, 2H).

Synthesis of sulfonyl chloride **9**. To 20 grams (138.8 mmole) of allyl sulfonate **8** was added 80 mL of phosphorous oxychloride and stirred at 135°C for 6 hours under Ar. Reaction mixture cooled to RT and ice water (100 mL) added carefully to quench excess phosphorous oxychloride and allowed to sit for 15 minutes. Extracted aqueous phase with chloroform (3 x 50 mL), combined organic phases concentrated in vacuo. Crude mixture distilled to afford sulfonyl chloride product **9** (125°C at 10 mtorr) as a colorless oil in 30 % yield (5.84 g). <sup>1</sup>H NMR (300 MHz, CDCl<sub>3</sub>): δ 6.05 (m, 1H), 5.71 (m, 2H), 4.31 (d, 2H). <sup>13</sup>C NMR (300 MHz, CDCl<sub>3</sub>): δ 128.07, 123.37, 68.98.

Synthesis of allyl sulfonate **10**. To a solution of propargyl alcohol (1.0 g, 17.8 mmoles) in dichloromethane (40 mL) and triethylamine (5 mL) at 0°C was added dropwise sulfonyl chloride **9** (2.5 g, 17.8 mmoles). After 30 minutes at 0°C reaction was warmed to room temperature and pentane was added. The reaction mixture was then filtered through Celite and the filtrate was concentrated in vacuo. The crude material was then purified by silica gel chromatography using 5:1 hexanes:EtOAc to give **10** in 85% yield as a colorless oil (2.42 g). <sup>1</sup>H NMR (300 MHz, CDCl<sub>3</sub>): δ 5.90 (m, 1H), 5.50

(m, 2H), 4.82 (m, 2H), 3.91 (m, 2H), 1.89 (td, 3H).  $^{13}\text{C}$  NMR (300 MHz,  $\text{CDCl}_3$ ):  $\delta$  121.31, 120.53, 82.84, 67.90, 55.38, 55.32, 52.31, 0.02.

Synthesis of sultone **1**. To a solution of ally sulfonate **10** (1.0 g, 6.24 mmole) in benzene (400 mL) was added Grubb's second generation catalyst (0.26 g, 0.31 mmole, 0.05 eq) and reaction was heated at 70°C for 5 hours and then room temperature overnight. The reaction mixture was then concentrated in vacuo. The crude product was then purified by silica gel chromatography using 2:1 hexane:EtOAc to afford **1** as a light brown solid in 99% yield (0.99 g).  $^1\text{H}$  NMR (300 MHz,  $\text{CDCl}_3$ ):  $\delta$  5.80 (m, 1H), 5.23 (m, 2H), 5.08 (s, 1H), 4.88 (s, 1H), 3.86 (m, 2H), 1.93 (s, 3H).  $^{13}\text{C}$  NMR (300 MHz,  $\text{CDCl}_3$ ):  $\delta$  138.02, 133.49, 115.34, 113.90, 72.93, 45.94, 20.71.

Synthesis of sulfonate ester **12**. To a solution of vinyl alcohol (1 g, 17.5 mmoles) in dichloromethane (40 mL) and triethylamine (5 mL) at 0°C was added dropwise sulfonyl chloride **9** (2.4 g, 17.5 mmoles). After 30 minutes at 0°C reaction was warmed to room temperature and pentane was added. The reaction mixture was then filtered through Celite and the filtrate was concentrated in vacuo. The crude material was then purified by silica gel chromatography using 6:1 hexanes:EtOAc to give **10** in 83% yield as a colorless oil (2.32 g).  $^1\text{H}$  NMR (300 MHz,  $\text{CDCl}_3$ ):  $\delta$  5.92 (m, 1H), 5.80 (m, 2H), 5.05 (d, 2H), 3.81 (d, 2H).  $^{13}\text{C}$  NMR (300 MHz,  $\text{CDCl}_3$ ):  $\delta$  124.39, 123.99, 121.06, 119.80, 72.76, 47.00.

Synthesis of sultone **13**. To a solution of ally sulfonate **12** (1.0 g, 6.16 mmole) in benzene (300 mL) was added Grubb's second generation catalyst (0.26 g, 0.31 mmole, 0.05 eq) and reaction was heated at 70°C for 5 hours and then at room temperature

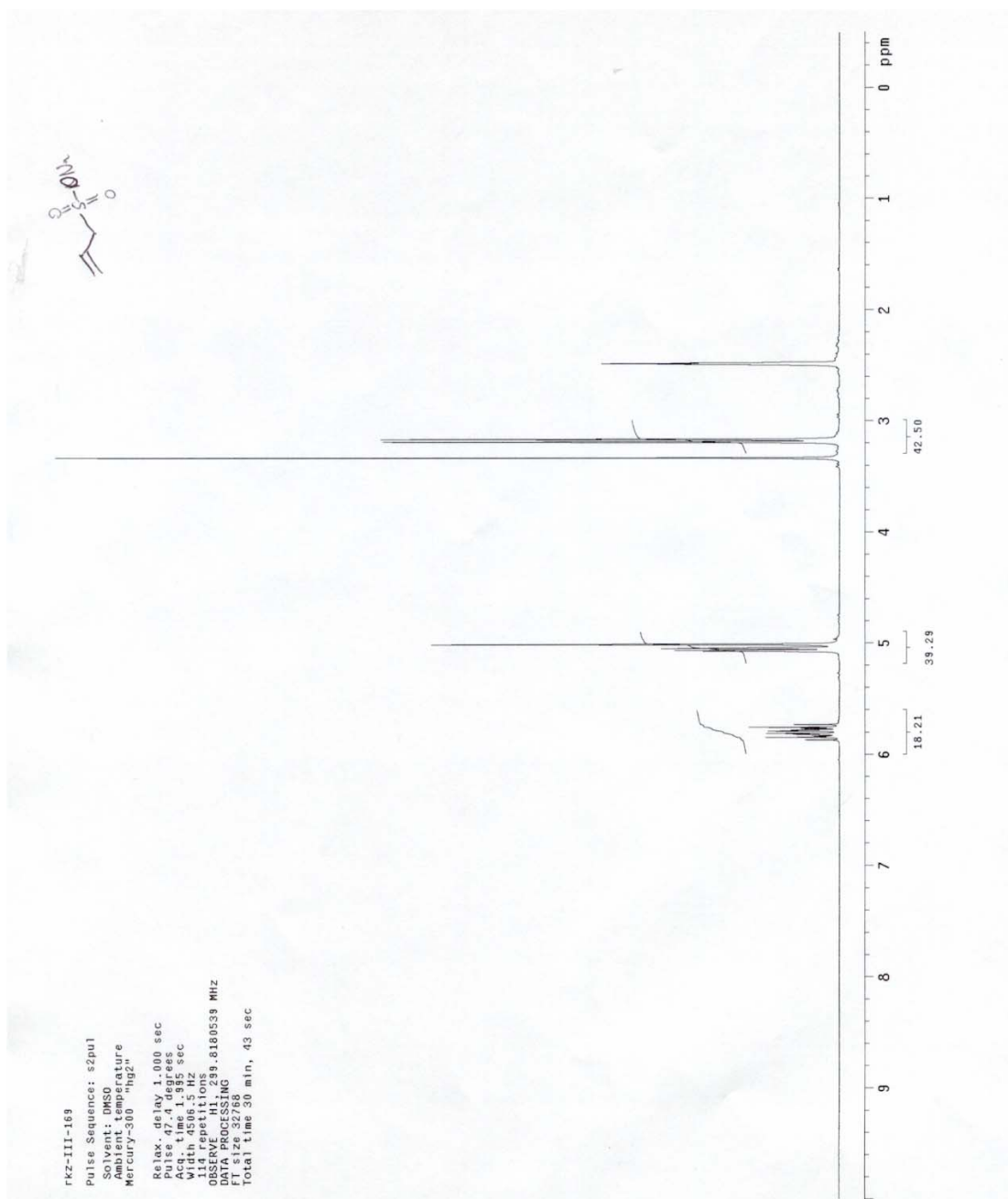
overnight. The reaction mixture was then concentrated in vacuo. The crude product was then purified by silica gel chromatography using 4:1 hexane:EtOAc to afford **13** as a light brown oil in 99% yield (0.98 g).  $^1\text{H}$  NMR (300 MHz,  $\text{CDCl}_3$ ):  $\delta$  5.92 (m, 1H), 5.42 (m, 2H), 4.71 (s, 1H), 3.84 (s, 1H), 2.16 (t, 2H).  $^{13}\text{C}$  NMR (300 MHz,  $\text{CDCl}_3$ ):  $\delta$  124.09, 119.39, 72.76, 47.00.

Synthesis of allyl sultone **19**. To a solution of 1,3 propane sultone (4 g, 32.76 mmole) in THF (40 mL) at  $-78^\circ\text{C}$  was added nBuLi (1.6 M in hexanes, 21.5 mL, 34.40 mmole) under Ar. Reaction was kept at  $-78^\circ\text{C}$  for 2 hours and then warmed to  $0^\circ\text{C}$ . Allyl bromide (3.96 g, 32.76 mmole) was then added dropwise to this reaction and allowed to react at  $0^\circ\text{C}$  for 2 hours. Reaction was quenched by addition of saturated aqueous  $\text{NH}_4\text{Cl}$  solution (50 mL). Extraction with EtOAc (3 x 50 mL) was then carried out and the organic phases were combined, dried over  $\text{Na}_2\text{SO}_4$ , filtered, and concentrated in vacuo. The crude reaction mixture was then purified by silica gel chromatography with 5:1 hexanes:EtOAc to afford 55% yield of the allyl sultone (2.93 g) as a clear oil.  $^1\text{H}$  NMR (300 MHz,  $\text{CDCl}_3$ ):  $\delta$  5.85 (m, 1H), 5.26 (m, 2H), 4.41 (m, 2H), 3.28 (m, 1H), 2.72 (m, 2H), 2.32 (m, 2H).  $^{13}\text{C}$  NMR (300 MHz,  $\text{CDCl}_3$ ):  $\delta$  132.32, 119.61, 67.00, 54.99, 33.23, 29.31.

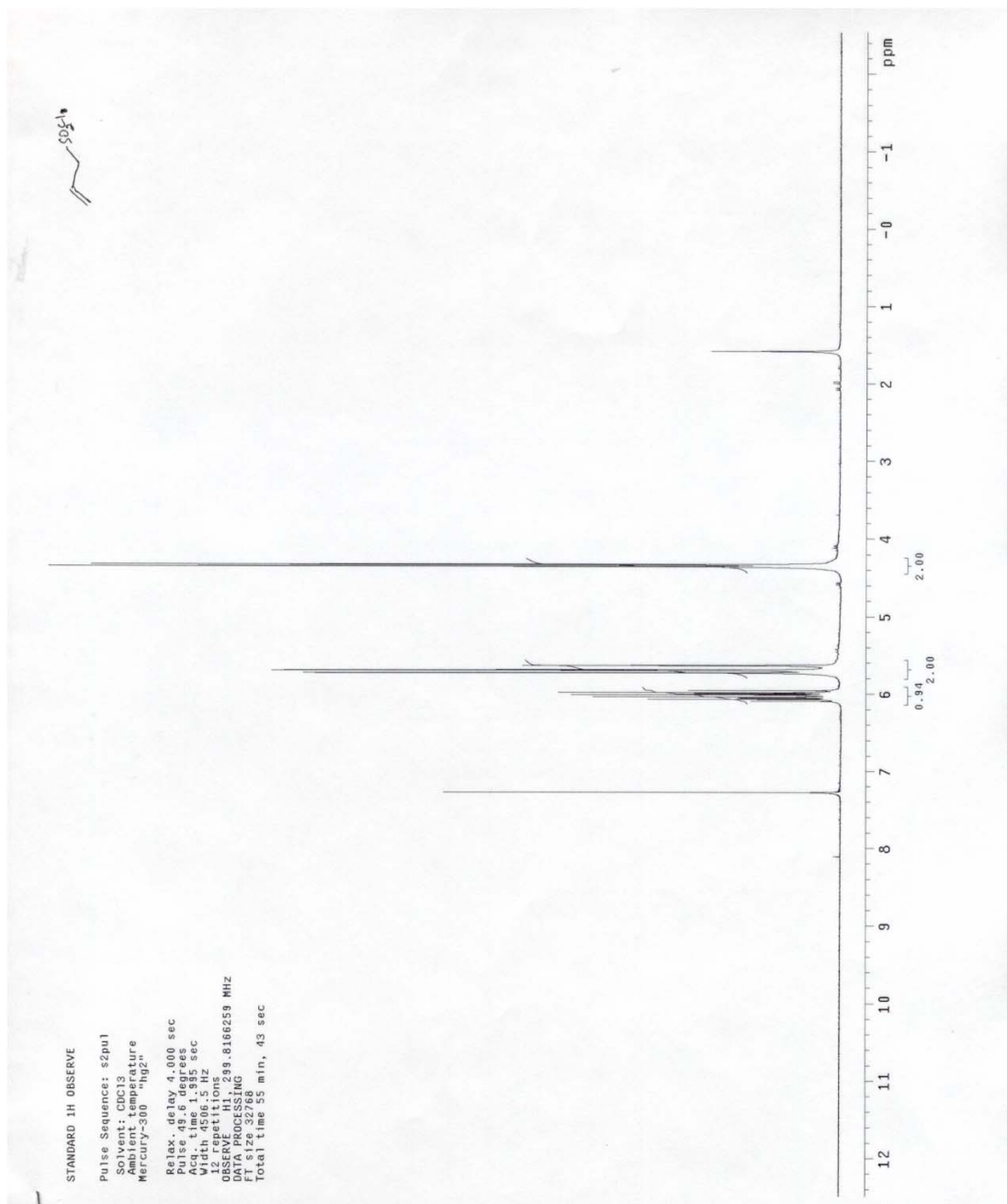
Synthesis of olefin functionalized SBA-15 **4**. SBA-15 was prepared by dissolving 4.0 g Pluronic 123 (MW 5500) in a teflon jar in 2.0 M HCl (120 mL) with water (6.0 mL). This mixture was stirred at  $40^\circ\text{C}$  until P123 fully dissolved. Tetraethylorthosilicate (8.4 mL) was then added to the mixture and stirred at  $40^\circ\text{C}$  for 24 hours. The Teflon jar was then aged at  $100^\circ\text{C}$  in an oven without stirring for 20 hours. The resulting white solid was then filtered, washed with water (4 x 400 mL) and dried on



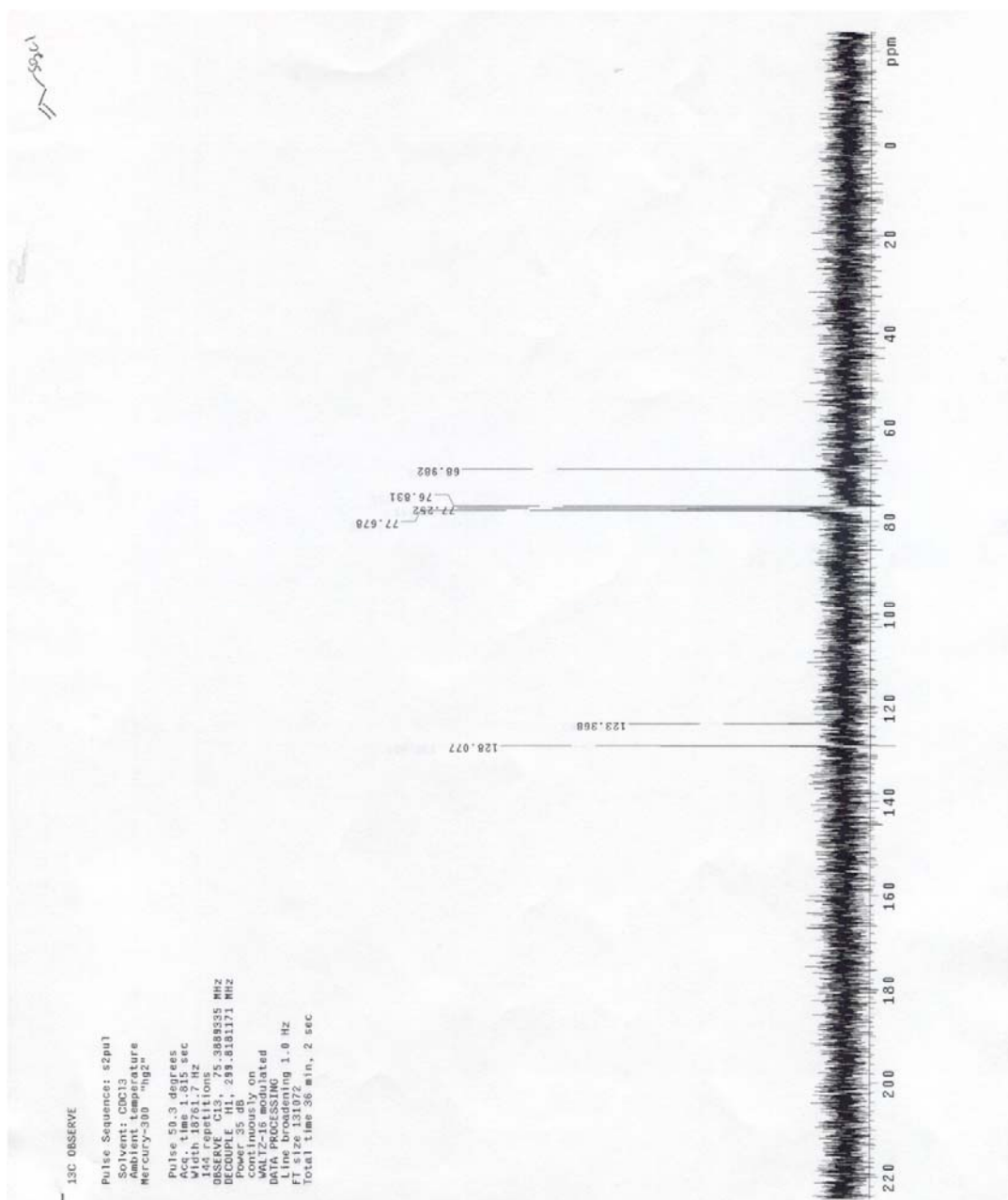
an aspirating filter overnight. The solid white powder was then calcined at 550 °C for 16 hours (6 hour slow ramp up to 550 °C from room temperature). This calcined SBA-15 (1 g) was then suspended in toluene (100 mL) and trimethoxyvinylsilane was added (0.30 g, 2.0 mmole) and stirred at 50 °C for 24 hours. The resulting white solid was then filtered, rinsed with toluene (3 x 100 mL) and dichloromethane (3 x 100 mL). This solid powder was then soxhlet extracted with dichloromethane (500 mL) overnight and dried in a 100°C oven to remove residual solvent. The solid SBA-15 functionalized material was then characterized by TGA to determine an organic loading of 1.5 mmole/g. Solid state CP/MAS NMR was also carried out and clearly exhibited incorporation of the organic vinyl group.  $^{13}\text{C}$  NMR (200 MHz):  $\delta$  135.0, 126.0.



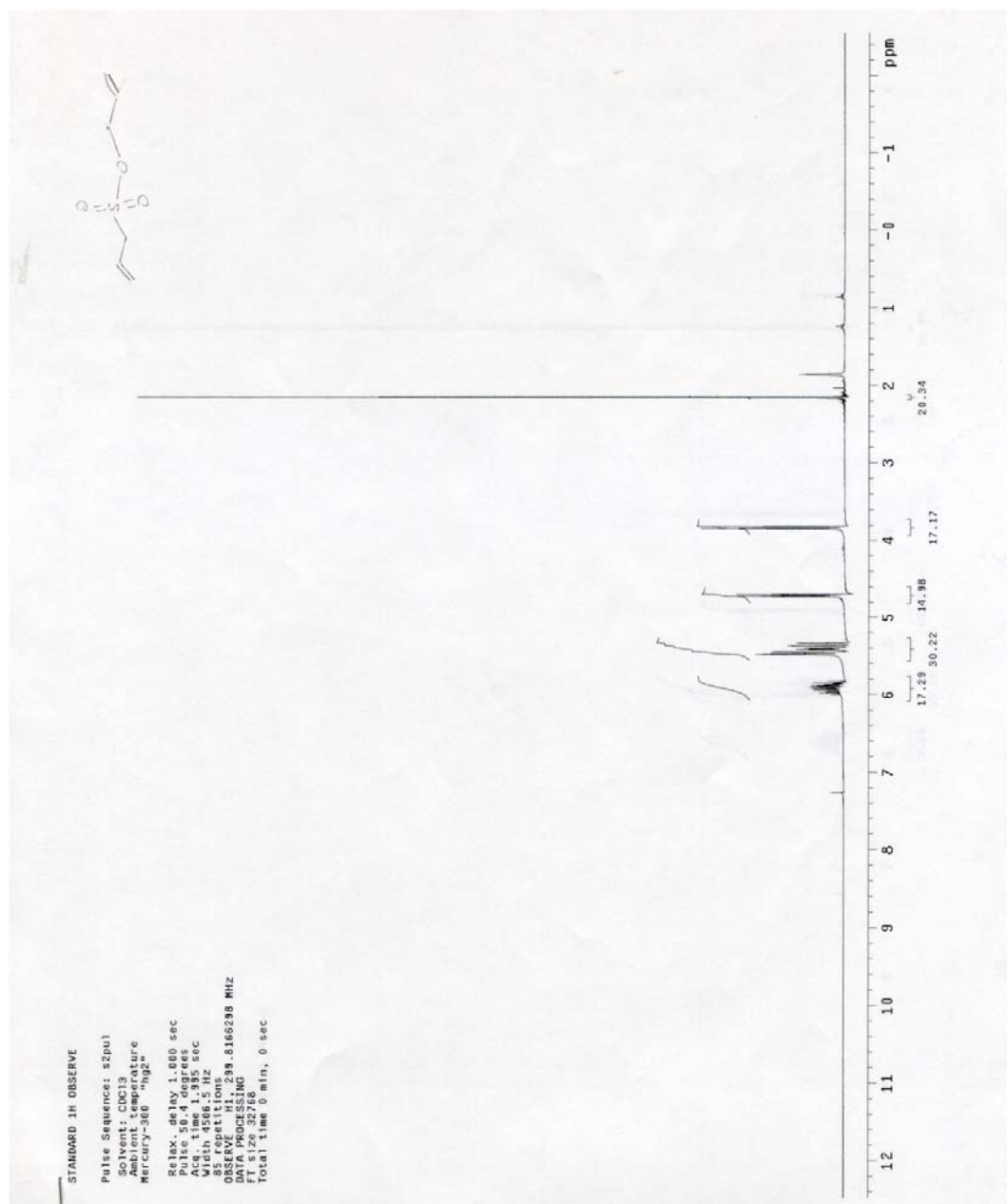
**Figure 2.22** Ally sulfonate **8** <sup>1</sup>H NMR.



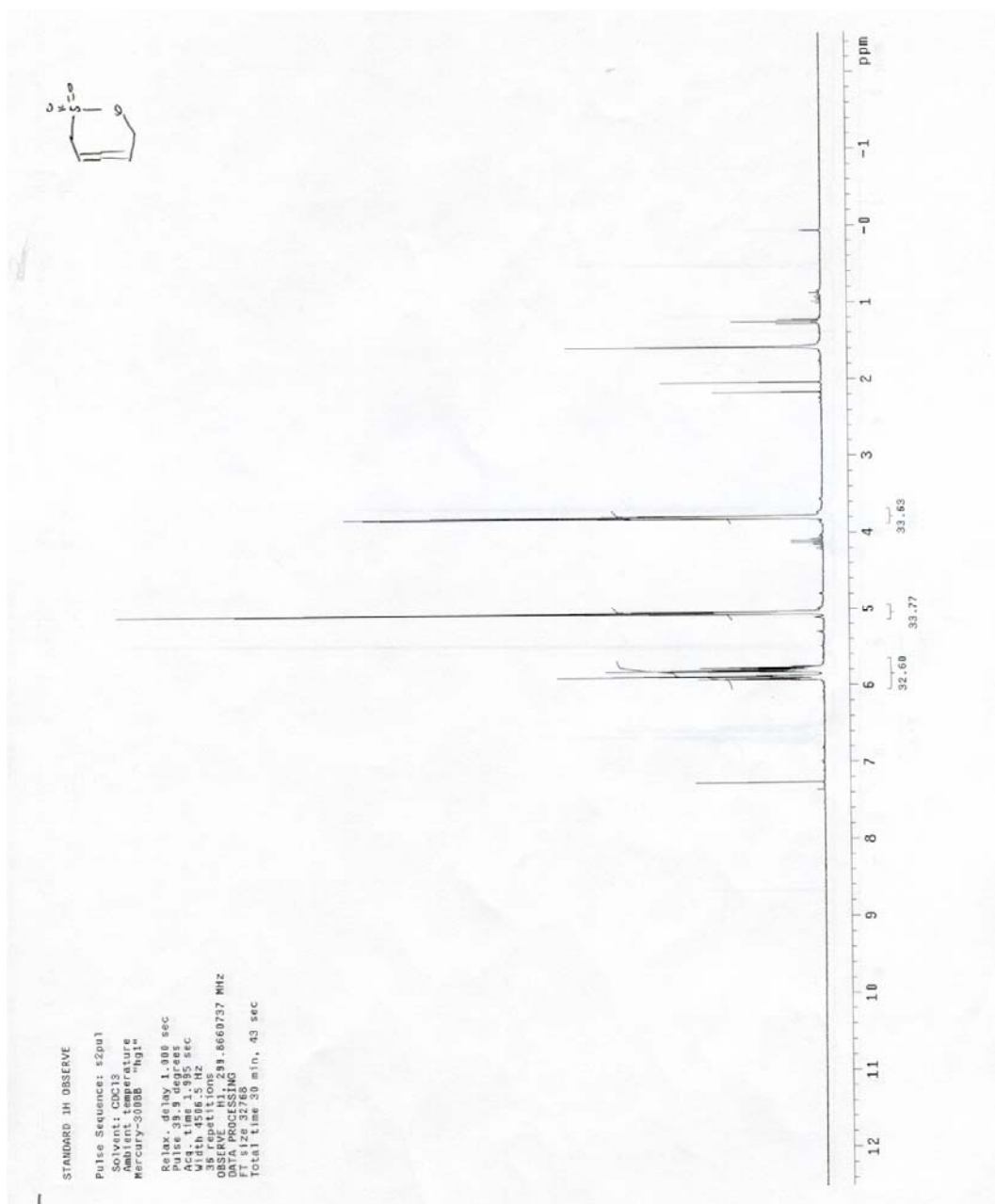
**Figure 2.23** Sulfonyl chloride **9**  $^1\text{H}$  NMR.



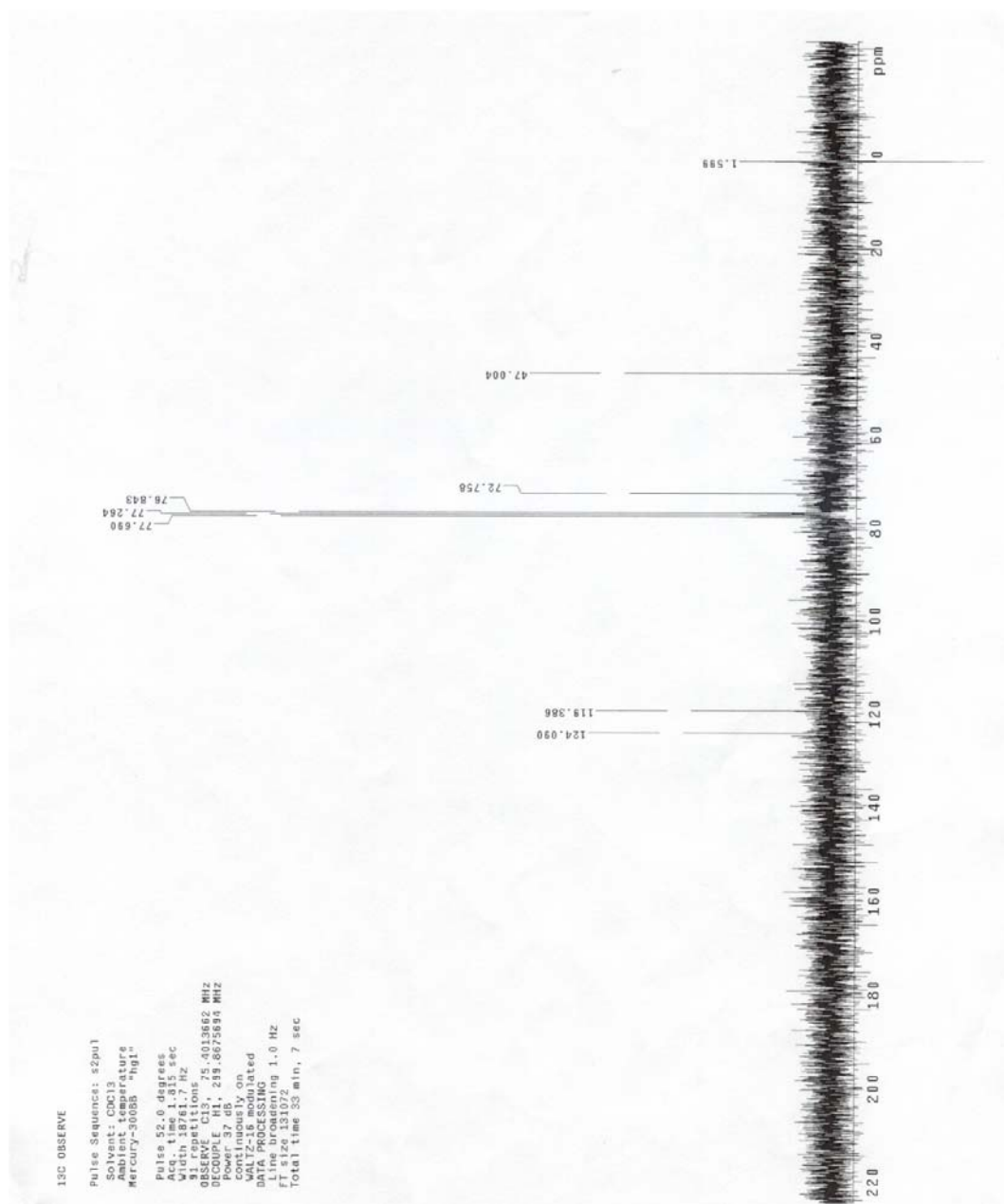
**Figure 2.24** Sulfonyl chloride **9**  $^{13}\text{C}$  NMR.



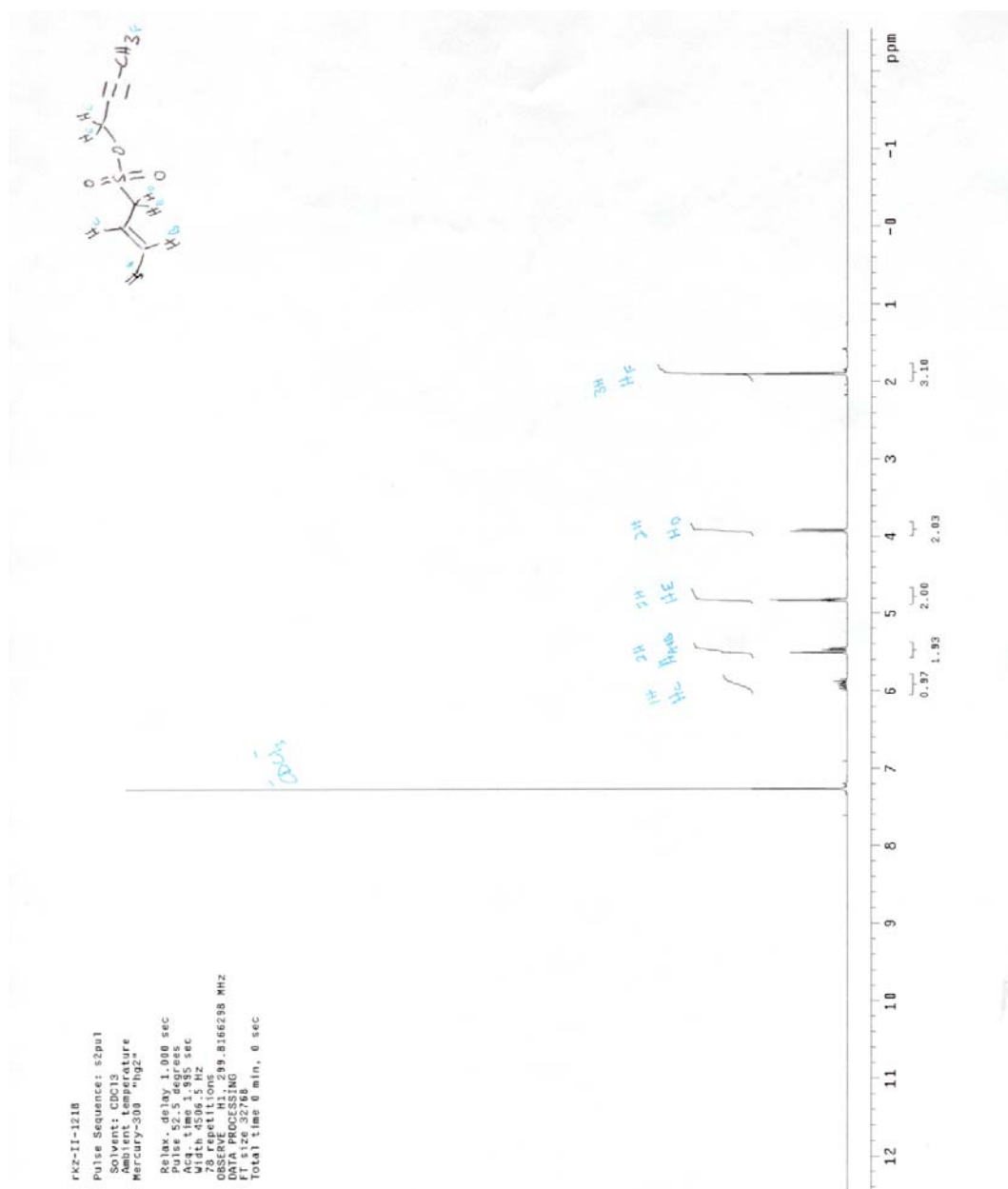
**Figure 2.25** Sulfonate ester **12** <sup>1</sup>H NMR.



**Figure 2.26** Sultone 13 <sup>1</sup>H NMR.

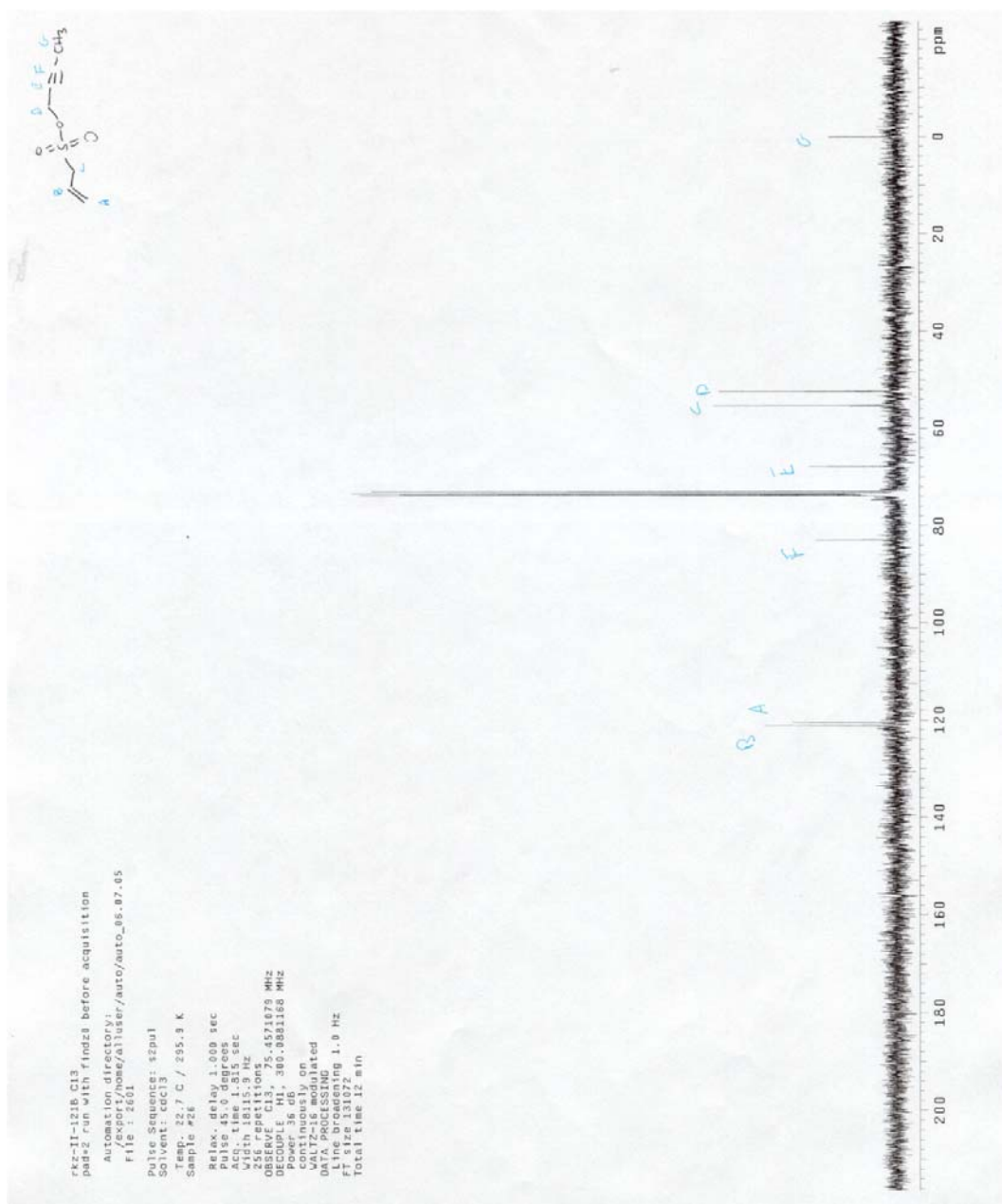


**Figure 2.27** Sultone **13**  $^{13}\text{C}$  NMR.

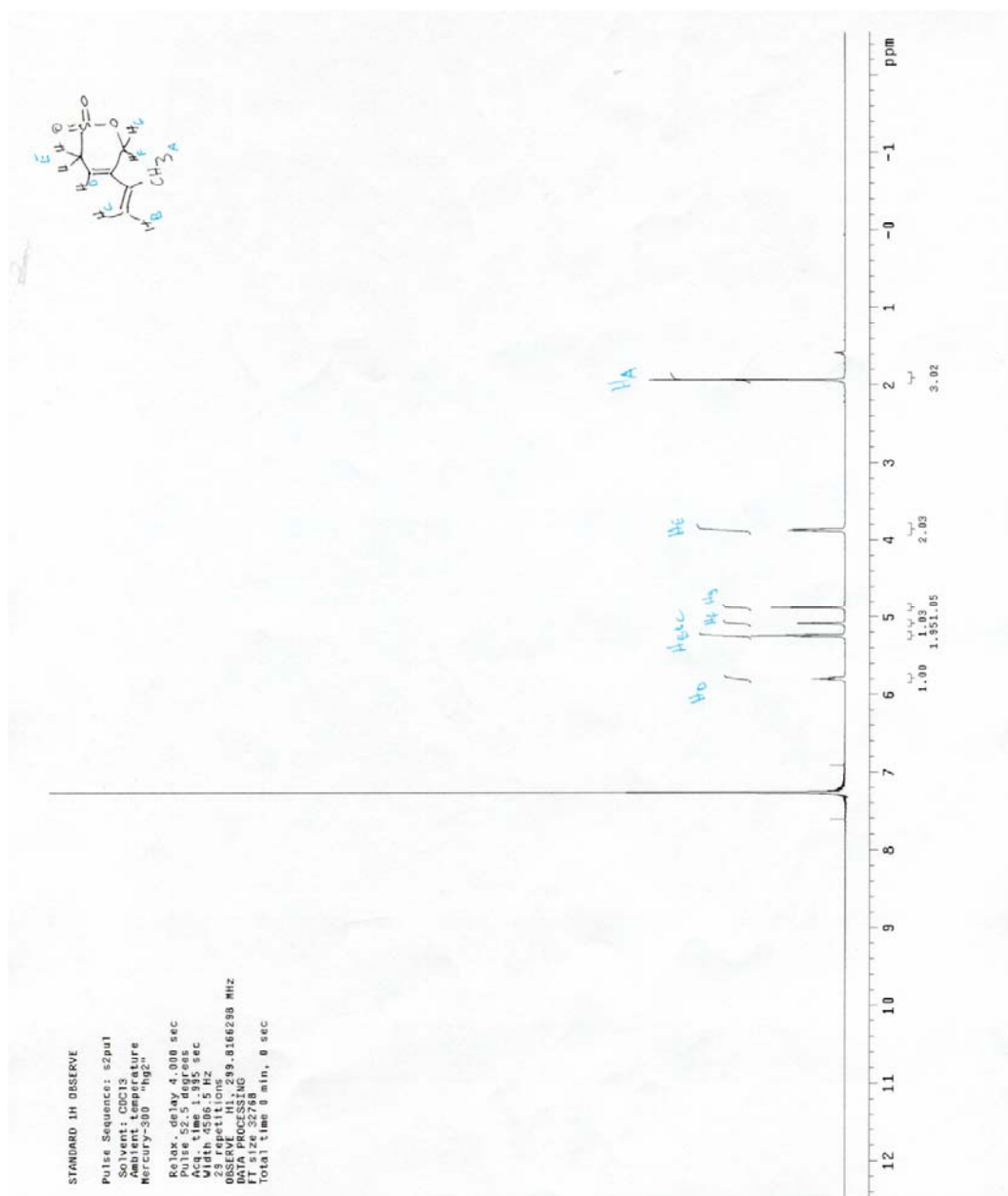


**Figure 2.28** Sulfonate ester **10**  $^1\text{H}$  NMR.

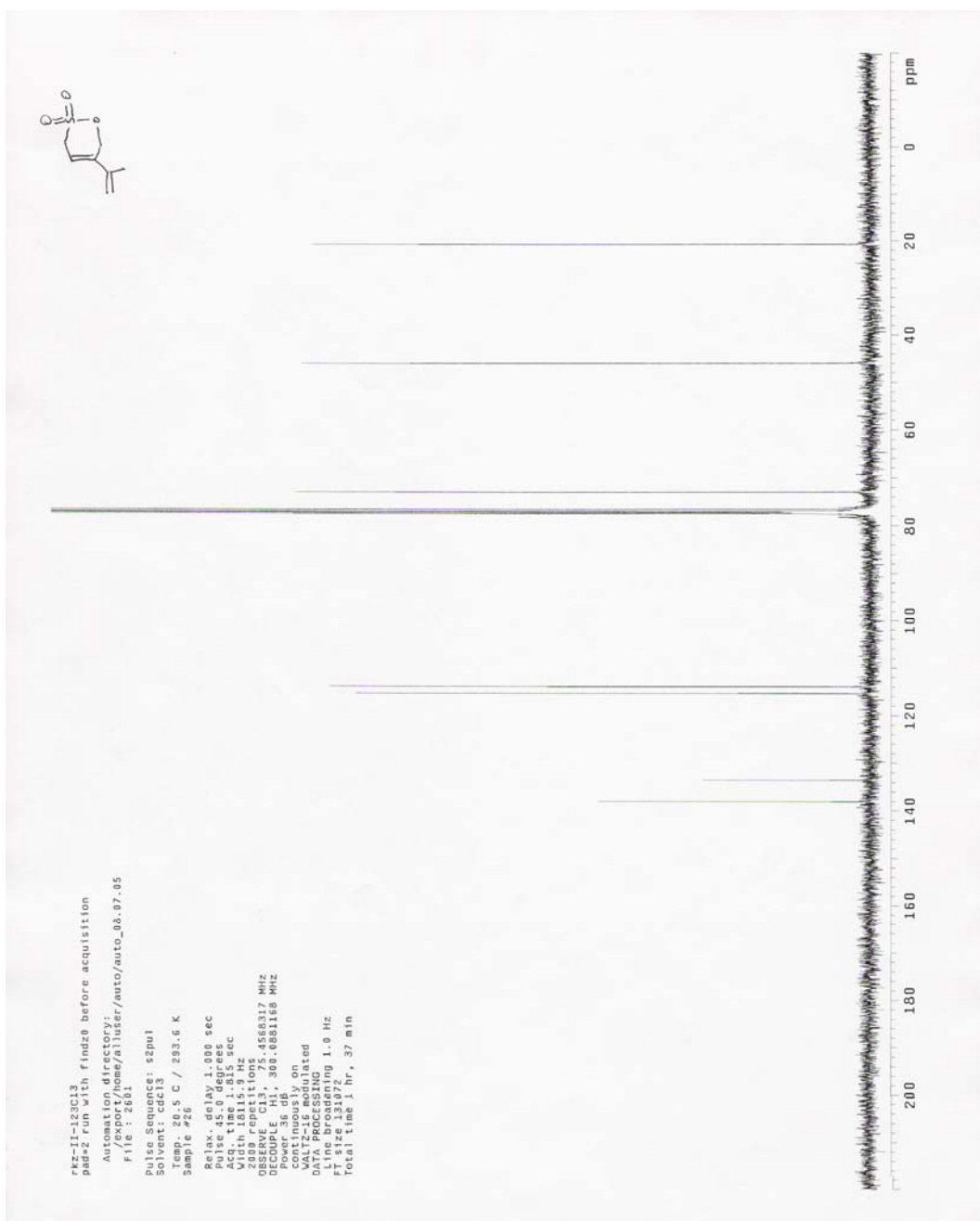




**Figure 2.29** Sulfonate ester **10**  $^{13}\text{C}$  NMR.

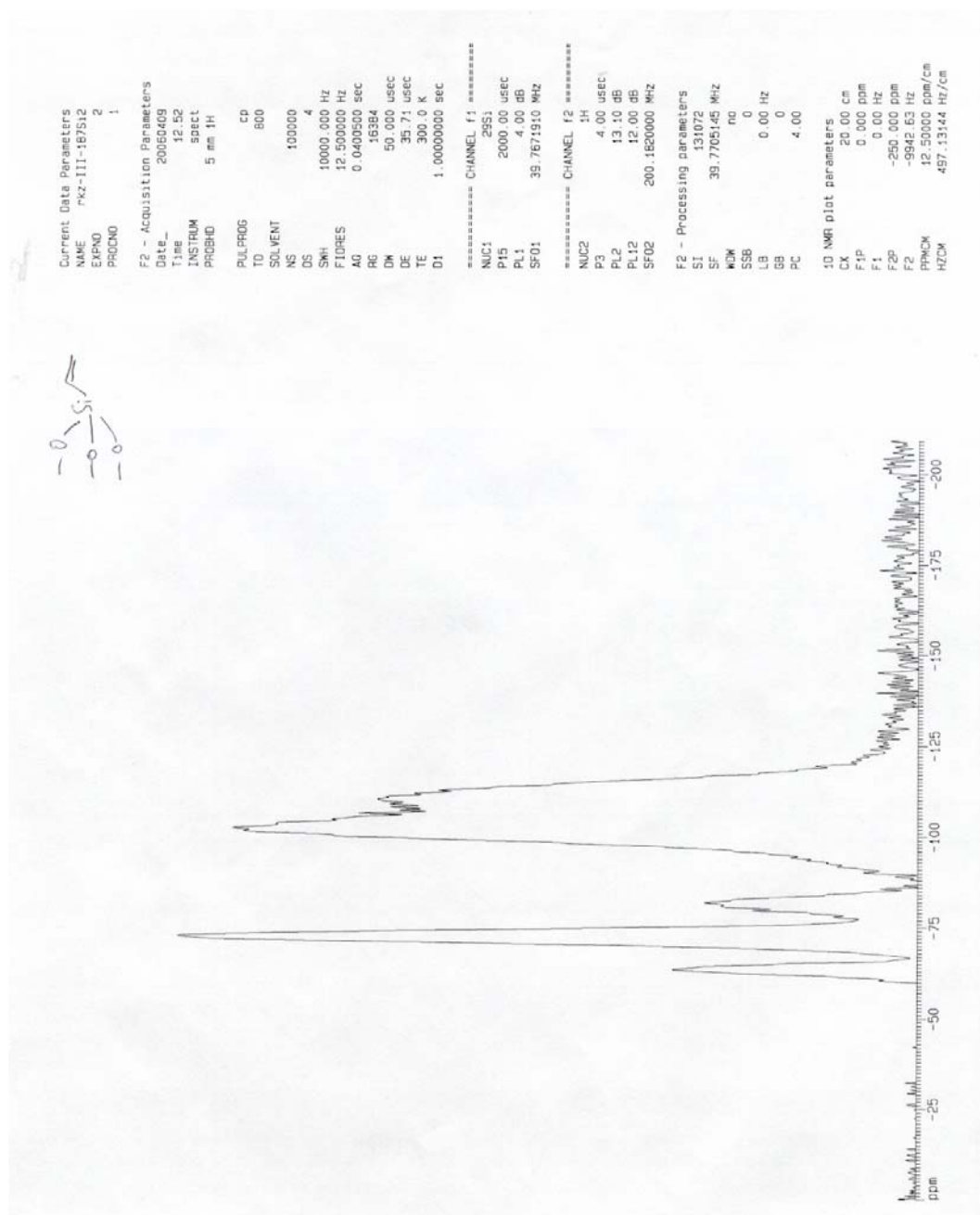


**Figure 2.30** Sultone **1** <sup>1</sup>H NMR.

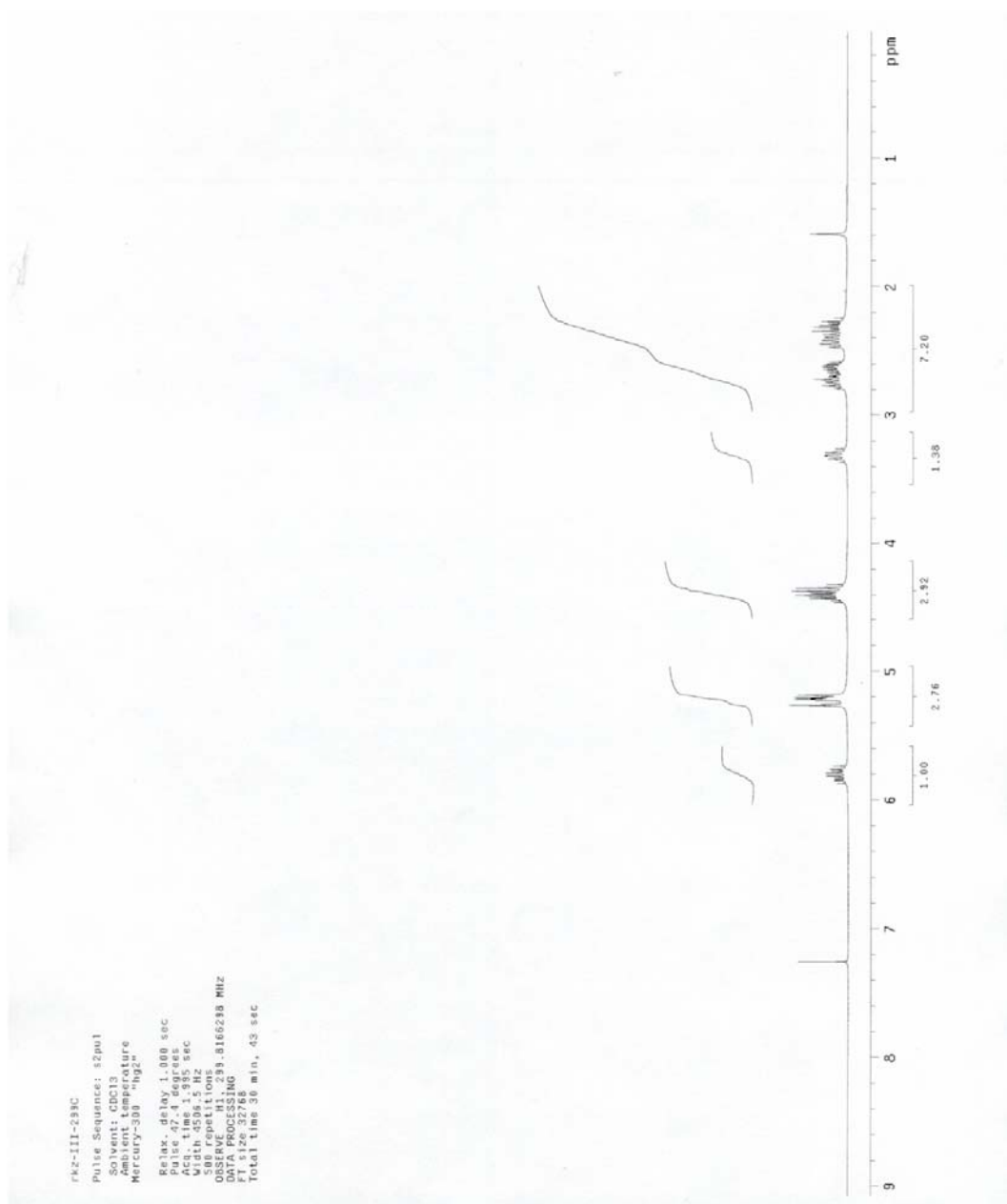


**Figure 2.31** Sultone 1  $^{13}\text{C}$  NMR.

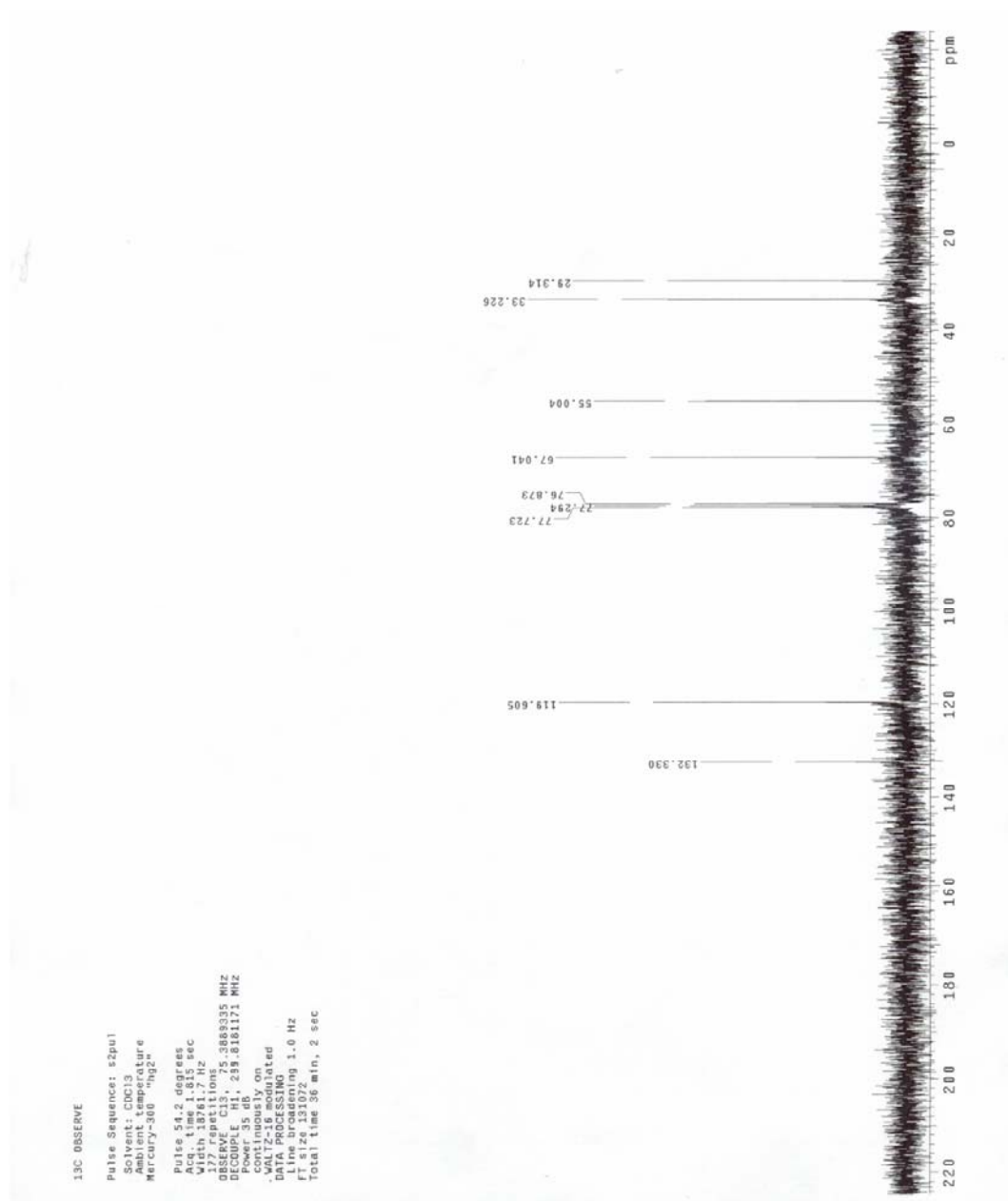




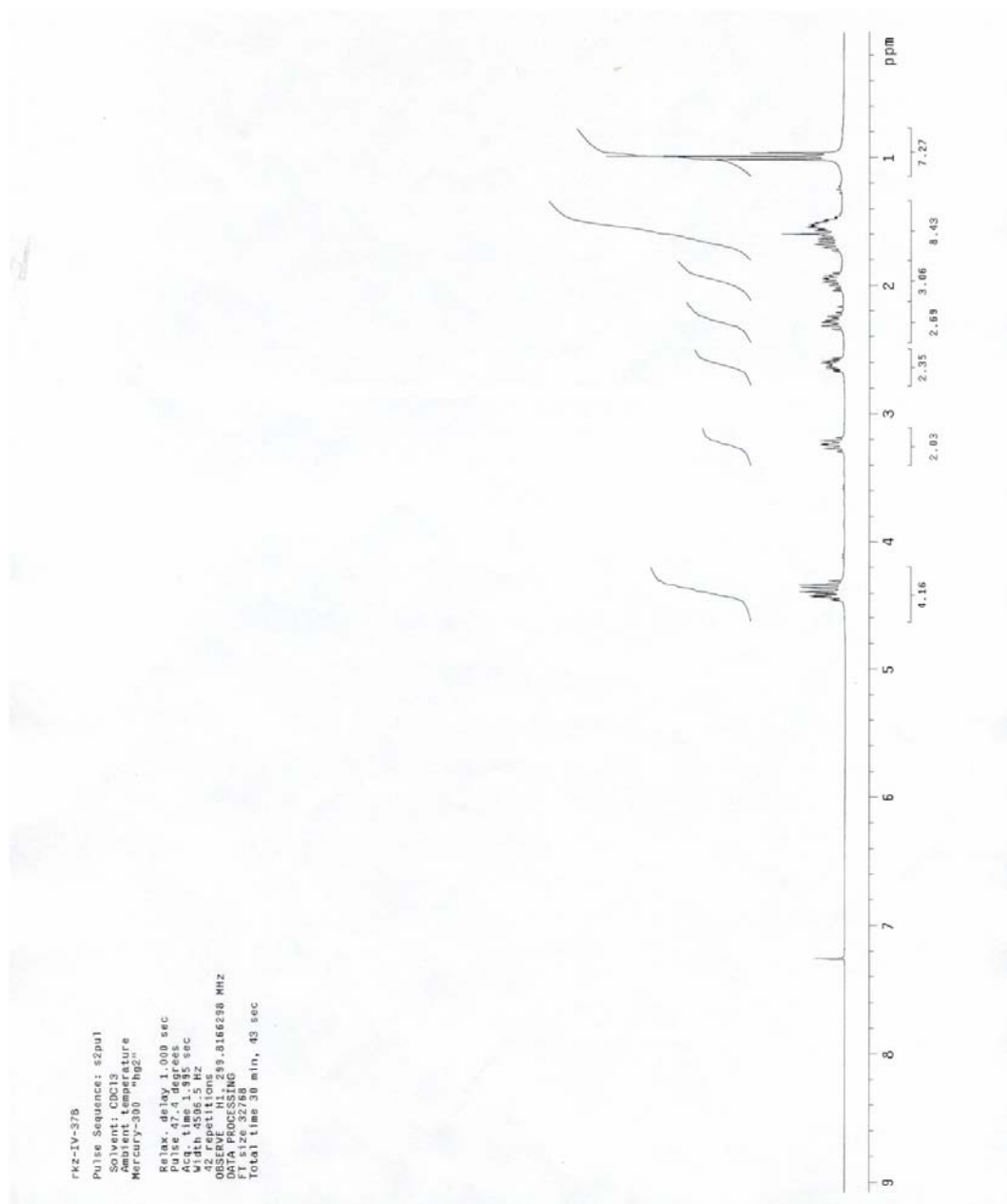
**Figure 2.33** Olefin functionalized SBA-15 4  $^{29}\text{Si}$  NMR.



**Figure 2.34** Allyl sultone **20**  $^1\text{H}$  NMR.



**Figure 2.35** Ally Sultone **20**  $^{13}\text{C}$  NMR.



**Figure 2.36** Olefin reduction side product of hydrosilylation reactions.



## 2.6 References

- [1] Kresge, C. T.; Leonowicz, M. E.; Roth, W. J.; Vartuli, J. C.; Beck, J. S. *Nature* **1992**, *359*, 710-712.
- [2] Wight, A. P.; Davis, M. E. *Chem. Rev.* **2002**, *102* (10), 3589-3613.
- [3] Rahimi, A.; Farhangzadeh, S. *Iran. Poly. J.* **2001**, *10* (1), 29-32.
- [4] Dufaud, V.; Davis, M. E. *J. Am. Chem. Soc.* **2003**, *125*, 9403-9413.
- [5] Darmstadt, J. K.; Reinheim, V. K.; Darmstadt-Arheilgen, W. U. Method for making aromatic bisphenols. US Patent 4,931,594, 1990.
- [6] Randolph, U.; Bachem, N.; Wulff, C. Ion exchange modified with mercapto amines. US Patent 5,212,206, 1993.
- [7] Li, S. M. Isomerization of by-products of bi-phenol synthesis. US Patent 4,825,010, 1989.
- [8] Powell, J. B.; Uzelmeier, C. W. Process for preparing a bisphenol. US Patent 5,105, 026, 1992.
- [9] Wehmeyer, R. M.; Tasset, E. L.; Walters, M. E. Polymeric substrate containing mercapto and sulfonic groups. US Patent 6,051,658, 2000.
- [10] Wieland, S.; Panster, P. *Stud. Sur. Sci. Catal.*, *108*, **1997**.
- [11] (a) Das, D.; Lee, J. -F.; Cheng, S. *Chem. Commun.* **2001**, 2178-2179. (b) Wieland, S.; Panster, P. *Stud. Surf. Sci. Catal.* **1997**, *108*, 67-74. (c) Jerabek, K.;

- Odnoha, J.; Setinek, K. *Appl. Catal.* **1988**, *37*, 129-138. (d) Gupta, S. R.; Dwivedi, M. C. *Chem. Age India* **1971**, *22*, 339-348. (e) Jerabek, K.; Li, G. H.; Setinke, K. *Collect. Czech. Chem. Commun.* **1989**, *54*, 321-325.
- [12] (a) Van Rhijn, W. M.; De Vos, D.; Sels, B. F.; Bossaert, W. D.; Jacobs, P. A. *J. Chem. Soc., Chem. Commun.* **1998**, 317-218. (b) Bradley, R. D.; Ford, W. T. *J. Org. Chem.* **1989**, *54*, 5437-5443. (c) Zhao, D.; Sun, J.; Li, Q.; Stucky, G. D. *Chem. Mater.* **2000**, *12*, 1961-1968. (d) Margolese, D.; Melero, J. A.; Christiansen, S. C.; Chmelka, B. F.; Stucky, G. D. *Chem. Mater.* **2000**, *12*, 2448-2459.
- [13] Mbaraka, I. K.; Radu, D. R.; Lin, V. S.; Shanks, B. H. *J. Catal.* **2003**, *219*, 329-336.
- [14] Hermanson, G. T. *Bioconjugate Techniques*. Academic Press, 1996. Pp. 88-89.
- [15] King, J.F.; Lam, J. Y. L. Skonieczny, S. *J. Am. Chem. Soc.* **1992**, *114* (5), 1743-1749.
- [16] Dauban, P.; Dodd, R. H. *Org. Lett.* **2000**, *15*, 2327-2330.
- [17] Karsch, S.; Freitag, D.; Schwab, P.; Metz, P. *Synthesis* **2004**, *10*, 1696-1712.
- [18] Le Flohic, A.; Meyer, C.; Cossy, J.; Desmurs, J.-R.; Galland, J.-C. *Synlett* **2003**, *5* (10), 667-670.
- [19] Smith, M. B.; Wolinsky, J. *J. Org. Chem.* **1981**, *46*, 101-106.

**Chapter 3****Acid-Base Bi-functional Heterogeneous Catalyst Design**

This chapter was reproduced in part with permission from Zeidan, et. al., *Angew. Chem. Int. Ed. Eng.*, 6332-6335 (2006). Copyright 2006 Wiley-VCH.

### 3.1 Abstract

Direct synthesis of mesoporous silica that contains both organic amines and acids is reported. Simultaneous immobilization of primary amines and sulfonic acids on SBA-15 (SBA-15-A/B) creates a heterogeneous catalyst that exhibits cooperative catalytic behaviour in the aldol condensation reaction due to its combined acidic and basic properties. Immobilization of the acid and base groups maintains their respective chemical reactivity, whereas the homogeneous analogues of these functional groups in solution neutralize and are not active. By varying the pKa of the acid component in the acid-base bi-functional catalysts, improved reactivity is observed with lower acidity as the effect on the equilibrium between free and neutralized acid and base is examined.

### 3.2 Introduction

One of the recurring principles of enzyme catalysis that enables reactions to be carried out with incredible reaction rates and selectivities is that of cooperativity between neighboring functional groups.<sup>1</sup> Enzymes are assembled through a complex network of interactions that give rise to primary, secondary and tertiary structure elements. The rigid amide backbone allows for precise placement of functional groups near to one another, and the rigid backbone allows for the formation of a well defined active site. This active site has a three dimensional structure containing binding pockets and reactive functional groups arranged in a precise manner. The binding pockets are responsible for orienting substrates, differentiating between different size substrates and conforming to the transition state of the reaction to help lower the activation energy by stabilizing the transition structure.<sup>2</sup> It is the combinations of neighboring functional groups that operate in concert in a cooperative fashion that are responsible for carrying out the transformations. A number of interactions are observed between these functional groups during the course of the cooperative, catalytic behavior and the most common are electrostatic interactions, dipole-dipole interactions and acid-base interactions. As an extension of the work presented in Chapter 2, the possibility of using “co-condensation” to prepare multi-functional catalysts by incorporation of multiple functional groups was examined with the aim of emulating these types of interactions found in enzyme catalysis, particularly acid-base interactions.

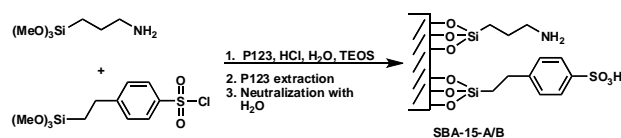
Having demonstrated that it was possible to observe cooperative catalysis<sup>3</sup> between functional groups immobilized on SBA-15 together through random distribution in a “co-condensation” approach, the next application of interest for this method was the

possibility of immobilizing incompatible functional groups together on the surface. A number of applications for a material with multiple functional groups could be envisioned, such as carrying out multi-step reaction sequences in one pot with each step catalyzed by a different functionality immobilized on the surface. Immobilizing incompatible functional groups may give rise to unique reactivity or cooperativity between such pairs (such as oxidants with reductants or acids with bases) in addition to the ability to carry out orthogonal reaction steps in sequence in one pot. Materials bearing amine functional groups have been reported to undergo cooperative catalysis with surface silanols.<sup>4</sup> Functionalized materials bearing amine functional groups together with thiols have also been reported.<sup>5-6</sup> Incompatible functionalities have also been used simultaneously when prepared on isolated supports and mixed in a physical mixture,<sup>7-11</sup> but this strategy has the drawback of preventing any sort of cooperative catalysis between these groups due to their physical separation. Cooperativity has been reported between immobilized amines with hydrogen bonding ureas as well.<sup>12</sup> During the course of this study, a similar approach was reported where amine and sulfonic acid containing materials were prepared in which the sites were physically separated on the same support.<sup>13</sup>

### **3.3 Results and Discussion**

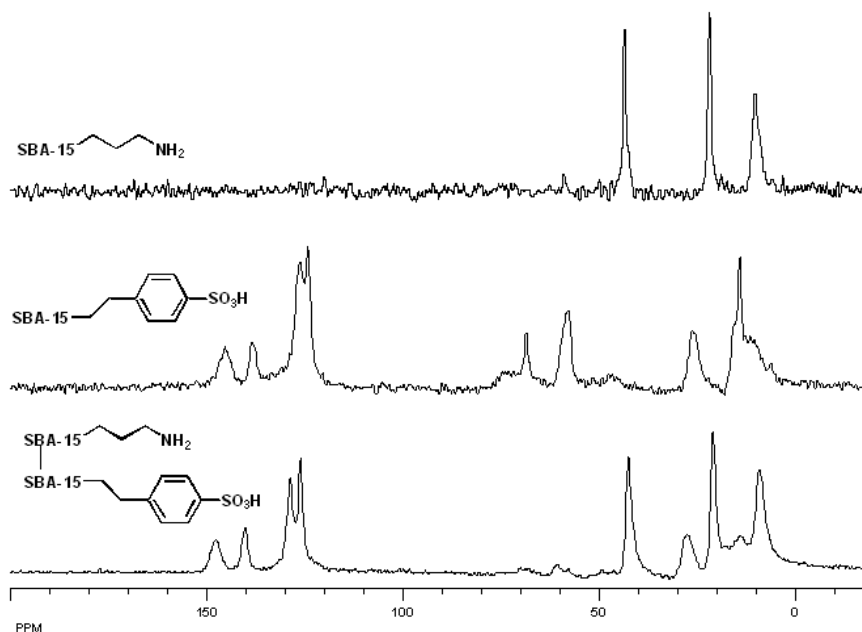
Drawing from the methods in Chapter 2, “co-condensation” methods of preparing SBA-15 mesoporous silica catalysts functionalized with organic groups were carried out.<sup>14</sup> Having worked extensively with sulfonic acid functionalized SBA-15, as well as previous experience with amine functionalized materials, initial experiments were carried out toward creating materials containing incompatible sulfonic acid and primary amine

functional groups simultaneously. Through “co-condensation” methods, SBA-15 type materials were prepared containing aromatic sulfonic acid sites and primary amine sites (Figure 3.1).



**Figure 3.1** Synthesis of acid-base bi-functional catalyst.

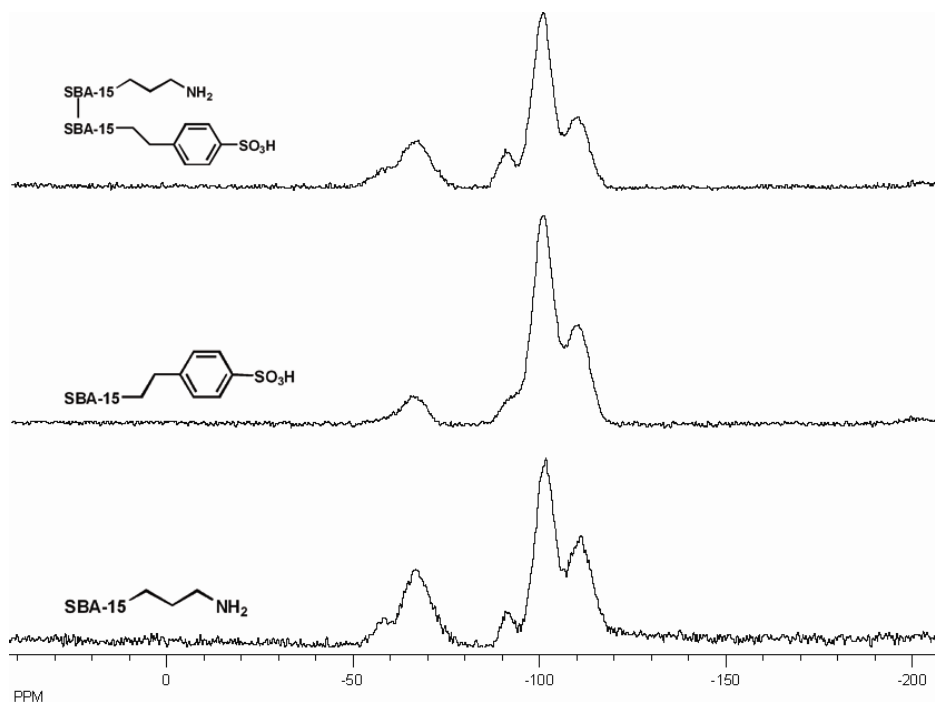
Using the commercially available sulfonyl chloride precursor shown above, which is first added to the pH 1 SBA-15 synthesis pot and stirred for 5 minutes to allow for hydrolysis of the sulfonyl chloride followed by addition of the aminopropyltrimethoxysilane, SBA-15-A/B was prepared which contained sulfonic acid and propyl amine sites randomly distributed throughout the material. The appropriate control catalysts were also synthesized, SBA-15 functionalized with only amine sites as well as SBA-15 functionalized with only sulfonic acid sites. Incorporation of these groups simultaneously was confirmed through spectroscopic methods to illustrate the co-habitation of the mutually incompatible functionalities. Solid state <sup>13</sup>C CP/MAS NMR experiments were carried out on the materials to illustrate incorporation of the organic groups into the material. These experiments clearly illustrate the incorporation of the aromatic sulfonic acid residue as well as the propyl aliphatic chain of the primary amine in the dual-functionalized catalyst (Figure 3.2).



**Figure 3.2**  $^{13}\text{C}$  CP/MAS solid state NMR of organically functionalized materials. Peaks at 60 ppm are due to residual ethoxy, and at 73 ppm due to P123 remaining after extraction.

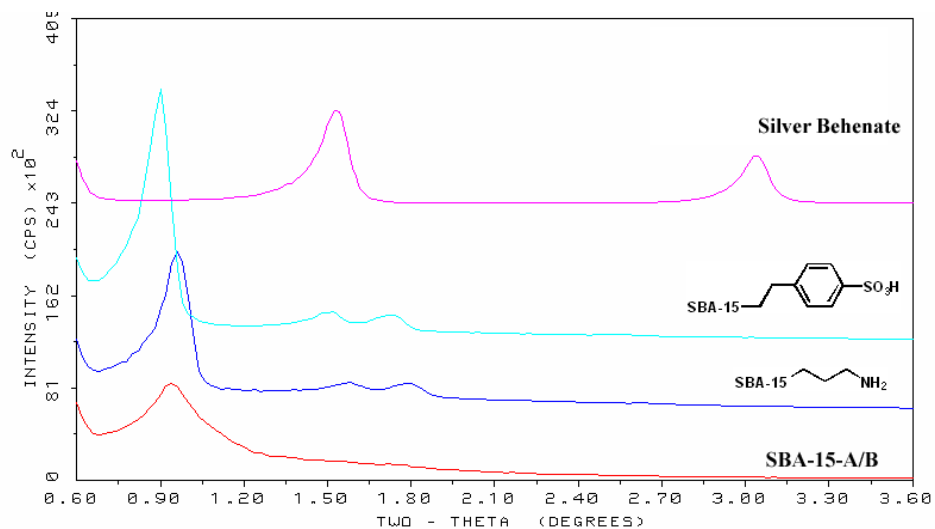
Similarly,  $^{29}\text{Si}$  CP/MAS solid state NMR experiments were also carried out to examine the silica environment and confirm inclusion of the organic groups into the silica structure (Figure 3.3). Each material clearly exhibits T type (-65 ppm) silica atoms indicative of silica atoms connected to three oxygen atoms and one carbon atom, confirming incorporation of the organic groups into the walls of the materials. Each material also exhibits Q type sites (-100 ppm) corresponding to quaternary silica atoms attached to four oxygen atoms making up the walls of the mesoporous material, as is typical of SBA-15 type materials.





**Figure 3.3**  $^{29}\text{Si}$  CP/MAS solid state NMR of organically functionalized materials.

Powder X-ray diffraction measurements were made on a Siemens D500 instrument in step mode in order to examine the ordering of the catalysts (Figure 3.4). A step size of 0.02 degrees and a scan rate of 0.3 degrees/minute were used. Silver behenate was run as a low angle standard. The materials all showed a low angle peak indicative of hexagonal ordering and typically showed some long range ordering peaks. The SBA-15-A/B shows less ordering in its structure as it has a higher organic loading, and this is typical of materials with high organic loading.



**Figure 3.4** XRD analysis of solid state catalysts.

These catalysts were also characterized by  $N_2$  adsorption and the organic loading estimated by TGA (Table 3.1).

**Table 3.1** Catalyst characterization data.

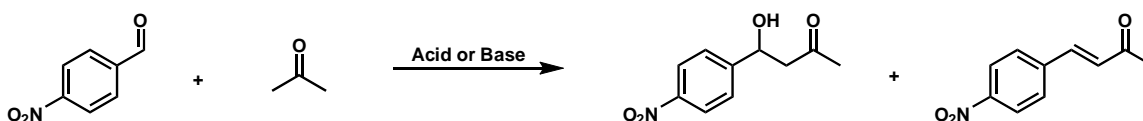
Catalyst	BET Surface Area (m <sup>2</sup> /g)	Mean Pore Diameter (Å)	Organic loading (mmole/g) <sup>a</sup>
SBA-15-CH <sub>2</sub> CH <sub>2</sub> CH <sub>2</sub> NH <sub>2</sub>	597	46	1.1
SBA-15-CH <sub>2</sub> CH <sub>2</sub> C <sub>6</sub> H <sub>4</sub> SO <sub>3</sub> H			
SBA-15-CH <sub>2</sub> CH <sub>2</sub> CH <sub>2</sub> NH <sub>2</sub>	718	62	0.51
SBA-15-CH <sub>2</sub> CH <sub>2</sub> C <sub>6</sub> H <sub>4</sub> SO <sub>3</sub> H	852	56	0.49

[a] Determined by TGA analysis

[b] 1.1 mmole/g is the total organic loading, corresponding to 0.55 mmole/g of each functional group

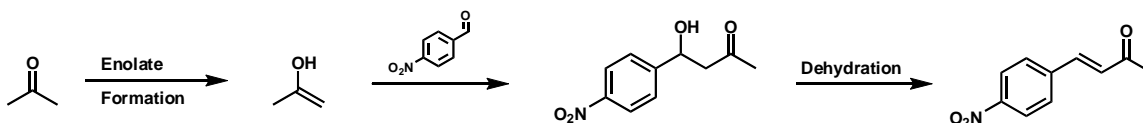
The materials exhibited similar physical properties, with surface areas on the order of 600-800 m<sup>2</sup>/g and mean pore diameters of roughly 50-60 Å typical of SBA-15 type materials.

Having characterized these catalysts, it was possible to use these materials as catalysts for carrying out reactions. Due to the nature of the dual-functionalized acid-base material, it was necessary to examine a different reaction for this catalyst. Ideally, a reaction should be used that is catalyzed by acids and bases in order to investigate the possibility of cooperativity between these groups. The aldol reaction was chosen as it meets these criteria in being catalyzed by acids or bases, as well as being a biologically relevant reaction involved in the creation of many natural products. The reaction between acetone and 4-nitrobenzaldehyde was chosen to examine the reactivity properties of the acid-base bi-functional catalyst (Figure 3.5).



**Figure 3.5** Aldol reaction between acetone and 4-nitrobenzaldehyde.

In order to understand the results of catalytic experiments, it is essential to examine the reaction mechanism and understand the chemical transformations that occur in this reaction (Figure 3.6). In the first step, an enolate is formed from acetone by removal of one of the alpha protons, either by direct deprotonation with a base, activation by an acid followed by deprotonation with the conjugate base of the acid, or through imine formation with amine catalysts. The enolate generated in the reaction mixture then attacks the electrophilic aldehyde generating the secondary alcohol bearing aldol addition adduct. Under the reaction conditions of acid or base, this secondary alcohol can eliminate and lose an equivalent of water generating the aldol dehydration product.



**Figure 3.6** Mechanism of aldol reaction.

This reaction was then carried out using the synthesized bi-functional catalysts to investigate cooperative interactions between the immobilized acid and base sites. Entry 1 (Table 3.2) was carried out using the acid-base functionalized catalyst and surprisingly good conversion, 62% yield, of the aldol products was observed. This level of conversion was surprising when considering the respective functional groups alone were not nearly as reactive, as shown in entries 2 and 3 (Table 3.2). In these entries the sulfonic acid alone exhibits 16% conversion and the amine alone exhibits 33% conversion, significantly lower than the acid-base functionalized catalyst. With the two functional groups being dispersed randomly in the synthesis, it is expected that there would be acid sites neighboring acid sites, base sites neighboring base sites, and some acid sites in proximity to base sites. If the catalytic activity is due to single acid or base sites, or neighboring acid/acid or base/base sites, the level of conversion as in entries 2 and 3 (Table 3.2), would be the achievable upper bound. The enhancement of reactivity beyond those cases is likely due to interactions between neighboring acid and base sites.

**Table 3.2** Acid-base bi-functional catalysis data.

Reaction scheme showing the reaction of 4-nitrobenzaldehyde with acetone catalyzed by SBA-15 functionalized catalysts at 50°C for 20 hours, yielding products A and B.

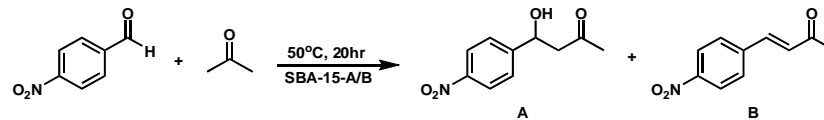
Entry	Catalyst	%A	%B	Total Yield (%) <sup>[a]</sup>
1		45	17	62
2		8	8	16
3		25	8	33
4	Physical Mixture <sup>[b]</sup>	30	14	44
5	SBA-15	0	0	0
6		0	0	0
7		3	5	8
8		3	1	4

[a] Yields determined by <sup>1</sup>H NMR with THF as an internal standard.  
 [b] Physical mixture is a 1:1 physical mixture of amine functionalized SBA-15 and sulfonic acid functionalized SBA-15

A physical mixture of acid and amine functionalized SBA-15 (on separate solids) shows an intermediate level of conversion that is significantly lower than the dual functionalized acid/base catalyst (entry 4, Table 3.2). The support alone causes no conversion (entry 5, Table 3.2). Interestingly, the homogeneous analogues of the sulfonic acid and amine show no conversion to either product as these functionalities apparently neutralize each other and salt out of the reaction mixture (entry 6, Table 3.2). This

illustrates one of the advantages of immobilizing incompatible functional groups: when they are used in solution together, no conversion is observed. Also, the individual acid and base homogeneous analogues give rise to very low conversions (entries 7 and 8, Table 3.2), much less than the acid/base bi-functional catalyst.

It is expected that the acid and base groups in SBA-15-A/B would be in equilibrium between the free acid and base and the ion pair that results from neutralization, and that the solvent would have a dramatic effect on this equilibrium, i.e., protic solvents would confer different properties than aprotic solvents due to differing abilities to stabilize the neutralized ion pair. In polar, protic solvents, the equilibrium would lie towards the ion pair as proton exchange would be rapid, and the protic solvent would stabilize the ion pair the most. Non-polar, aprotic solvents would cause slower exchange of protons and would stabilize an ion pair much less than a protic solvent, forcing the equilibrium in favor of the free acid and base. In order to investigate these possibilities, reactions were carried out in a variety of co-solvents to examine the effect of solvent polarity on conversion. In polar, protic solvents such as water and methanol (entries 1 and 2, Table 3.3) the conversion to both products is near 30%. Upon moving to polar, aprotic solvents, such as diethyl ether and chloroform, the conversion more than doubles to about 70% (entries 3 and 4, Table 3.3). Non-polar, aprotic solvents like hexane and benzene (entries 5 and 6, Table 3.3) give further improvements in conversion, approaching 90% in the case of hexanes (entry 5, Table 3.3). Thus, there is a clear effect on conversion that is related to solvent polarity, suggesting that the nature of the solvent does affect the equilibrium of proton exchange and hence the effective concentration of free acid and base.

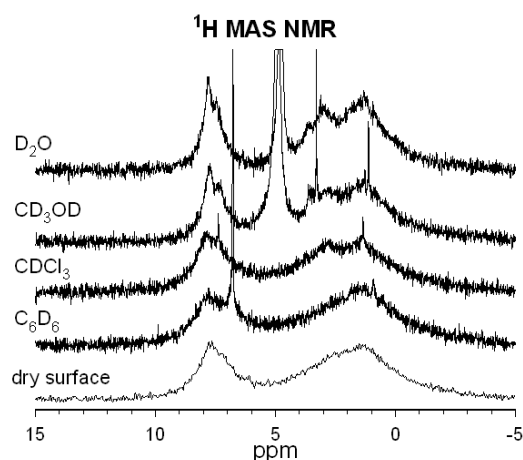
**Table 3.3** Solvent effect on catalysis.

Entry	1:1 cosolvent	%A	%B	Total Yield (%) <sup>[a]</sup>
1	H <sub>2</sub> O	27	7	34
2	MeOH	14	9	23
3	Et <sub>2</sub> O	52	13	65
4	CHCl <sub>3</sub>	60	9	69
5	Hexane	75	13	88
6	PhH	62	12	74

[a] Yields determined by <sup>1</sup>H NMR with THF internal standard

Solid state CP/MAS NMR was used to probe the local motion of the bi-functional catalyst. SBA-15-A/B was fully deuterated and then slurried in different deuterated solvents to study the changes in motion of the functional groups in these different environments (Figure 3.7). In D<sub>2</sub>O and CD<sub>3</sub>OD the resolution of the <sup>1</sup>H NMR resonances (from non-exchanging protons in the organic functional groups) sharpened, indicating a more mobile structure. However, in the non-polar solvents CD<sub>3</sub>Cl and C<sub>6</sub>D<sub>6</sub>, the resonances broadened and suggest more restricted motion of the two groups as the acid and base functional groups associate to avoid unfavorable interactions with non-polar solvents. The trend is in full agreement with the catalysis data as reactions in non-polar solvents causes the polar acid and base groups to associate to a greater extent, allowing for an increased cooperative effect. In polar solvents, the groups are more mobile as they favorably interact with the solvent and are less likely to interact with one another for cooperative catalysis to occur. Taken together, the catalytic and NMR data suggest that

the catalytic behavior of SBA-15-A/B is clearly dictated by multiple factors, two of which seem to be the state of the equilibrium between the acid and base and the ion pair and the interactions between the two functional groups as caused by polar/non-polar interactions with the solvent.



**Figure 3.7** Solvent effect on  $^1\text{H}$  MAS NMR lineshape. Sharp lines are due to incomplete deuteration of solvents.

In order to probe the bi-functionality of the catalyst, SBA-15-A/B was treated with acid to neutralize the amine functional groups, leaving only the sulfonic acid sites. SBA-15-A/B was washed with 1 M HCl or pTSA(aq), entries 1 and 2 respectively (Table 3.4), and it is clear that the material behaves like the immobilized sulfonic acid alone (entry 2, Table 3.1). Likewise, SBA-15-A/B was treated with propyl amine (entry 3, Table 3.4) and the resulting material where the sulfonic acid sites are neutralized behaved the same as the amine functionalized catalyst (entry 3, Table 3.1). These results illustrate the bi-functionality of SBA-15-A/B and the co-existent acidity and basicity. The experiments highlight the interesting properties achievable by immobilization of multiple



functional group types. In solution, the amine and sulfonic acid salt out and give rise to no conversion (entry 6, Table 3.1), and when the heterogeneous catalyst SBA-15-A/B is treated with homogeneous acids or bases the opposing functional group salts out and its respective behavior is lost. Whereas when the amine and sulfonic acid are immobilized on SBA-15-A/B the two opposing functional groups do not lose catalytic activity but rather function in a cooperative manner to give the most active catalyst used in this study.

**Table 3.4** Catalyst quenching experiments.

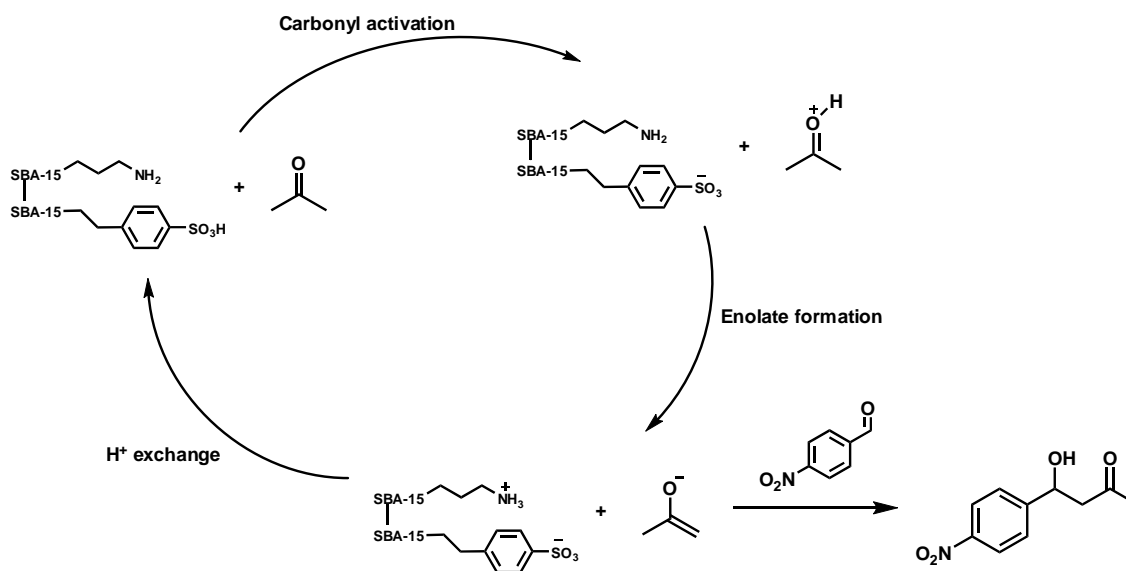
Entry	Catalyst	%A	%B	Total Yield (%) <sup>[a]</sup>
1		7	7	14
2		8	7	15
3		31	7	38

[a] Yields determined by <sup>1</sup>H NMR with THF internal standard

The nature of the equilibrium between the acid and base groups in this material could be very important to the tuning and understanding of its catalytic behavior, as a dramatic solvent effect was observed for this system. The proposed mechanism for acid/base

cooperative catalysis (Figure 3.8) illustrates the potential importance of acid/base interactions. Presumably the regeneration of the active catalytic species relies on the rate of proton exchange between the acid and base groups, which would be facilitated by surface silanols and water when immobilized on mesoporous supports.

In the case of sulfonic acids and amines, one would expect the equilibrium would lie heavily in favor of the inactive, neutralized ion pair and there would be only small amounts of the unneutralized acid/base species containing free sulfonic acids and amines. Sulfonic acids, being strong acids, would expectedly protonate the primary amine readily causing the equilibrium to lie heavily in the direction of the neutralized ion pair.



**Figure 3.8** Proposed cooperative mechanism of acid and base in aldol condensation.

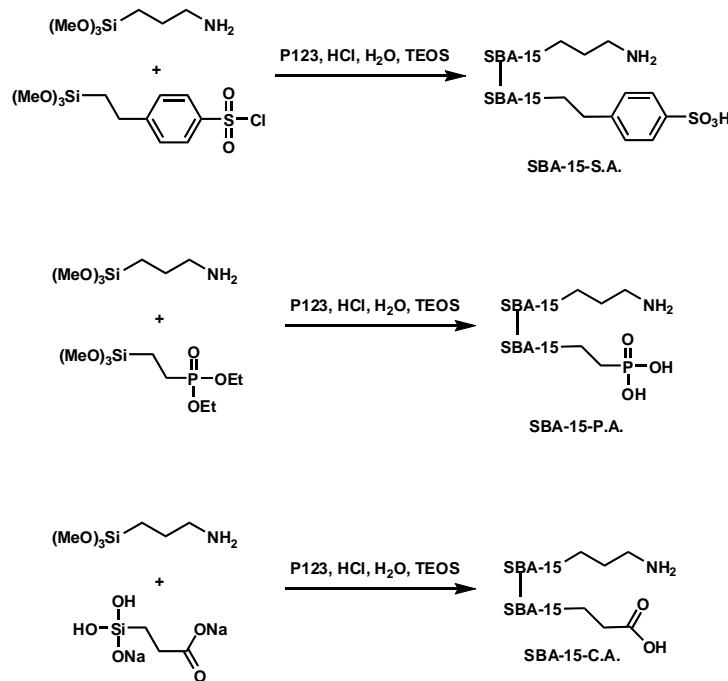
### 3.4 Experimental Section

“One-pot” synthesis. To triblock copolymer poly(ethylene glycol)-block-poly(propylene glycol)-block-poly(ethylene glycol) P123 (4.0 g, 0.688 mmole,  $M_n$  5,800) was added 2.0 M HCl (120.0 mL, 240.0 mmole) and H<sub>2</sub>O (6.0 mL, 333.0 mmole) and stirred at 40 °C until P123 fully dissolved. TEOS (8.2 mL, 37.8 mmole) was then added and allowed to stir at 40 °C for 45 minutes. Then 2-(4-chlorosulfonylphenyl)-ethyltrimethoxysilane (0.65 g, 50/50 w/w solution in dichloromethane, 1.0 mmole) was added first followed by 3-aminopropyltrimethoxysilane (0.19 mL, 1.0 mmole). The mixture was then stirred at 40 °C for 20 hours, and then aged at 100 °C for 24 hours. The resulting solid was filtered and rinsed with excess H<sub>2</sub>O (4 x 500 mL) until the slurry reached a neutral pH. The solid was then allowed to dry overnight on a filter. The dried solid was then extracted with EtOH (400 mL per gram) by refluxing in EtOH for 24 hr to remove P123. The solid was filtered and rinsed repeatedly with EtOH (4 x 500 mL), washed with copious water until neutral, and dried overnight to obtain a dry white solid. The solid was then further dried at 80 °C under vacuum for 24 hr.

Catalytic Experiments. The following general procedure was used for the aldol condensation.<sup>12</sup> 4-nitrobenzaldehyde (76 mg, 0.5 mmole) was dissolved in acetone (10 mL) and the catalyst was added (0.05 mmole total amines and/or sulfonic acids). The reaction was then sealed under Ar and heated at 50 °C for 20 hr. Acetone was then removed in vacuo and the product was analyzed by <sup>1</sup>H NMR in CDCl<sub>3</sub> with THF as an internal standard. In the case of the co-solvent studies, 10 mL of a 50:50 mixture of acetone and co-solvent was used.

### 3.5 Acid pKa Effect

In order to examine this equilibrium, it was reasoned that a careful choice of acids to pair with the amino group could allow for a change in the equilibrium toward more free acid/base sites and potentially lead to higher catalytic activity; if weaker acids with higher pKa's were chosen. Sulfonic acids have a pKa of approximately -2, weaker phosphoric acids have pKa near 3 and even weaker carboxylic acids have pKa's around 5. These three acids of varying strengths were incorporated into SBA-15 through a one-pot synthesis procedure under acidic conditions with P123 as a structure directing agent (Figure 3.9).



**Figure 3.9** Catalyst syntheses with different acid groups.

These different acid functionalized materials were used in the aldol condensation between acetone and 4-nitrobenzaldehyde. The catalysis data are shown below in Table

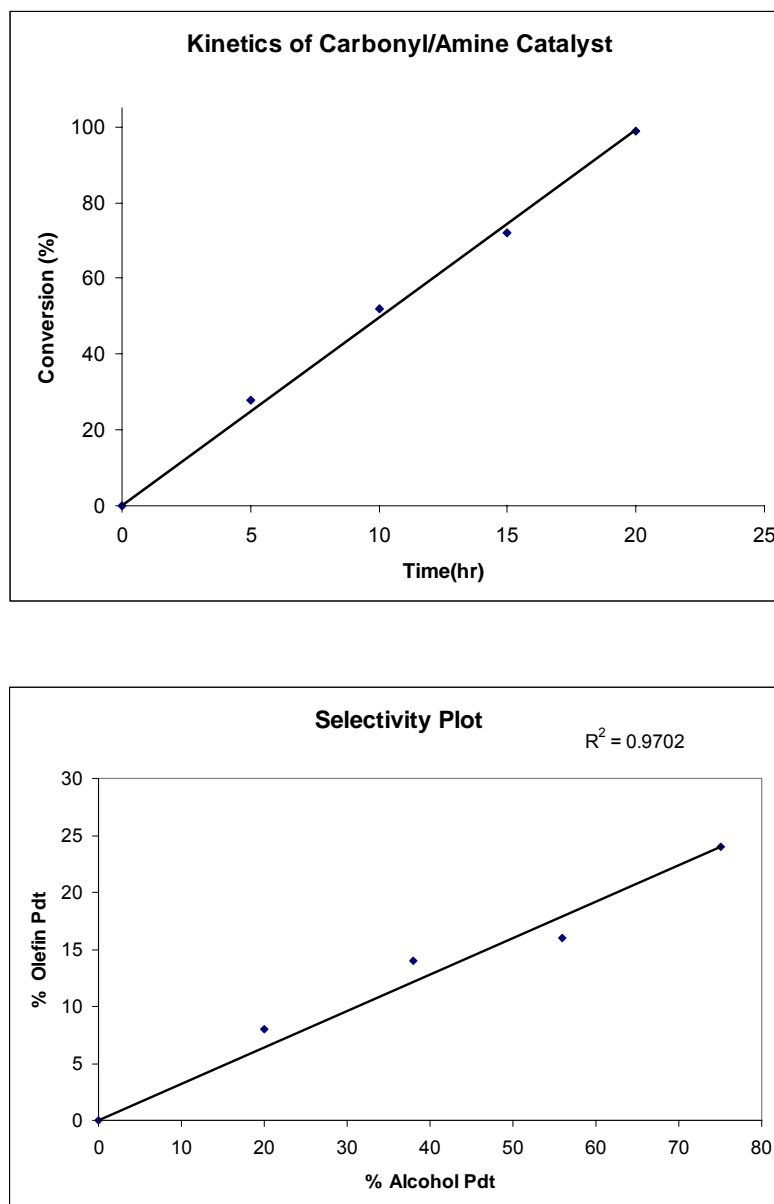
3.5. The hypothesized trend in catalytic behavior is clearly realized and illustrated by these results in that the conversion increases significantly with decreasing acid strength. The combination of sulfonic acid with amines (Entry 1, Table 3.5) gives rise to 62% conversion of aldol product, illustrating cooperative catalysis between these groups. When using a slightly weaker acid in the phosphoric acid/amine catalyst (Entry 2, Table 3.5) a significant improvement in conversion is observed to 78%. Employing an even weaker acid, the carboxylic acid/amine material (Entry 3, Table 3.5), further enhancement is observed and the reaction is nearly quantitative. Entries 4-7 (Table 3.5) serve as control experiments to illustrate the catalytic ability of these functional groups when used independently and to exemplify the types of improvements one can achieve by immobilizing different functional groups that have the ability to behave in a cooperative manner. The carboxylic acid and phosphoric acid groups alone are not efficient catalysts of this reaction and do not give rise to any conversion independently. However, when paired with a group that is mutually incompatible with the acids (a primary amine), these materials are transformed into efficient catalysts for the aldol reaction. The contradictory nature of moving from weaker acids yet obtaining better catalysts is most likely due to this equilibrium between acid and base, and having a weaker acid component actually allows for more free acid and base (the active catalytic sites) to remain on the surface.

**Table 3.5** Acid-base variations catalysis data.

Reaction scheme: 4-nitrobenzaldehyde + acetone  $\xrightarrow[50^\circ\text{C}]{\text{Catalyst}}$  4-nitro-1-phenylbutan-1-ol (A) + 4-nitro-1-phenylbut-3-en-1-one (B)

Entry	Catalyst (10 mol%)	%A	%B	Total Conversion
1		45	17	62
2		62	16	78
3		75	24	99
4		0	0	0
5		0	0	0
6		8	8	16
7		25	8	33

Kinetic experiments were run on the carbonyl functionalized catalyst (Entry 3, Table 3.5) and the data show that the conversion is linear with time and gives a constant selectivity throughout the course of the reaction and are presented below in Figure 3.10.

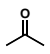
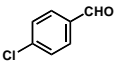
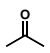
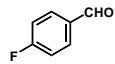
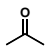
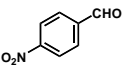
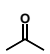
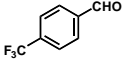
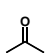
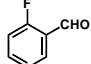
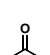
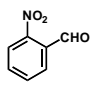

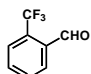


**Figure 3.10** Reaction kinetics and selectivity plot for aldol reaction with SBA-15-C.A.

In order to examine the effect of the electron density of the aldehyde partner on conversion, a variety of aldehyde partners were chosen for the aldol condensation and SBA-15-C.A. was used as the catalyst. Entries 1-4 (Table 3.6) illustrate the importance of an electron-withdrawing group at the para position for this reaction. The conversion varies with the electron donating ability of the para substituent. When a chloro group is

at the 4 position (entry 1), poor conversion to the aldol product is observed. However, in switching to a fluoro, nitro and trifluoromethyl (Entries 2-4) group, conversion improves significantly and according to the electron withdrawing capability of these groups ( $\text{Cl} < \text{F} < \text{NO}_2 < \text{CF}_3$ ). When these electron withdrawing groups are moved to the ortho position, where they may be able to impart a steric blockage of the aldehyde position, conversions decrease significantly, but in this case seem to track with the steric bulk of the substituent rather than electron withdrawing nature (ie  $\text{F} > \text{NO}_2 > \text{CF}_3$ ).

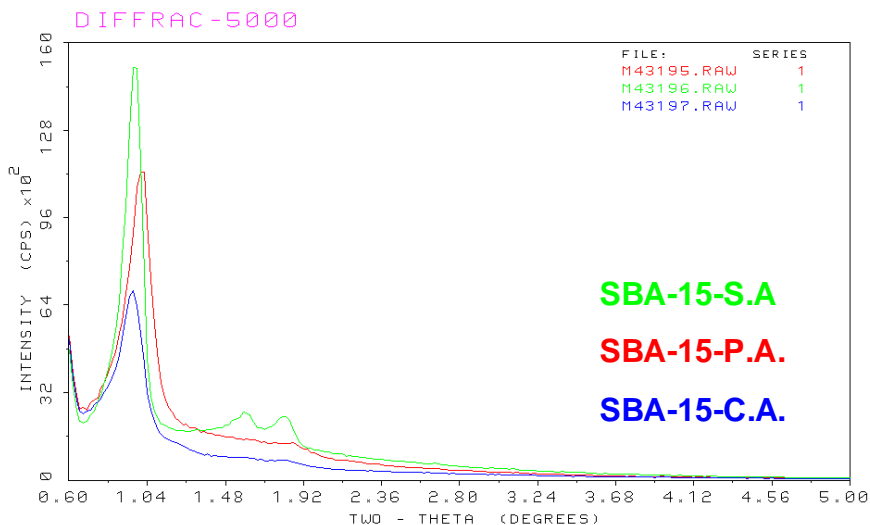
**Table 3.6** Substrate scope.

$  \begin{array}{c}  \text{R}^1-\text{C}(=\text{O})-\text{R}^2 + \text{R}^3-\text{CHO} \xrightarrow[50^\circ\text{C, 20 hr}]{\text{SBA-15-C.A.}} \text{R}^3-\text{CH}(\text{OH})-\text{CH}(\text{R}^2)-\text{C}(=\text{O})-\text{R}^1 + \text{R}^3-\text{CH}=\text{CH}-\text{C}(=\text{O})-\text{R}^1 \\  \text{A} \qquad \qquad \qquad \text{B}  \end{array}  $					
Entry	Ketone	Aldehyde	Alcohol Product (% A)	Olefin Product (% B)	Total Conversion (%)
1			12	12	24
2			49	42	91
3			75	24	99
4			66	33	99
5			40	20	60
6			32	14	46
7			26	8	34

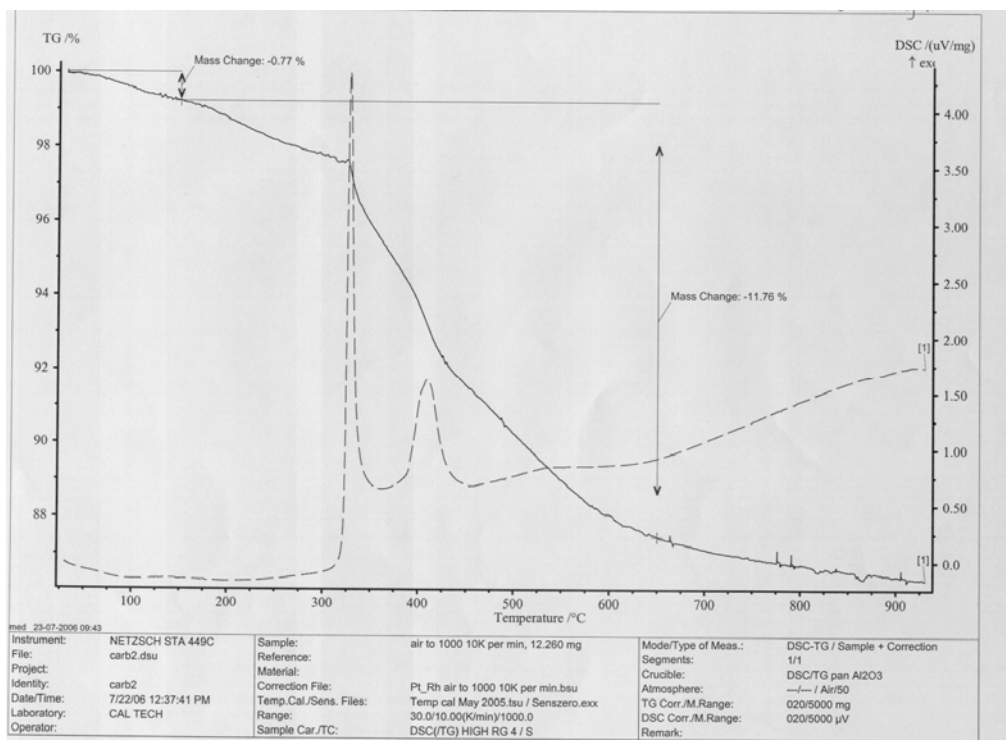


### 3.6 Catalyst Characterization

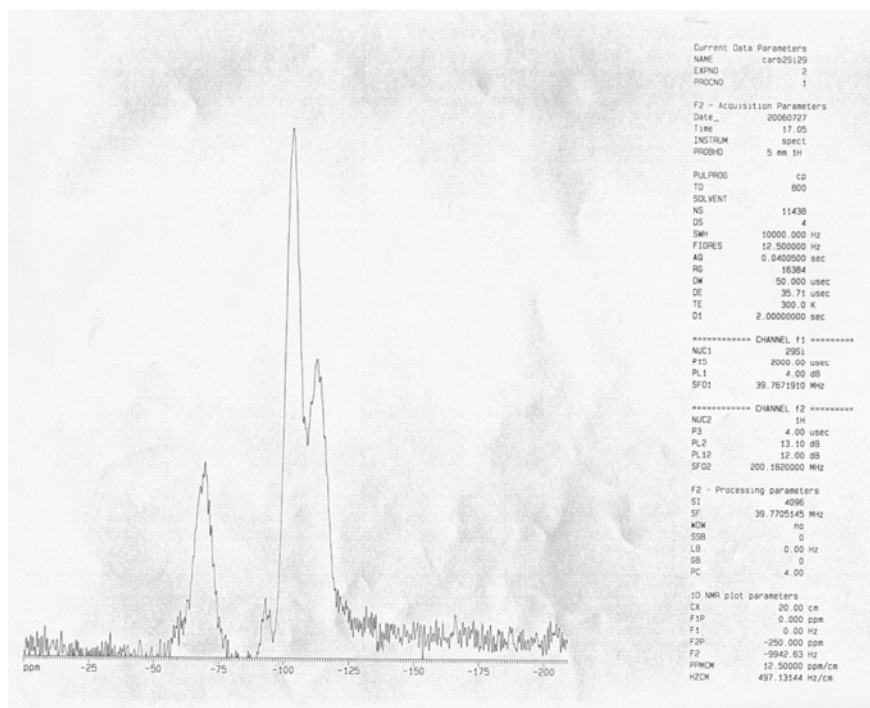
The acid-base functionalized catalysts described above with varying acid components were characterized by a number of different methods and the data are presented below (Figure 3.11). The powder XRD were run on a Siemens D5000 instrument in step mode. The step size was 0.02 degree, and the scan rate was 0.3 degrees/minute. The slit configuration was as follows: there are two consecutive 0.3 degree slits in front of the incident beam, a 0.3 degree slit after the diffracted beam, a 0.05 degree slit before the diffracted beam monochromator, and a 0.15 degree slit before the detector.



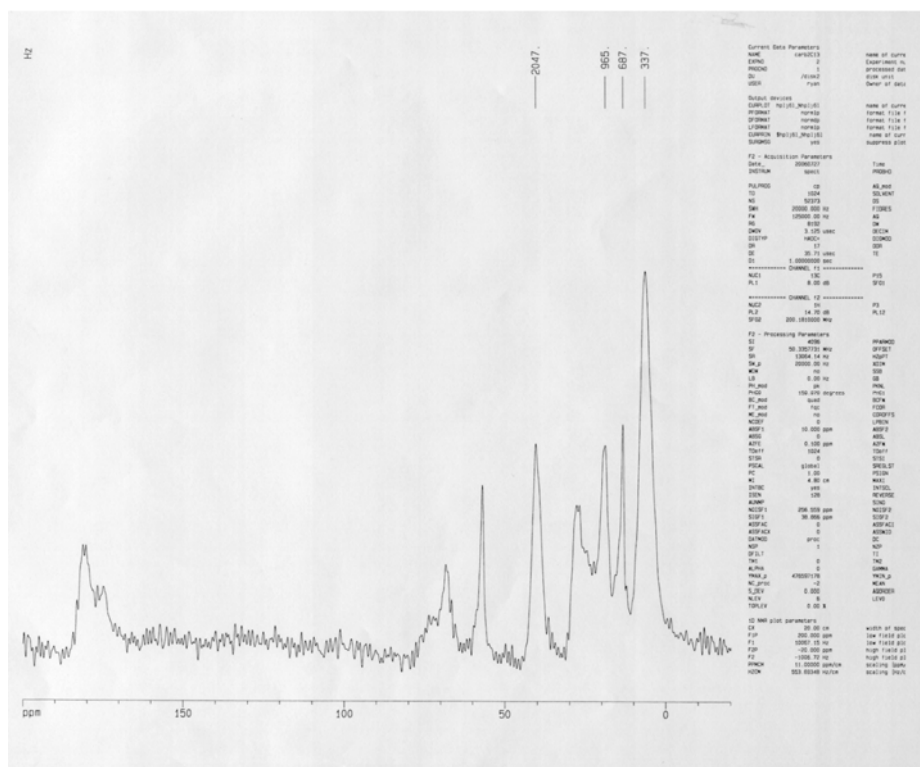
**Figure 3.11** XRD diffraction pattern of heterogeneous catalysts.



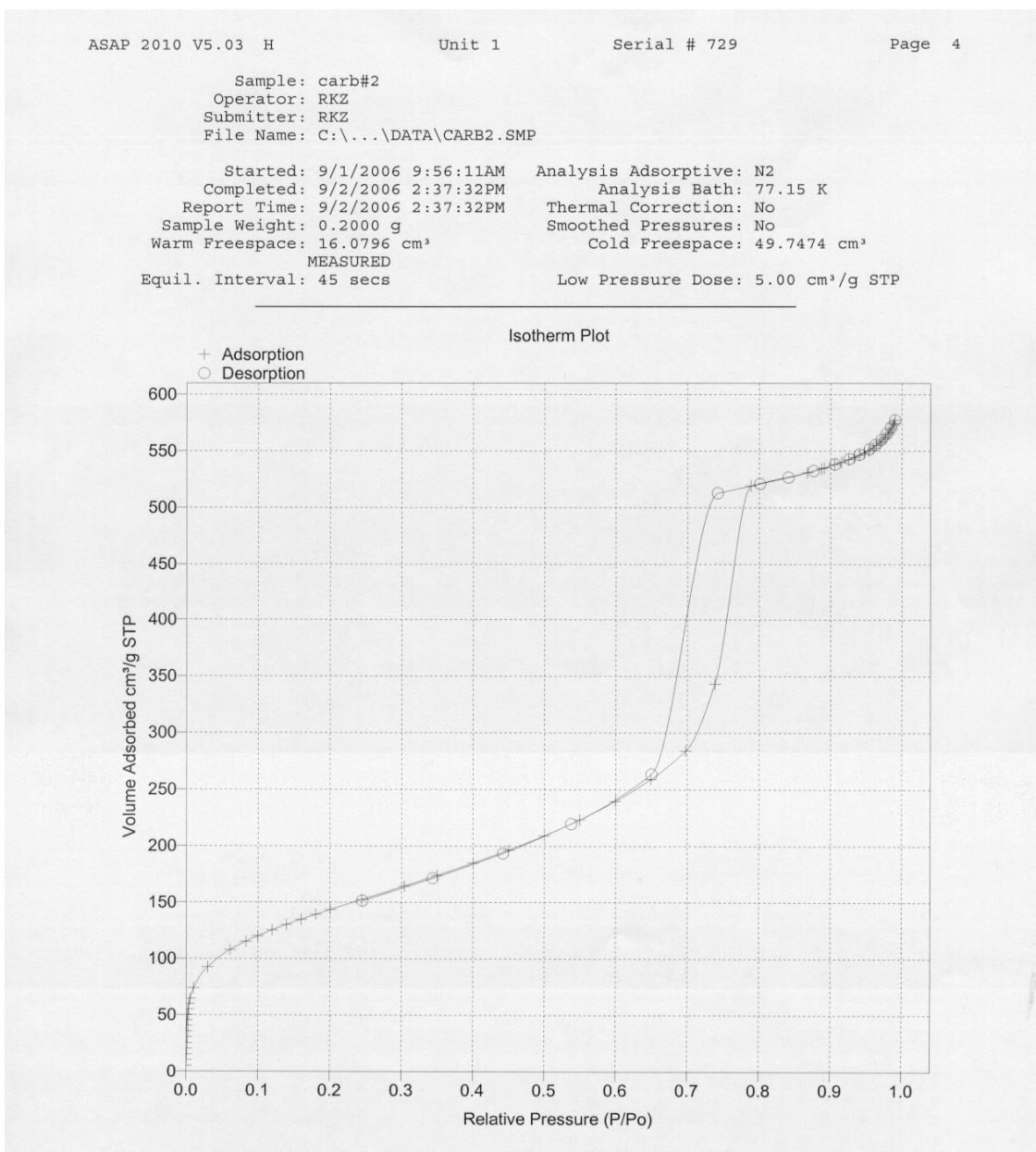
**Figure 3.12** TGA analysis of SBA-15-C.A.



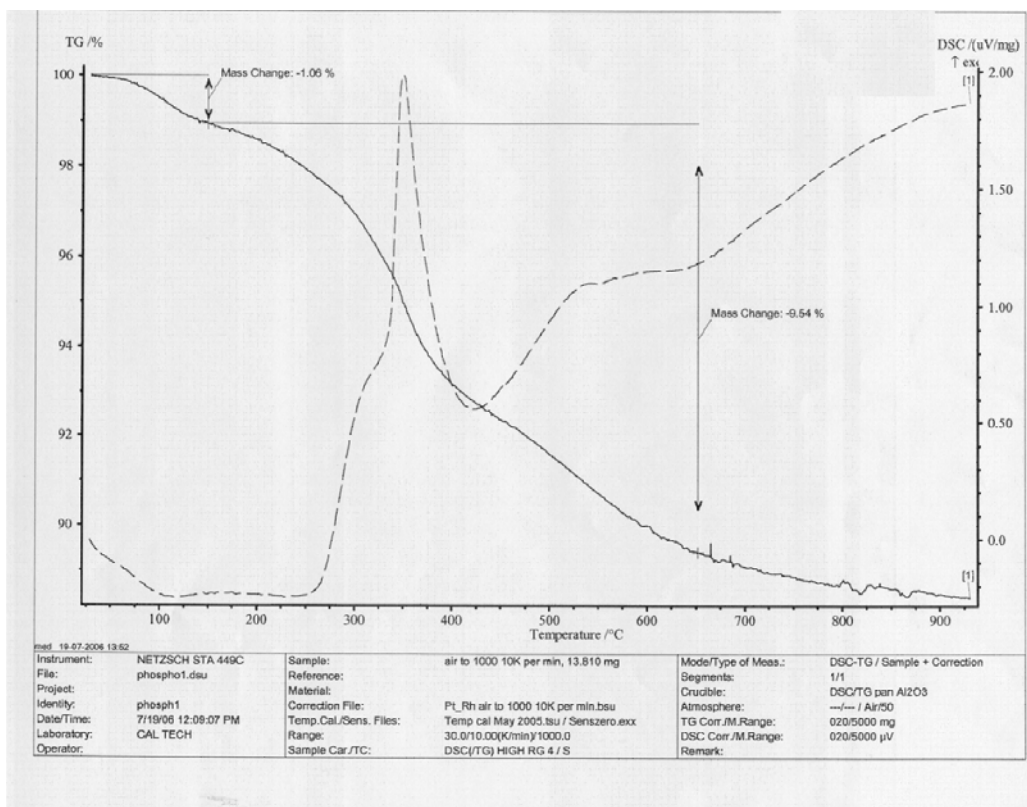
**Figure 3.13**  $^{29}\text{Si}$  solid state CP/MAS NMR of SBA-15-C.A.



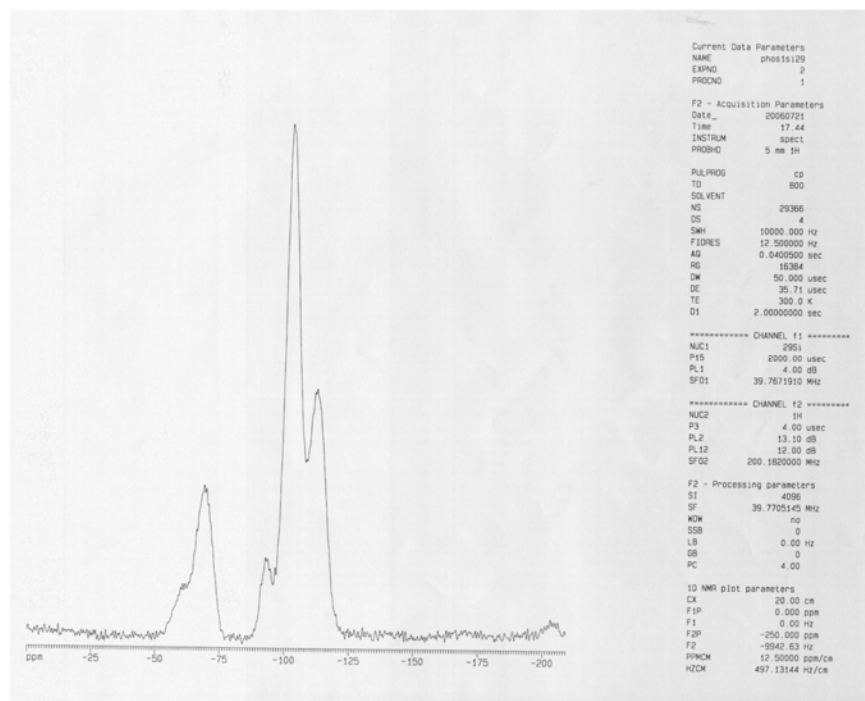
**Figure 3.14**  $^{13}\text{C}$  solid state CP/MAS NMR of SBA-15-C.A. Carbonyl shoulder may likely represent small amounts of carboxylate anion or anhydride on surface.



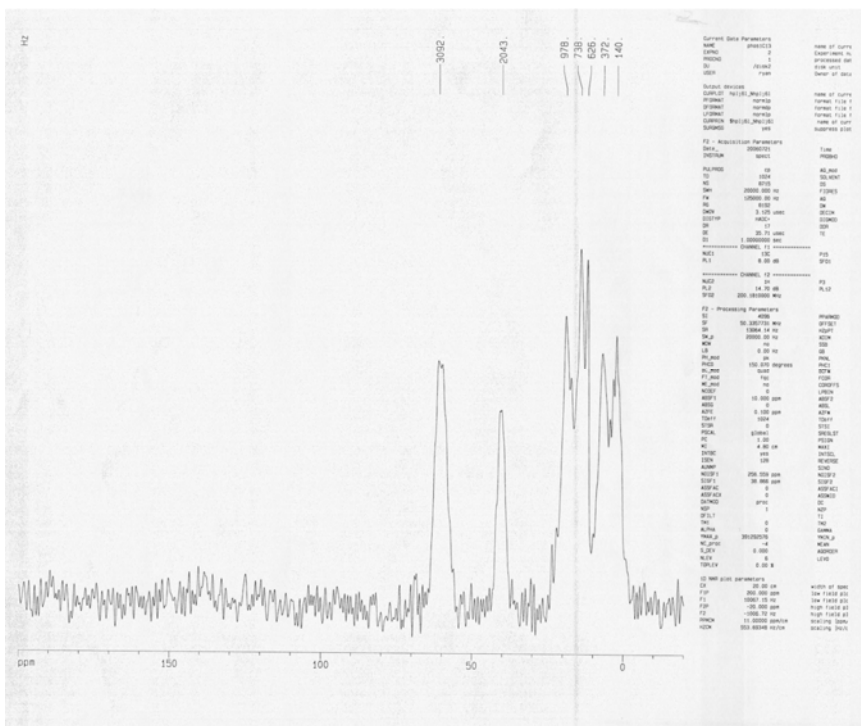
**Figure 3.15** N<sub>2</sub> adsorption isotherm of SBA-15-C.A. BET surface calculated of 496 m<sup>2</sup>/g and BJH desorption average pore diameter of 63 Å.



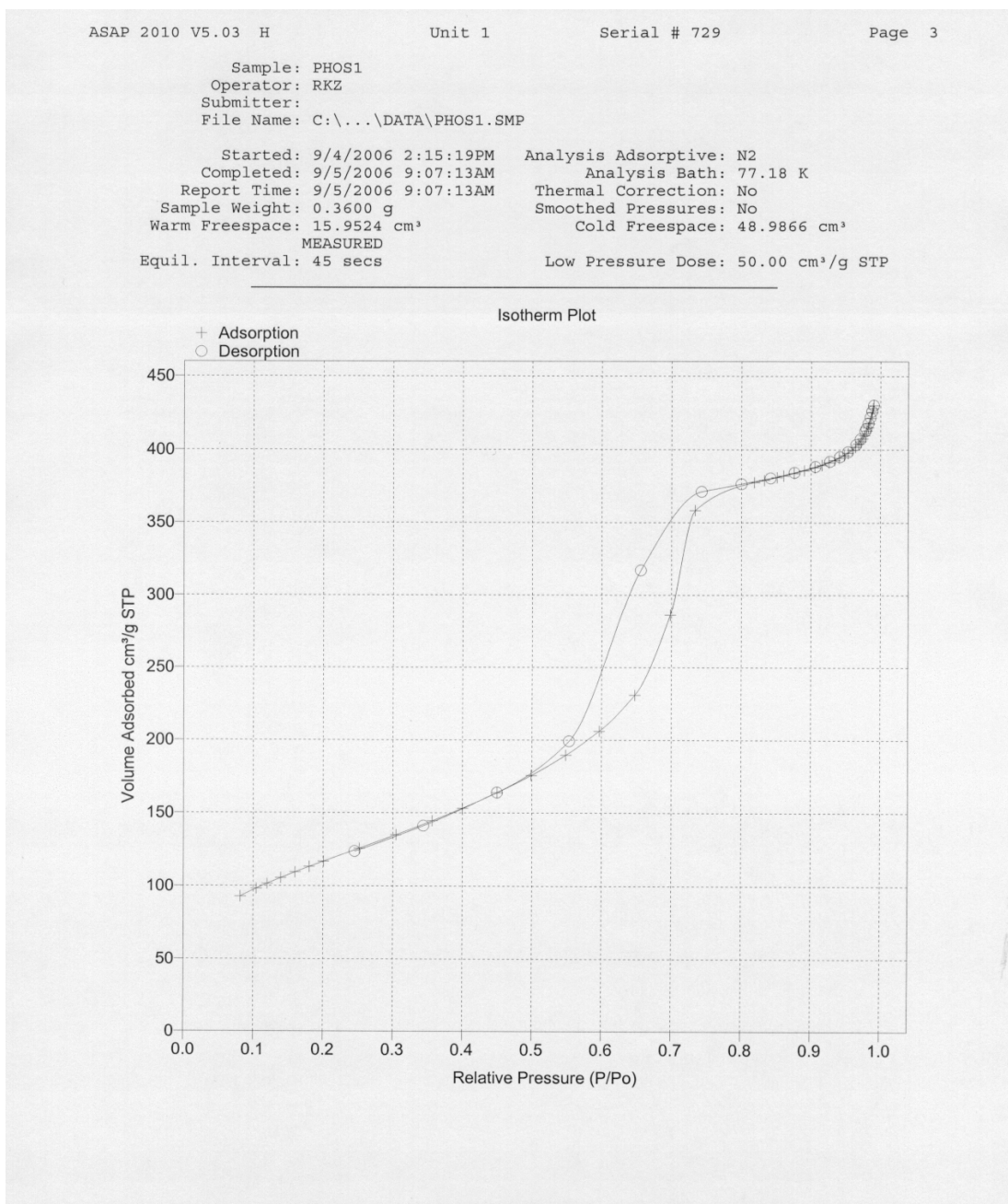
**Figure 3.16** TGA analysis of SBA-15-P.A.



**Figure 3.17**  $^{29}\text{Si}$  solid state CP/MAS NMR of SBA-15-P.A.



**Figure 3.18**  $^{13}\text{C}$  solid state CP/MAS NMR of SBA-15-P.A.



**Figure 3.19** N<sub>2</sub> adsorption isotherm of SBA-15-P.A. BET surface area of 426 m<sup>2</sup>/g with a BJH desorption pore diameter of 54 Å.

### 3.7 Experimental Section

**“One-pot” catalyst synthesis.** Siloxane starting materials were purchased from Gelest. Triblock copolymer poly(ethylene glycol)-block-poly(propylene glycol)-block-poly(ethylene glycol) P123 (4.0 g, 0.688 mmole, Mn 5800) was weighed into a teflon bottle. Then 2.0 M HCl (120.0 mL, 240.0 mmole) and H<sub>2</sub>O (6.0 mL, 333.0 mmole) were added and stirred at 40 °C until P123 fully dissolved. TEOS (8.2 mL, 37.8 mmole) was then added to the reaction and allowed to stir at 40 °C for 45 minutes pre-hydrolysis time. Then 2-(4-chlorosulfonylphenyl)-ethyltrimethoxysilane (0.65 g, 50/50 w/w solution in dichloromethane, 1.0 mmole) was added first to allow for hydrolysis of the sulfonyl chloride followed by 3-aminopropyltrimethoxysilane (0.19 mL, 1.0 mmole). The respective acid component was substituted for the sulfonyl chloride for the different acid functionalization. The mixture was then allowed to stir at 40 °C for 20 hr. It was then aged at 100 °C for 24 hr. The mixture was then cooled to RT and the resulting solid was filtered and rinsed with excess H<sub>2</sub>O repeatedly (4 x 500 mL). The solid was then allowed to dry overnight on an aspirating filter. The dried solid was then extracted with EtOH (400 mL per gram) by refluxing in EtOH for 24 hr to remove P123. The solid was again filtered and rinsed repeatedly with EtOH (4 x 500 mL), and then dried overnight on the aspirator to obtain a dry white solid. The solid was then further dried at 80 °C under vacuum for 24 hr. Solids were characterized by solid state NMR on a Bruker 200 MHz NMR using CP/MAS with spinning at 4 KHz. TGA analysis was carried out on the dry solids on a Netzsch STA 449C with a heating rate of 10°C/min. N<sub>2</sub> adsorption was carried out after drying the catalysts at 90 °C for 24 hours on a Micromeritics 2010



instrument. The organic loading per functional group of SBA-15-S.A was 0.55 mmole/g, for SBA-15-P.A. was 0.57 mmole/g, and for SBA-15-C.A. was 0.62 mmole/g. Characterization data for SBA-15-S.A. has already been reported.<sup>1</sup>

**Catalytic Experiments.** The following general procedure was used for the aldol condensation. 4-nitrobenzaldehyde (76 mg, 0.5 mmole) was dissolved in acetone (10 mL) and the respective catalyst was added (0.05 mmole total amines and/or acids). The reaction was then sealed under Ar and heated at 50 °C for 20 hr. The reaction was then filtered to remove the solid catalysts (washed with acetone and then chloroform (3x10 mL each). The filtrate was then concentrated in vacuo and the resulting product was analyzed by <sup>1</sup>H NMR in CDCl<sub>3</sub> with THF as an internal standard.

### 3.8 References

- [1] Fersht, Alan. *Structure and Mechanism in Protein Science*, 1999. W.H. Freeman. Chapter 2, pp. 54-58.
- [2] Silverman, Richard B. *The Organic Chemistry of Enzyme-Catalyzed Reactions*, 2000. Academic Press.
- [3] Zeidan, R. K.; Dufaud, V.; Davis, M. E. *J. Cat.* **2006**, 239, 299-306.
- [4] Bass, J. D.; Solovyov, A.; Pascall, A. J.; Katz, A. *J. Am. Chem. Soc.* **2006**, 128, 3737-3747.
- [5] Coutinko, D.; Madhugiri, S.; Balkus, K. J. *J. Porous Mater.* **2004**, 11, 239-254.
- [7] Bass, J. D.; Katz, A. *Chem. Mat.* **2006**, 18, 1611-1620.
- [8] Gelman, F.; Blum, J.; Avnir, D. *Angew. Chem.* 2001, **113**, 3759-3761; *Angew. Chem. Int. Ed.* 2001, **40**, 3647-3649
- [9] Voit, B. *Angew. Chem. Int. Ed.* **2006**, 45, 2-5.
- [10] Motokura, K.; Fujita, N.; Mori, K.; Mizugaki, T.; Ebitani, K.; Kaneda, K. *J. Am. Chem. Soc.* **2005**, 127, 9674-9675.
- [11] Helms, B.; Guillaudeu, S. J.; Xie, Y.; McMurdo, M.; Hawker, C. J.; Frechet, J. M. *J. Angew. Chem.* **2005**, 117, 6542-6545; *Angew. Chem. Int. Ed.* **2005**, 44, 6384-6387.
- [12] Huh, S.; Chen, H. T.; Wiench, J. W.; Pruski, M.; Lin, V. *Angew. Chem. Int. Ed.* **2005**, 44, 1826-1830; *Angew. Chem.* **2005**, 117, 1860-1864.
- [13] Alauzun, J.; Mehdi, A.; Reye, C.; Corriu, R. J. P. *J. Am. Chem. Soc.*, **2006**, 128, 8718-8719.

- [14] Zeidan, R.K.; Hwang, S.J.; Davis, M. E. *Angew. Chem. Int. Ed.* **2006**, *45*, 6332-6335.

**Chapter 4****Labeling Method for Cyclodextrins**

This chapter was reproduced in part with permission from Zeidan, et. al., *Bioconjugate Chemistry* 17, 1624-1626 (2006). Copyright 2006 American Chemical Society.

#### 4.1 Abstract

A method for installing a distinguishable label onto cyclodextrins or cyclodextrin-containing polymers is reported. Cyclodextrins (CD) and cyclodextrin-containing polymers are exposed to labeled ( $^2\text{H}$  or  $^{14}\text{C}$ ) ethylene oxide (EO) vapor and the alcohol groups on the CD ring open the EO to give ether-linked labeled methylenes and a terminal alcohol. This method provides for the incorporation of an easily tracked and quantified label without the use of solvents or purification steps. The method can be generalized for use with materials that contain nucleophiles other than alcohols, e.g., amines.

## 4.2 Introduction

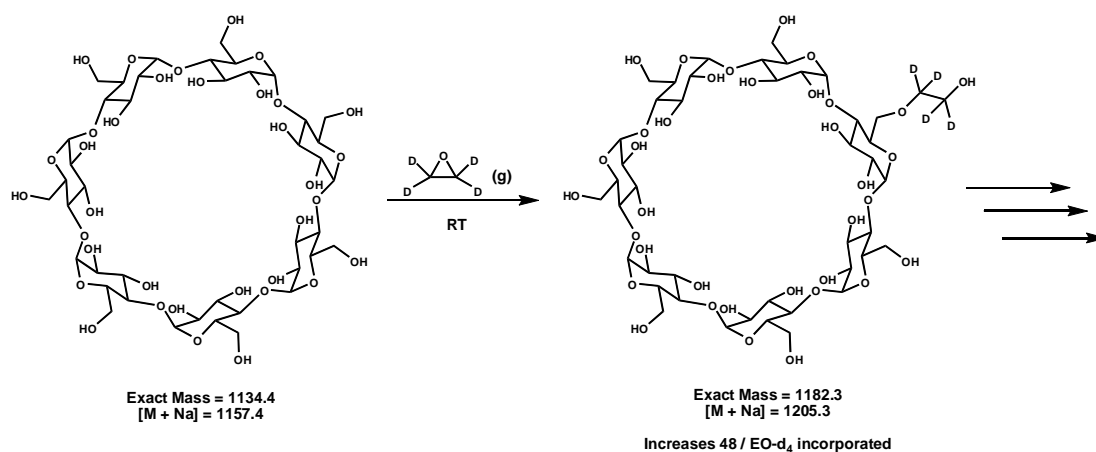
Cyclodextrin compounds have increasingly seen applications in a growing number of areas. Due to the unique structural, biological and chemical properties of these materials, cyclodextrins have been used for a number of purposes.<sup>1</sup> The pharmaceutical industry has taken advantage of the ability of cyclodextrins to form inclusion compounds to aid in solubility of small molecule therapeutics and the biocompatibility of cyclodextrins allows for their use in medicinal applications. Recently, polymeric materials bearing cyclodextrin monomers have been prepared for use as targeted drug delivery agents.

The ability to label cyclodextrins with a traceable and quantifiable functionality would aid in using cyclodextrins in bioavailability studies as well as allow for precise biodistribution studies.<sup>2</sup> A method that would achieve chemical modification of the cyclodextrin through a simple reaction with minimal effects on the chemical properties of the cyclodextrin would be ideal.

## 4.3 Results and Discussion

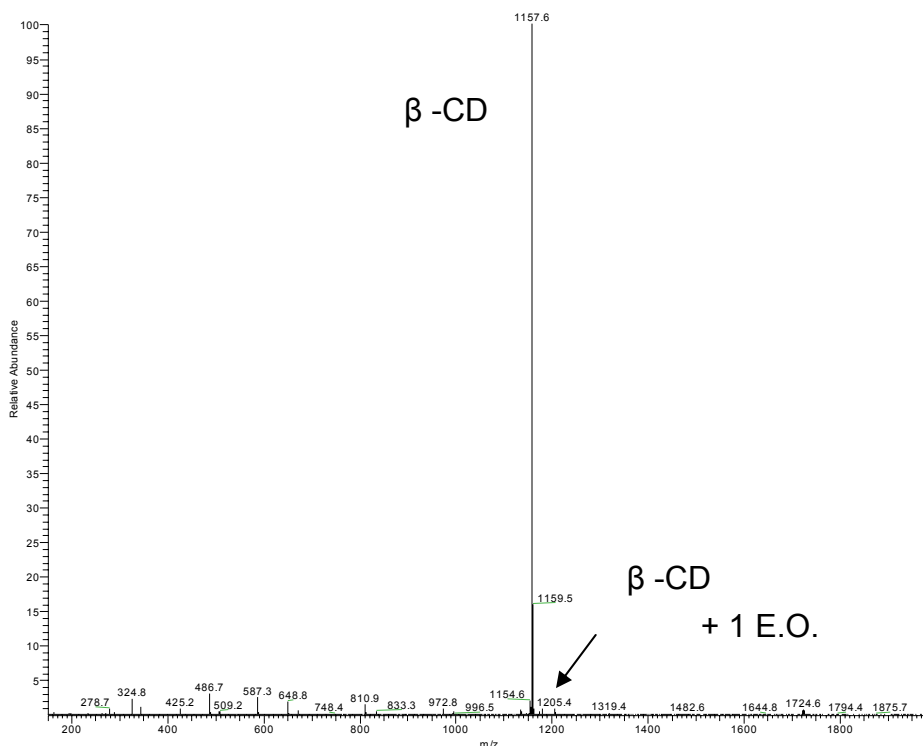
A simple method was envisioned that utilizes the reactivity between ethylene oxide and primary alcohols, as reported by LeMaistre and Seymour using aqueous ethylene oxide and reacting it with sucrose.<sup>3</sup> The carbohydrate nature of cyclodextrins with many reactive alcohol nucleophiles could allow for similar reactivity and incorporation of ethylene oxide into cyclodextrins.

The reaction with  $\beta$ -cyclodextrin was used as model system to test the application of this labeling method with cyclodextrin materials. Commercially available isotopically labeled d4-ethylene oxide was used as an ethylene oxide source in order to incorporate a simple label that could be observed through mass spectrometry. Importantly, radioactively labeled ethylene oxide could also be synthesized, allowing for simple extension of this method to radioactive labeling. Radioactive labeling has the advantage of being quantifiable and traceable when incorporated into a substance. Experiments were carried out in the simplest manner possible in order to create a simple labeling method, and reaction between cyclodextrin and ethylene oxide were carried out by exposing solid  $\beta$ -cyclodextrin to gas phase ethylene oxide without any solvent (Figure 4.1).



**Figure 4.1** Schematic of reaction of  $\beta$ -cyclodextrin with ethylene oxide-d4.

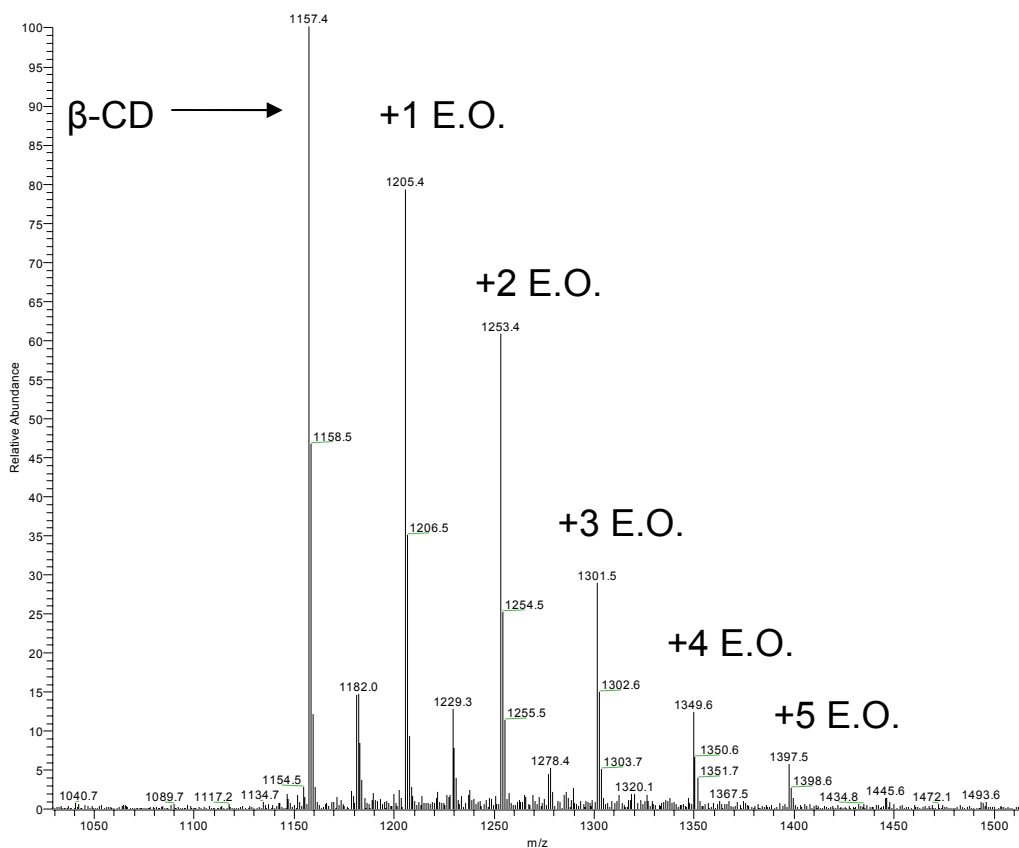
When  $\beta$ -cyclodextrin was treated with gas phase d4-ethylene oxide no reaction was observed (Figure 4.2). Presumably interactions with water carried by cyclodextrins were causing quenching of the labeled ethylene oxide and generating ethylene glycol.



**Figure 4.2** ESI/MS analysis of  $\beta$ -CD that was not dried and treated with EO-d<sub>4</sub>.

The same experiment was then carried out with  $\beta$ -CD that was dried at 100°C for 24 hours prior to use, and then treated with EO-d<sub>4</sub> for 5 minutes. It is clear that there are observable species in the mass spectrum that correspond to various levels of ethylene oxide incorporation into the  $\beta$ -CD (Figure 4.3). The parent peak at 1157.4 corresponds to  $[M+Na]$  for the parent  $\beta$ -CD. The corresponding peak for 1 addition of EO is at  $[M+Na] = 1205.4$ , and is clearly present. The corresponding peaks for 2, 3, 4, and 5 EO additions are also observed, as well as trace peaks corresponding to 6 and 7 additions at  $m/z$  of 1445 and 1493. The distribution of labeled products is also very clearly an exponentially decreasing trend as the  $m/z$  increases to values indicative of highly labeled species. By using shorter exposure time and lower reaction temperatures, less EO-d<sub>4</sub> is incorporated.

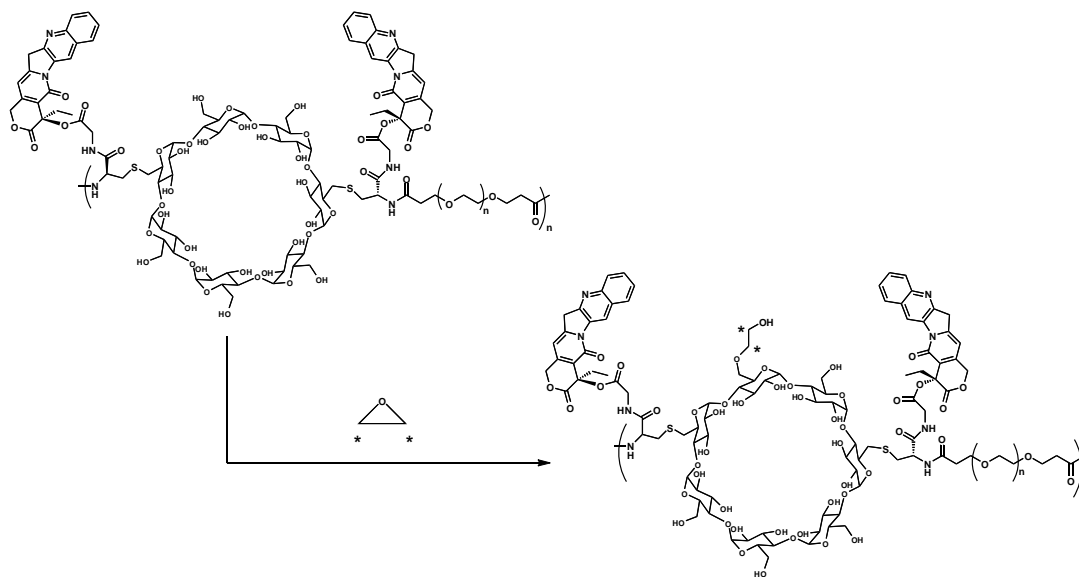




**Figure 4.3** ESI/MS analysis of labeled  $\beta$ -CD.

Having illustrated the reactivity between isotopically labeled ethylene oxide and cyclodextrins, it was desirable to extend the methodology to a traceable and quantifiable method taking advantage of this reactivity. Synthesis of  $^{14}\text{C}$  labeled ethylene oxide was carried out using  $^{14}\text{C}$  bromoethanol under basic conditions to generate the labeled ethylene oxide. This radioactively labeled ethylene oxide was then used to treat IT-101, a

cyclodextrin containing polymer conjugate of Camptothecin,<sup>4-7</sup> in order to incorporate the radioactive label (Figure 4.4).



**Figure 4.4** Schematic of radioactively labeled EO reaction with IT-101.

The labeled IT-101 contained 1.01 mCi/mg of radioactivity that corresponds to ca. 1.5 EO molecules added per polymer chain. The labeling was performed in the absence of solvents on the polymer conjugate, and when the “hot” IT-101 is dissolved in water it forms particles with average size of 43 nm (analysis was performed by The Southwest Research Institute). This size is consistent with published data of IT-101 that are not radiolabeled.<sup>4-7</sup> These data suggest that substantial levels of radiolabel can be incorporated into IT-101 and its properties are not significantly modified from the parent compound.

A TLC analysis was done to ensure that there was no ethylene glycol caused by the quenching of EO with residual water in the labeled polymer. It was of significance to

illustrate the lack of radiolabeled ethylene glycol in the labeled polymer to ensure that false results were not obtained due to ethylene oxide impurities (Figure 4.5).

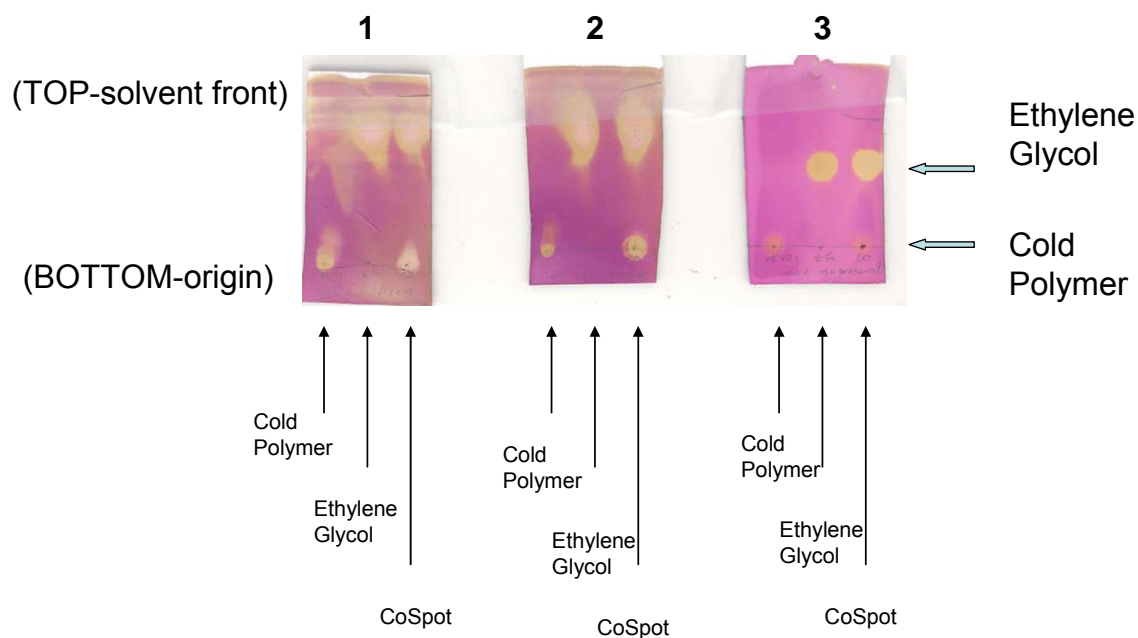


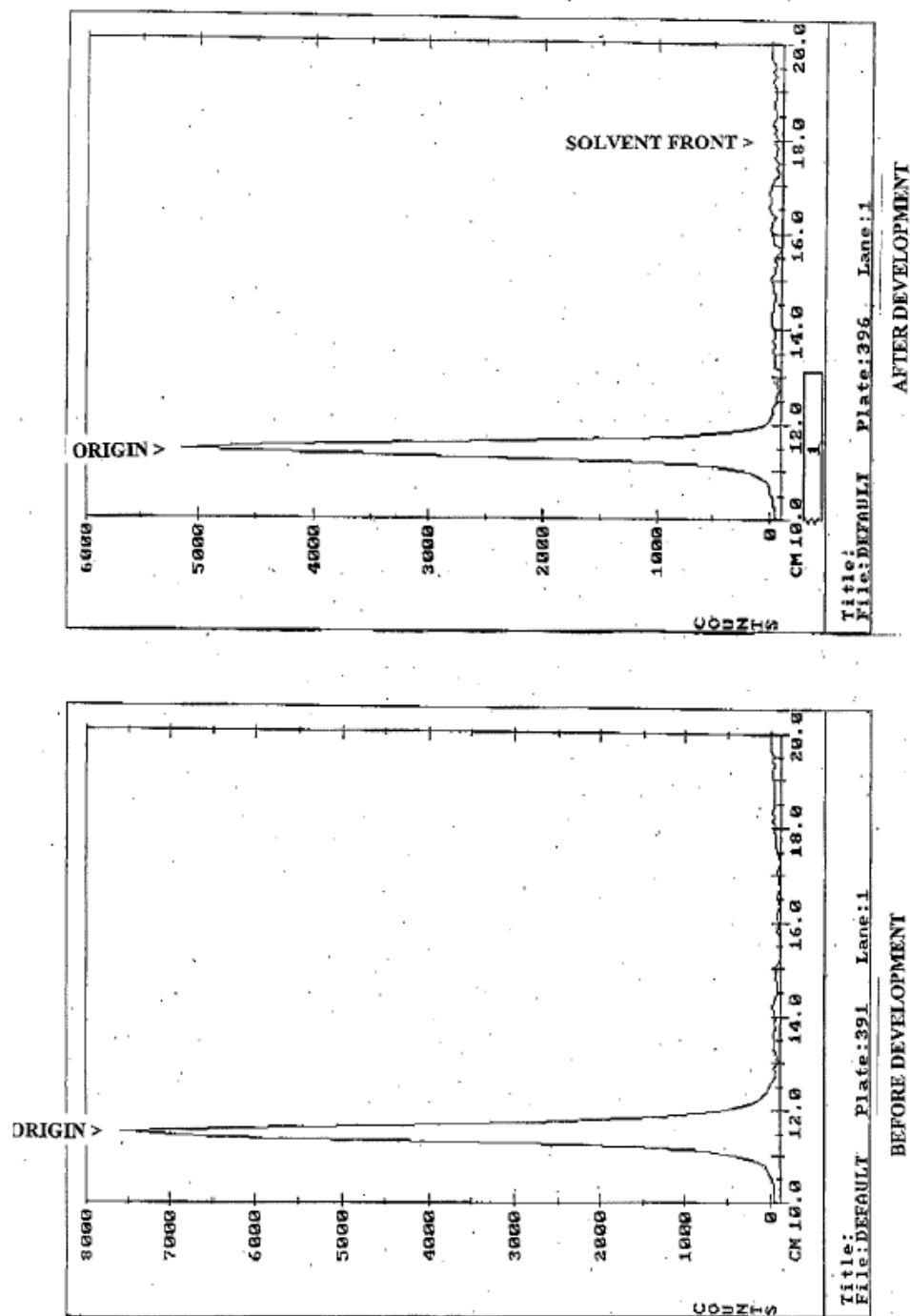
Plate **1** was run in 40%H<sub>2</sub>O:60% MeCN

Plate **2** was run in 10%H<sub>2</sub>O:90% MeOH

Plate **3** was run in 100% Isopropanol

**Figure 4.5** TLC analysis of labeled polymer.

Corresponding TLC analysis was carried out using the radioactively labeled polymer with a radioscan detector in order to ensure no radioactive impurities remained in the labeled polymer before use in animal studies (Figure 4.6).



FY6, [14C]  
 Lot# 116-089-000  
 Silica gel plate; 100% Isopropanol

**Figure 4.6** Radioscan of TLC plate with  $^{14}\text{C}$  ethylene oxide reacted IT-101.

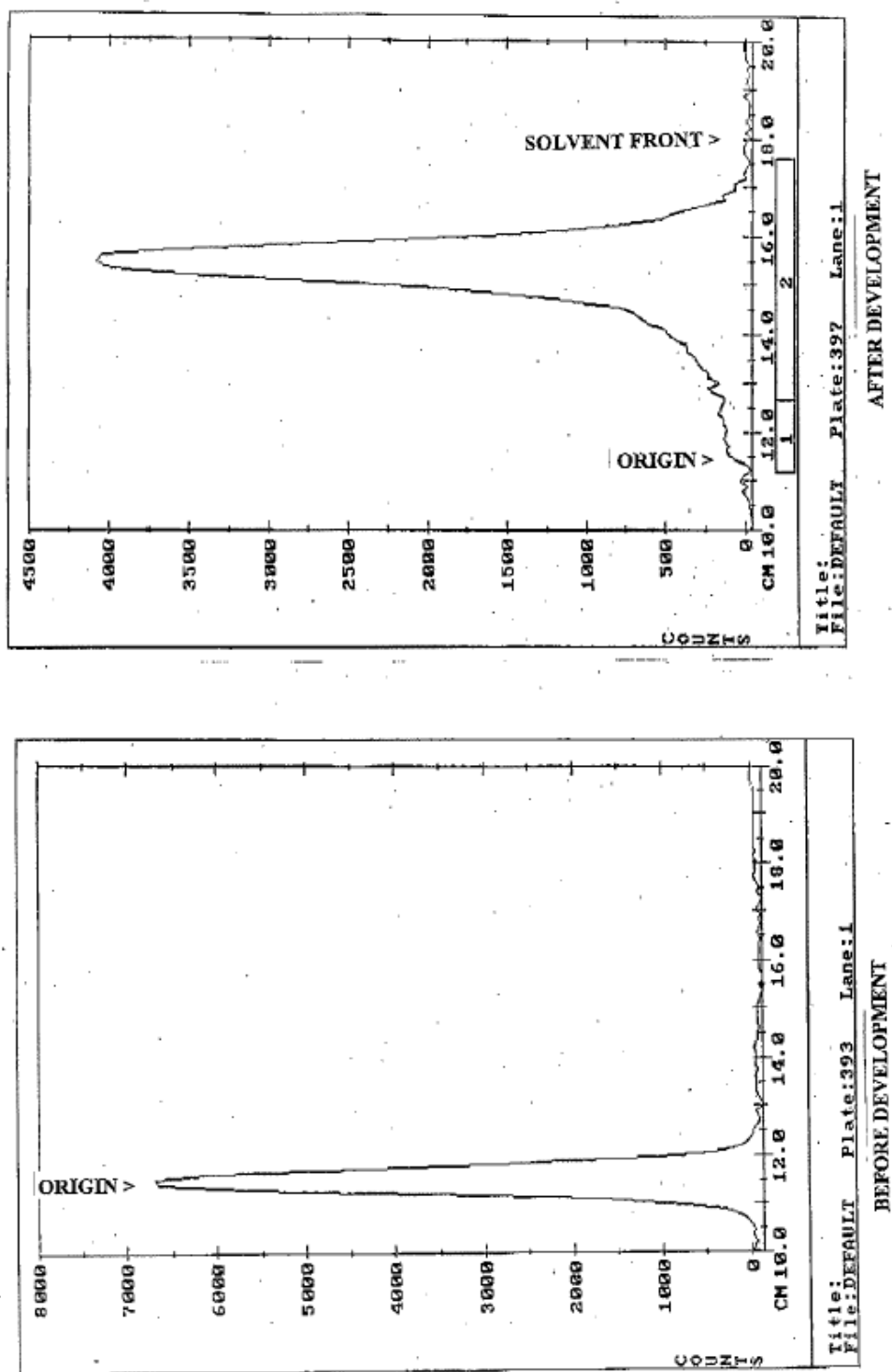


Figure 4.7 Radioscan of TLC plate with  $^{14}\text{C}$  ethylene glycol.

These radioscan illustrated the lack of ethylene glycol impurities in the radiolabeled polymers. Animal studies using radiolabeled IT-101 are in progress and will be reported at a later time.

#### 4.4 Experimental Section

**General.** Deuterated ethylene oxide was obtained as a gas from Sigma Aldrich.  $\beta$ -cyclodextrin was obtained from Wacker.

**Labeling with ethylene oxide-d4.**  $\beta$ -cyclodextrin (50 mg) was dried at 100°C under vacuum for 12 hours overnight in order to completely remove residual water (water reacts with ethylene oxide to form ethylene glycol if not removed). After drying, the solid  $\beta$ -cyclodextrin sample was then allowed to cool to RT. The lecture bottle with ethylene oxide-d4 was then attached to the reaction flask and gas was flowed over the material for 2 minutes at 17 psi. The reaction vessel was then placed under vacuum to remove unreacted ethylene oxide-d4. The resulting white solid was then analyzed by ESI-MS to test for EO incorporation. Deuterium NMR experiments were performed also to confirm the presence of the EO incorporation.

**Labeling with  $^{14}\text{C}$  ethylene oxide.** The cyclodextrin-containing polymer conjugate of camptothecin, IT-101<sup>4-7</sup> (1.6 g), was reacted with 1 mmol ethylene oxide [ $1,2\text{-}^{14}\text{C}$ ], 50 mCi/mmol, under anhydrous conditions. Ethylene oxide, [ $1,2\text{-}^{14}\text{C}$ ] was generated from bromoethanol, [ $1,2\text{-}^{14}\text{C}$ ] under basic conditions, dried and vacuum transferred into a 50

mL glass pressure vessel containing IT-101. The resultant mixture, at approximately 0.5 atm, was allowed to incubate for four days. The excess ethylene oxide, [1,2-<sup>14</sup>C] was removed by vacuum transfer and no further work-up was performed. The specific activity was measured by gravimetric assay to be 1.01 uCi/mg. Yield 1440 uCi, remaining a light yellow solid.

## 4.5 References

- [1] Davis, M.E.; Brewster, M.E. *Nat. Rev. Drug. Disc.* **2004**, *3*, 1023-1035.
- [2] Beumer, J.H.; Beijnen, J.H.; Schellens, J.H. *Clin. Pharmacokinet.* **2006**, *45*, 33-58.
- [3] LeMaistre, J. W.; Seymour, R. B. *J. Org. Chem.* **1948**, *13*, 782-785
- [4] Cheng, J.J., Khin, K.T., Jensen, G.S., Liu, A., and Davis, M.E. *Bioconj. Chem.* **2003**, *14*, 1007-1017.
- [5] Cheng, J.J.; Khin, K.T.; Davis, M.E. *Mol. Pharm.* **2004**, *1*, 183-193.
- [6] Schluep, T.; Cheng, J.J.; Kim, K.T.; Davis, M.E. *Cancer Chemother. Pharmacol.*, **2006**, *57*, 654-662.
- [7] Schluep, T.; Hwang, S.J.; Cheng, J.J.; Heidel, J.D.; Bartlett, D.W.; Davis, M.E. *Clin. Cancer Res.* **2006**, *12*, 1606-1614.



## **Chapter 5**

### **Design of a Polymer with Dual-fold Mechanism of Degradation**

## 5.1 Abstract

A new method of synthesizing materials that have a dual-control method of decomposing is described. Compounds containing an aromatic disulfide group can be photolyzed at 260 nm to generate sulfur radicals that quickly recombine. However, in the presence of a second stimulus, in this case hydrogen peroxide, the resulting radicals can be trapped by oxidation to a sulfonic acid species that causes a permanent splitting of the disulfide. This report demonstrates the use of this technique to split two different disulfide monomers as well as the synthesis of some unique polymers containing this functional group.

## 5.2 Introduction

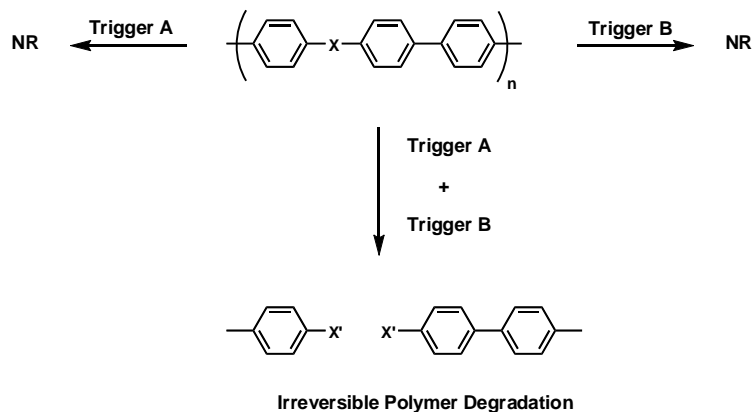
A variety of polyamide polymers have been synthesized for a number of different applications. The most widespread polyamides would have to be the Kevlar class of aramids<sup>1</sup> produced by the DuPont Chemical Company. These polymers exhibit a number of interesting properties, including incredible strength properties leading to their widespread use as a bulletproof vest material. These polyamides have incredible strength for a number of reasons, such as the rigid amide backbone, hydrogen bonding interactions between amides, and pi-pi stacking interactions. The properties allow for fibers to be extruded with a variety of physical characteristics that allow for their use in a number of applications, such as incorporation into clothing.

A number of synthetic challenges exist in preparing polyamide polymers,<sup>2</sup> and these difficulties greatly delayed the preparation and industrial application of these materials. The polarity of these amide rich polymers caused significant solubility issues, especially in polymers prepared with hydrophobic monomers such as hexamethylene or phenyl, and solvents such as 30 wt. % sulfuric acid were required to dissolve and manipulate these polymers. These solvents were not only expensive and extremely dangerous to work with on large scale syntheses, but also were very corrosive to most processing equipment preventing industrial preparation. A number of methods were designed to get around these limitations and allow for large scale preparation of polyamides, thus allowing for their widespread use industrially. For example, a very polar amine solvent, NMP, was found to be suitable for manipulating polyamides and provided an alternative to strong acid solvents. Importantly, this solvent is much less caustic and compatible with extrusion and processing equipment. Secondly, the addition of salts ( $\text{CaCl}_2$ ) in the NMP

solution of polyamide was found to disrupt hydrogen bond formation between polymer strands increasing the solubility of these very polar polymers and allow for fiber formation at higher concentration solutions of polymer, aiding in the ability to efficiently form large diameter fibers. These methods allow for simplified formation of polyamide polymers and revolutionized this area of polymer synthesis.

Characterization challenges<sup>2</sup> also complicate the preparation and utilization of these polymers in a number of applications. Solubility issues prevent the use of mass spectrometry methods such as electrospray or MALDI to characterize the molecular weight of these polymers. Similarly, these solubility issues preclude the use of gel permeation chromatography to determine the MW of the polymers.

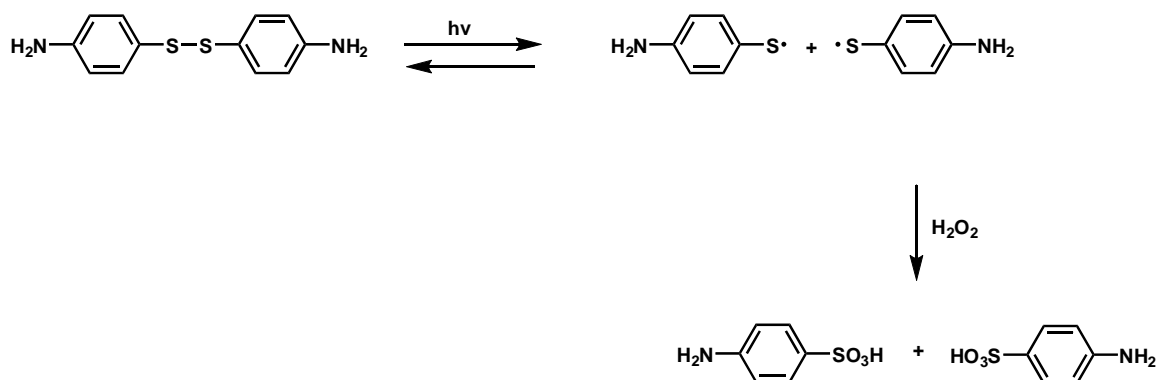
A polymer bearing a functional group that can be degraded under very precise reaction conditions could be useful for a number of applications, such as adhesives that could be readily degraded or medical fibers with a well defined degradation pathway. In designing a polymer that would have a very precise degradation mechanism, an approach that incorporates a degradation mechanism triggered by two independent stimuli only when applied simultaneously would have a number of advantages. By incorporating a mechanism that requires two simultaneous triggers, undesirable degradation by incident application of one trigger would be avoided, such as in a photodegradable polymer (Figure 5.1).



**Figure 5.1** Design of a dual trigger degradable polymer.

Important properties of these simultaneous triggers would be their orthogonality as well as mutual compatibility (i.e., could not use destructive methods such as oxidants with reductants) and very fast reactivity. Suitable triggers would include photochemical reactions, electrochemical reactions, and chemically activated reactions. Ideally, these triggers alone would cause no decomposition of the polymer and only bring about degradation when used in combination. Other desirable properties would include non-harmful and biologically compatible triggers (non-toxic or poisonous reagents) and the production of harmless by-products upon degradation.

An approach to preparing dual-trigger degradable polymers is outlined below in Figure 5.2. It has been reported that aromatic disulfide compounds bearing para-amino substituents can be homolytically split into two sulfur radicals upon irradiation at 260 nm.<sup>3</sup> These radicals then rapidly recombine on the order of femtoseconds to regenerate the parent disulfide. This property may be utilized in designing a two-trigger degradation mechanism and this first trigger would be photolytic.



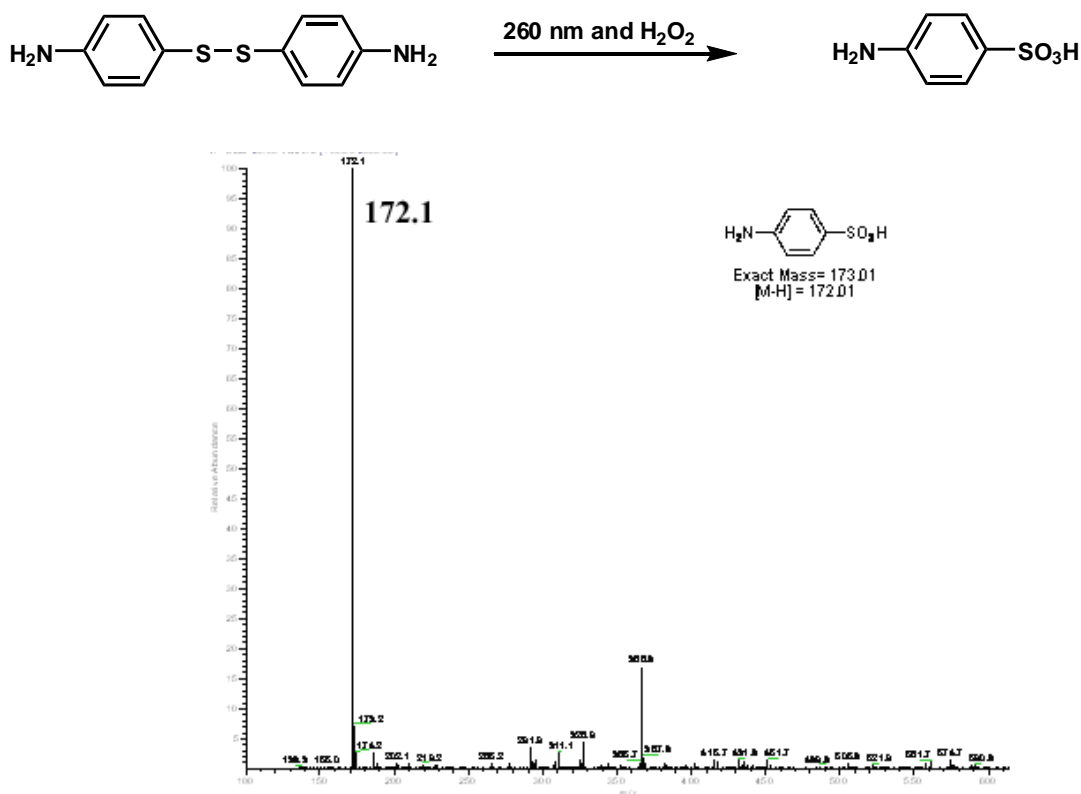
**Figure 5.2** Disulfide cleavage and possible oxidation.

As shown in Figure 5.2, if it were possible to irradiate the aromatic disulfide in the presence of hydrogen peroxide, it could be possible to trap the formed sulfur radicals and carry out an in situ oxidation to sulfonic acids, irreversibly cleaving the disulfide linkage. This approach would have the desirable property that neither trigger alone would lead to polymer cleavage, and both triggers are biocompatible reagents. Also of importance, the aromatic disulfide para-amino groups provide a handle for incorporating this monomer into a variety of polymer materials.

### 5.3 Results and Discussion

In order to test the feasibility of this in situ oxidation approach, a model study was carried out using the simple 4,4'-aminodiphenyl disulfide monomer as a substrate. This compound was dissolved in an acetonitrile solution with 15% hydrogen peroxide and irradiated at 260 nm for 2 minutes. The solution was then examined to detect oxidation

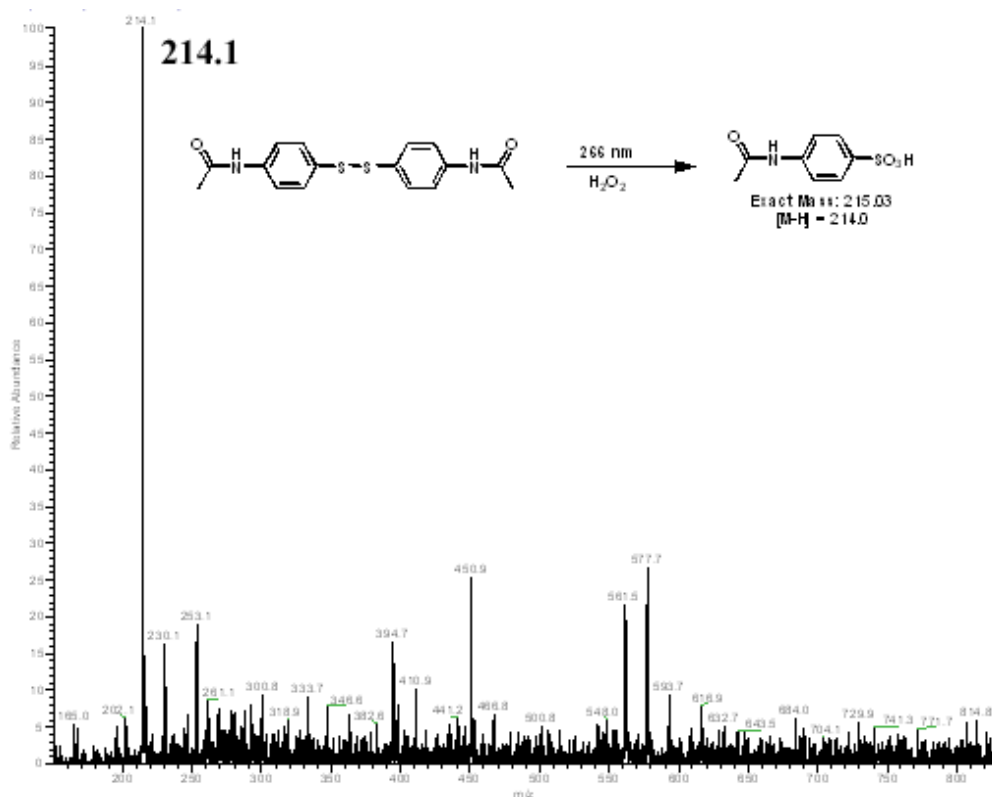
product and ESI/MS analysis clearly shows quantitative cleavage of the disulfide to the aromatic sulfonic acid cleavage product (Figure 5.3).



**Figure 5.3** Model system for degradation.

The most direct method of incorporating this disulfide monomer into a polymeric material would be through reaction with the para-amino groups. A variety of linkages could be envisioned, and a very simple approach would be to use these amines to form amide linkages by reacting with carboxylic acids or acid chlorides to form polyamide polymers. However, by converting the amines into amides, the electronics of the

aromatic ring would be greatly altered, potentially affecting formation of the sulfur radicals upon irradiation. In order to test the effect of forming amides at the para position, a model compound was prepared in which the amines are amide protected with acetamide groups (Figure 5.4). As illustrated below, when this model compound was treated with identical reaction conditions as the unprotected monomer, quantitative cleavage to the sulfonic acid was also observed in 2 minutes.

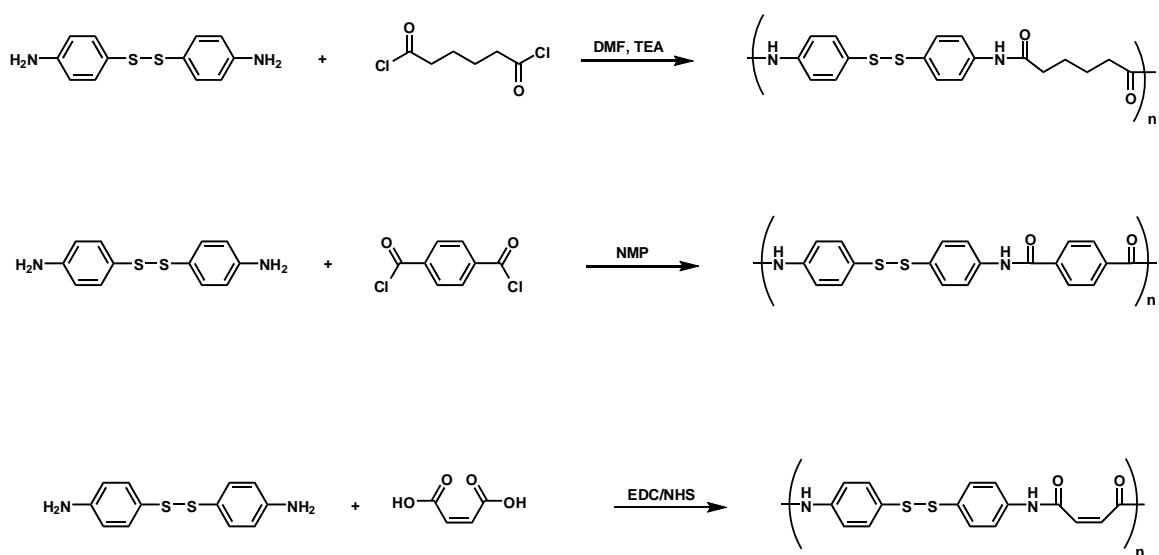


**Figure 5.4** Acetate protected monomer degradation.

Having demonstrated the tolerance for amides in this cleavage mechanism, this monomer was then used in a variety of syntheses towards preparing polyamides containing this disulfide as one monomer with a number of di-carboxylic acids as the other monomer. A number of strategies were examined towards this end, and

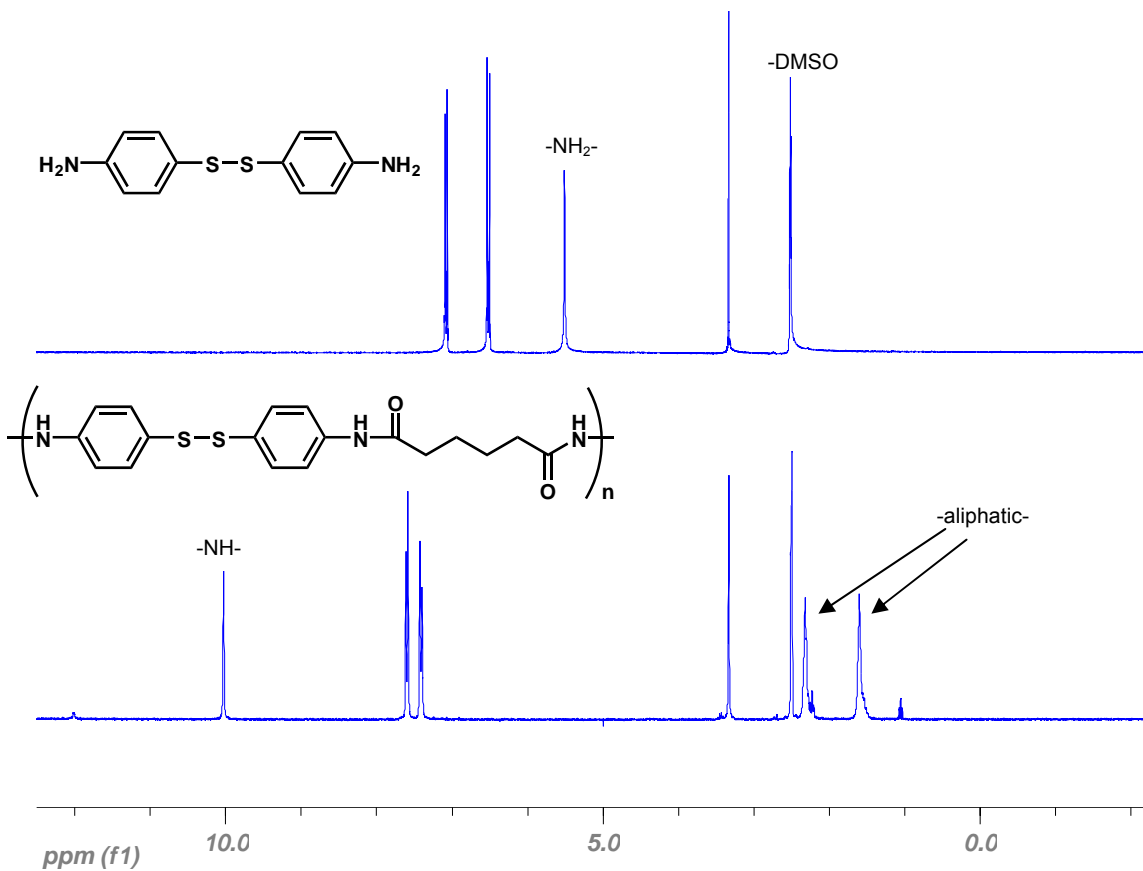


synthetically this approach presented difficulties. Solubility of the monomer was a limiting factor in attempting interfacial polymerizations such as those employed in the synthesis of 6,6-nylon. A number of peptide coupling conditions were attempted without success towards preparing polymers containing this monomer. Fortunately, changing the approach to utilize reactivity with acid chlorides in DMF or NMP solvents was effective at preparing polymers of this type (Figure 5.5).



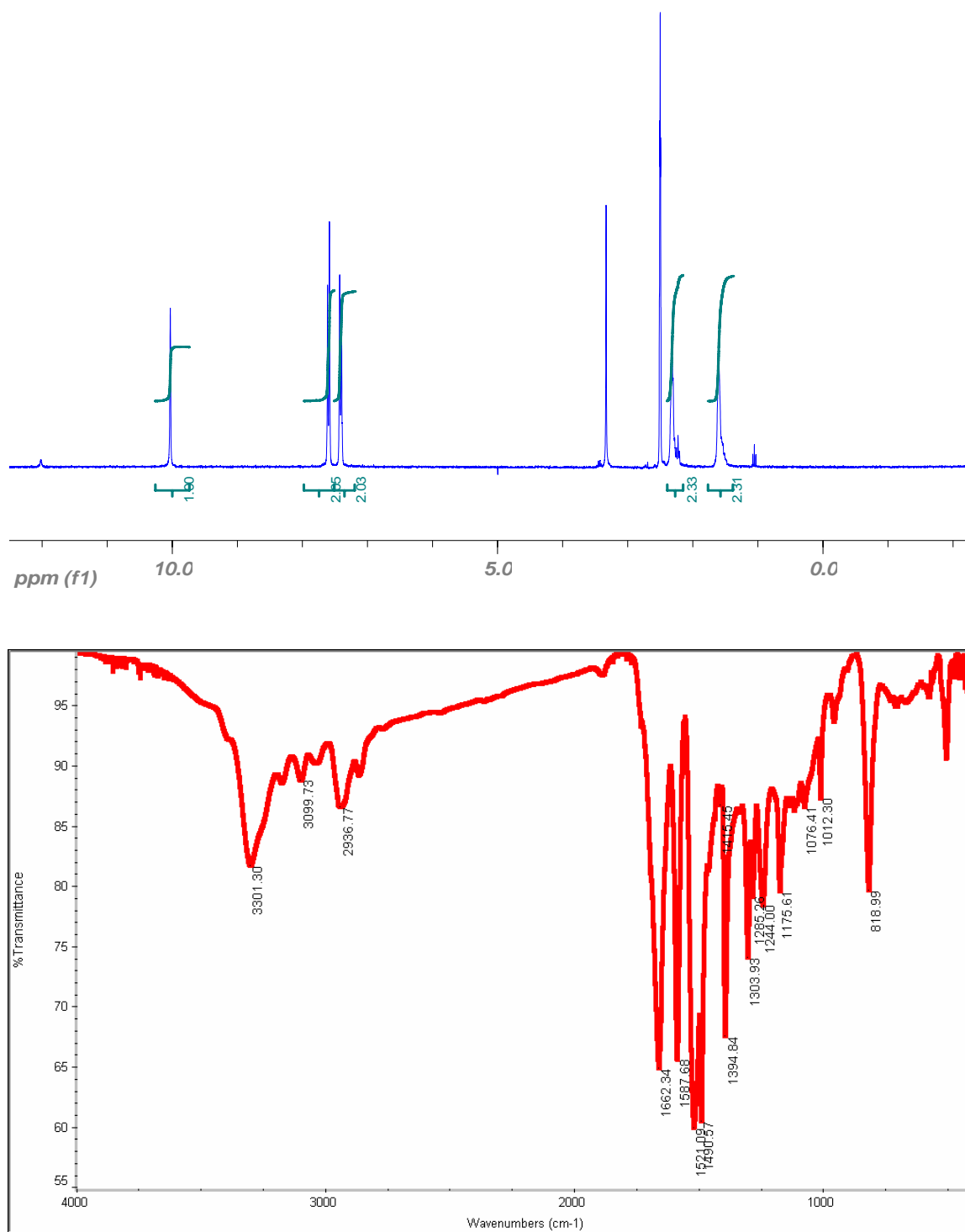
**Figure 5.5** Polyamide preparation.

These polymers were characterized by  $^1\text{H}$  NMR analysis as shown below in Figure 5.6. The chemical shift of the aromatic rings changed dramatically upon polymerization, due to conversion of anilines to amides, and clearly exhibited conversion of the monomer as shown below.

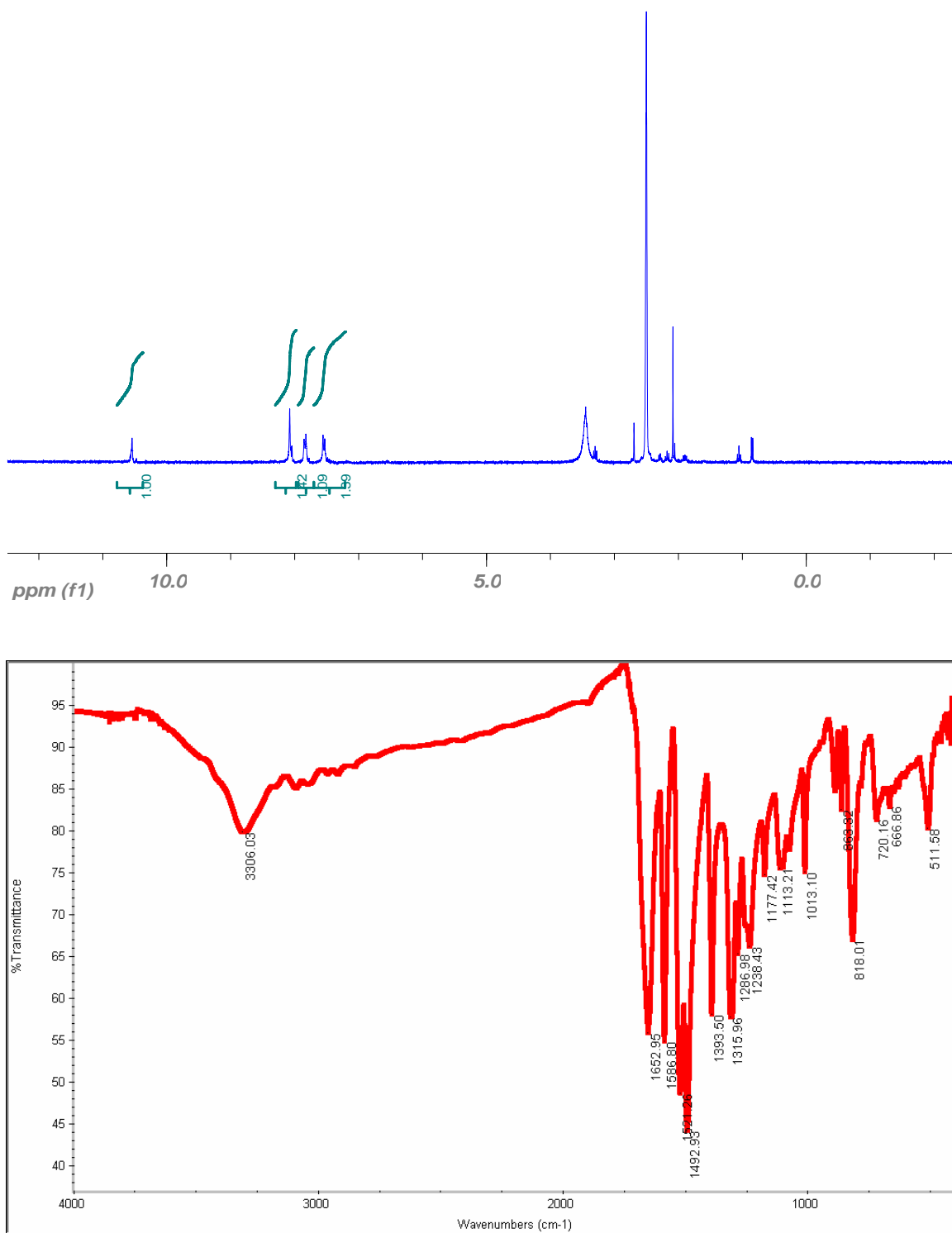


**Figure 5.6**  $^1\text{H}$  NMR analysis of polyamide.

Analogously,  $^1\text{H}$  NMR analysis was carried out for the remaining polyamides, as well as IR analysis to observe the formation of amide bonds. Each of the prepared polymers demonstrated full conversion of the monomer as indicated by complete shift of the aromatic region, and very little end group was detected, an indication of high molecular weight polymers.



**Figure 5.7**  $^1\text{H}$  NMR and IR analysis of polymer 2.



**Figure 5.8**  $^1\text{H}$  and IR analysis of polymer 3.

Numerous attempts were made at determining the molecular weight of these polymers more precisely using mass spectrometry. Due to the limited solubility of the polymers in salt-free solutions (necessary for MALDI analysis), molecular weight values were not achievable using MALDI/TOF. Solutions prepared in NMP, owing to its non-volatility, were not able to fly under the measurement conditions. GPC determination of MW was also not achievable as NMP mobile phase is destructive towards GPC column beds. The  $^1\text{H}$  NMR serves as the only indication of molecular weight and indicates that these polymers are of high MW.

The possibility of preparing a polymer with a dual-trigger method of degradation has been summarized. Proof-of-principle experiments were carried out using the monomer 4,4-aminophenyl disulfide as well as the acetamide protected variant and illustrated the ability of this disulfide to be photolyzed to sulfur radicals followed by in situ oxidation of the radicals to sulfonic acids, leading to irreversible monomer cleavage in both cases. The incorporation of this monomer into a number of polymers was also illustrated using very specialized conditions designed for such high polarity materials.

## 5.4 Experimental Section

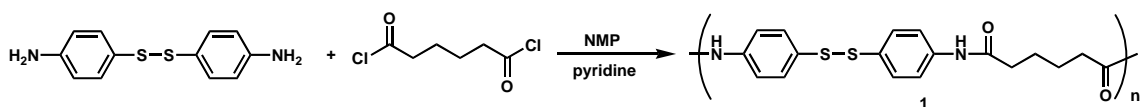
**Degradation of 4-aminophenyl-disulfide monomer.** A 2 mM solution of 4-aminophenyl-disulfide was prepared in acetonitrile. 0.7 mL of this solution was then placed in a Starna quartz cuvette. To this solution was added 0.5 mL of a 15 wt%  $\text{H}_2\text{O}_2$  solution followed by irradiation with 266 nm light for 1 min with mixing. The solution was then analyzed by mass spectrometry which showed formation of the degraded

sulfonic acid. HPLC trace also illustrates product fully degraded. Mass spectrum confirms degradation of the 4-aminophenyl disulfide monomer to the corresponding aminobenzene sulfonic acid.

**Preparation of 4-amidophenyl-disulfide.** To a solution of 4-aminophenyl-disulfide (2.48 g, 9.99 mmole) in toluene (150 mL) was added excess acetic anhydride (1.9 mL). The resulting solution was heated at 130 °C for 1 hour. Cooled reaction to RT and a white solid precipitate formed. Collected solid by filtration, washed with toluene (3x100 mL) and dried under vacuum to obtain 4-amidophenyl-disulfide in 85% yield (2.8 g). <sup>1</sup>H NMR (300 MHz, DMSO-d<sub>6</sub>): δ 10.06 (s, 2H), 7.58 (d, 4H), 7.42 (d, 4H), 2.04 (s, 6H). <sup>13</sup>C NMR (300 MHz, DMSO-d<sub>6</sub>): δ 168.46, 139.50, 130.13, 129.31, 119.64, 23.99.

**Degradation of 4-amidophenyl-disulfide.** A 0.2 mM solution of 4-amidophenyl-disulfide in acetonitrile was prepared. To 0.7 mL of this solution in a quartz cuvette was added 0.5 mL 15 wt% H<sub>2</sub>O<sub>2</sub>. This solution was then irradiated at 266 nm for 1 min with mixing. The resulting solution was analyzed by HPLC and by mass spectrometry, which confirmed degradation of the 4-amidophenyl-disulfide.

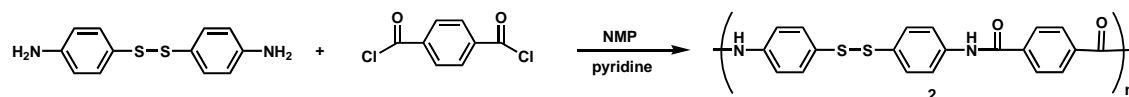
#### Synthesis of adipic dichloride polymer analog (1).



To 4-aminophenyl-disulfide (0.75 g, 3.0 mmole) was added NMP (17.5 mL) and pyridine (50 uL). This solution was stirred until fully dissolved. To this was then added adipic dichloride (0.44 mL, 3.0 mmole). The resulting solution was stirred for 6 hours at room temperature under Ar. The reaction mixture was then poured into excess EtOH (100 mL) and a white solid immediately precipitated. The white solid was collected by

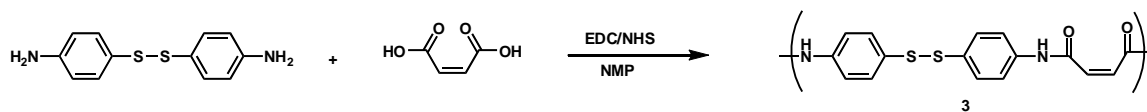
filtration, washed with boiling EtOH (3 x 100 mL) and then dried under aspirator for 12 hours. The solid product was then collected and dried under vacuum for another 12 hours. 821 mg of **1** was obtained as a solid white powder after drying. Product was characterized by <sup>1</sup>H NMR in DMSO-d<sub>6</sub> and by infrared analysis (KBr pellet).

### Synthesis of terephthalic dichloride analog (**2**).



To 4-aminophenyl-disulfide (0.75 g, 3.0 mmole) was added NMP (17.5 mL) and pyridine (50 uL). This solution was stirred until fully dissolved. To this was then added terephthalic dichloride (0.61 g, 3.0 mmole). The resulting solution was stirred for 6 hours at room temperature under Ar. The reaction mixture was then poured into excess EtOH (100 mL) and a white solid immediately precipitated. The white solid was collected by filtration, washed with boiling EtOH (3 x 100 mL) and then dried under aspirator for 12 hours. The solid product was then collected and dried under vacuum for another 12 hours. 1.05 g of **2** was obtained as a solid white powder after drying. Product was characterized by <sup>1</sup>H NMR in DMSO-d<sub>6</sub> and by infrared analysis (KBr pellet).

### Synthesis of conjugated olefin analog (**3**).

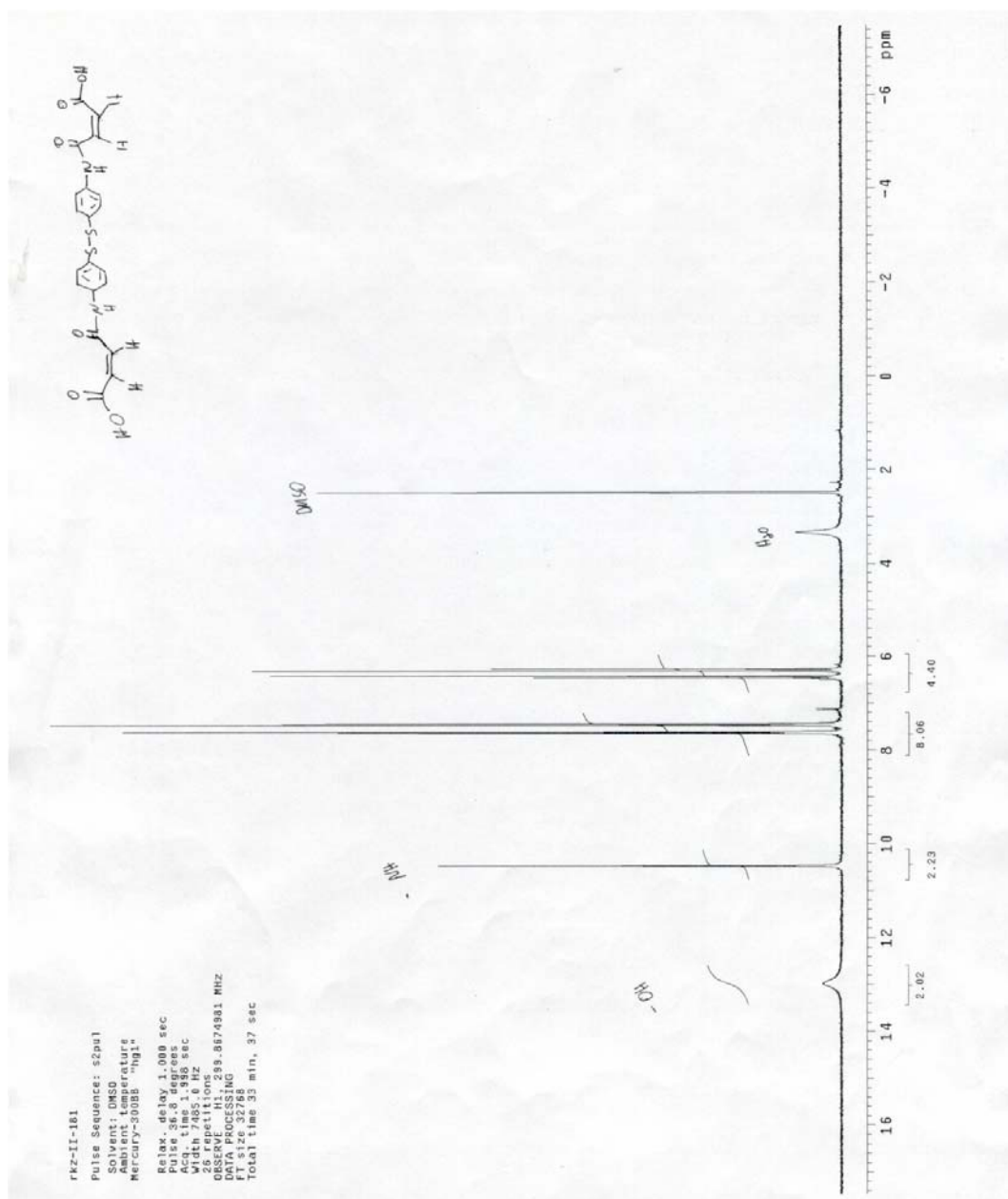


To 4-aminophenyl-disulfide (0.75 g, 3.0 mmole) was added NMP (17.5 mL) and EDC (0.93 g, 6.0 mmole) and NHS (0.69 g, 6.0 mmole). This solution was stirred until

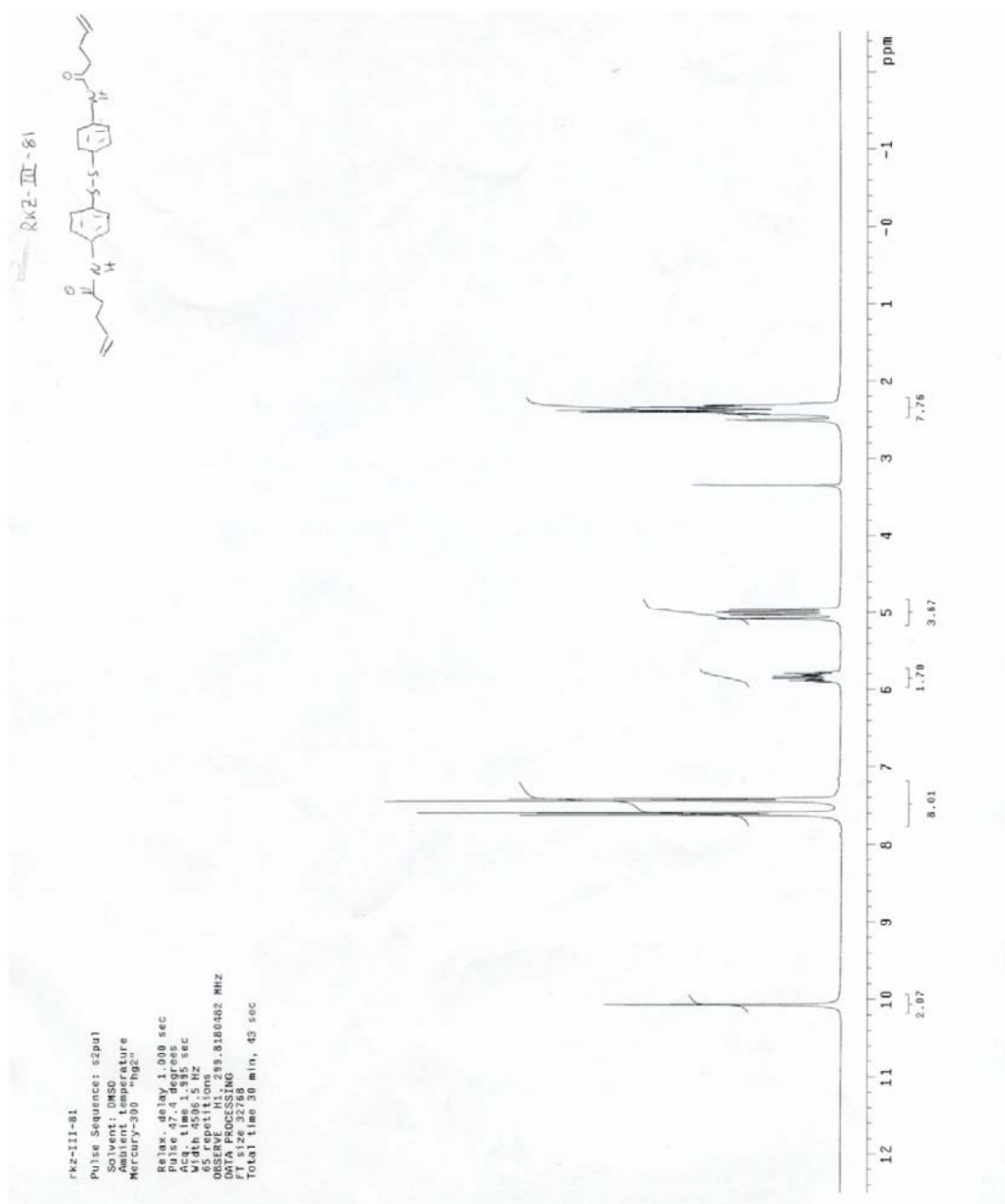
fully dissolved. To this was then added maleic acid (0.35 g, 3.0 mmole). The resulting solution was stirred for 24 hours at room temperature under Ar. The reaction mixture was then poured into excess EtOH (100 mL) and a purple solid immediately precipitated. The purple solid was collected by filtration, washed with boiling EtOH (3 x 100 mL), water (3x100 mL) and then dried under aspirator for 12 hours. The solid product was then collected and dried under vacuum for another 12 hours. 0.90 g of **3** was obtained as a solid purple powder after drying. Product was characterized by  $^1\text{H}$  NMR in DMSO- $d_6$  and by infrared analysis (KBr pellet).

**Preparation of modified monomers.** To a solution of 4-aminophenyl-disulfide (2.48 g, 9.99 mmole) in toluene (150 mL) was added 2.5 equivalents of the corresponding acid chloride or anhydride. The resulting solution was heated at 130 °C for 1 hour. Cooled reaction to RT and a white solid precipitate formed. Collected solid by filtration, washed with toluene (3x100 mL) and dried under vacuum to obtain modified monomers, the  $^1\text{H}$  NMR of which are shown below.

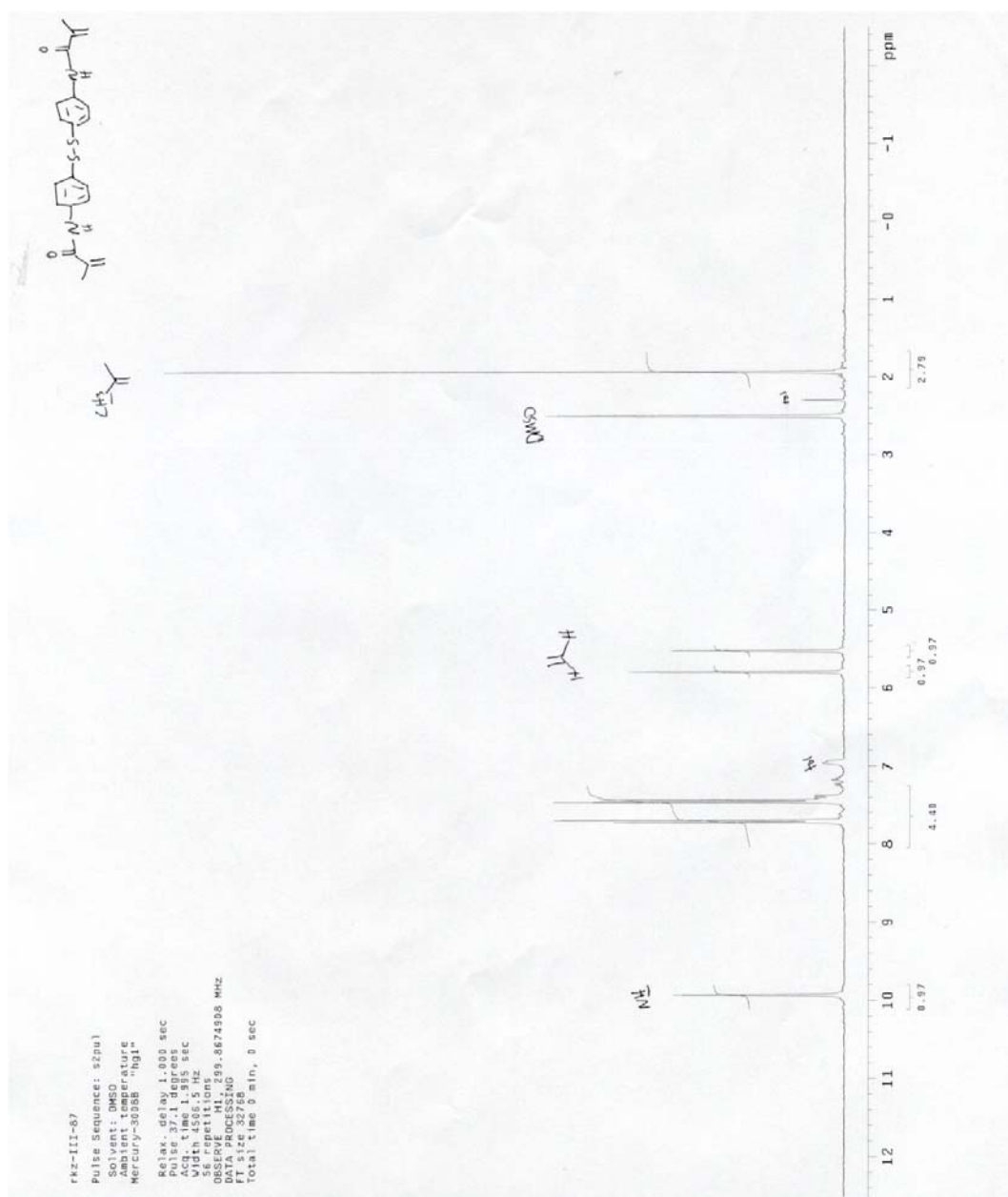




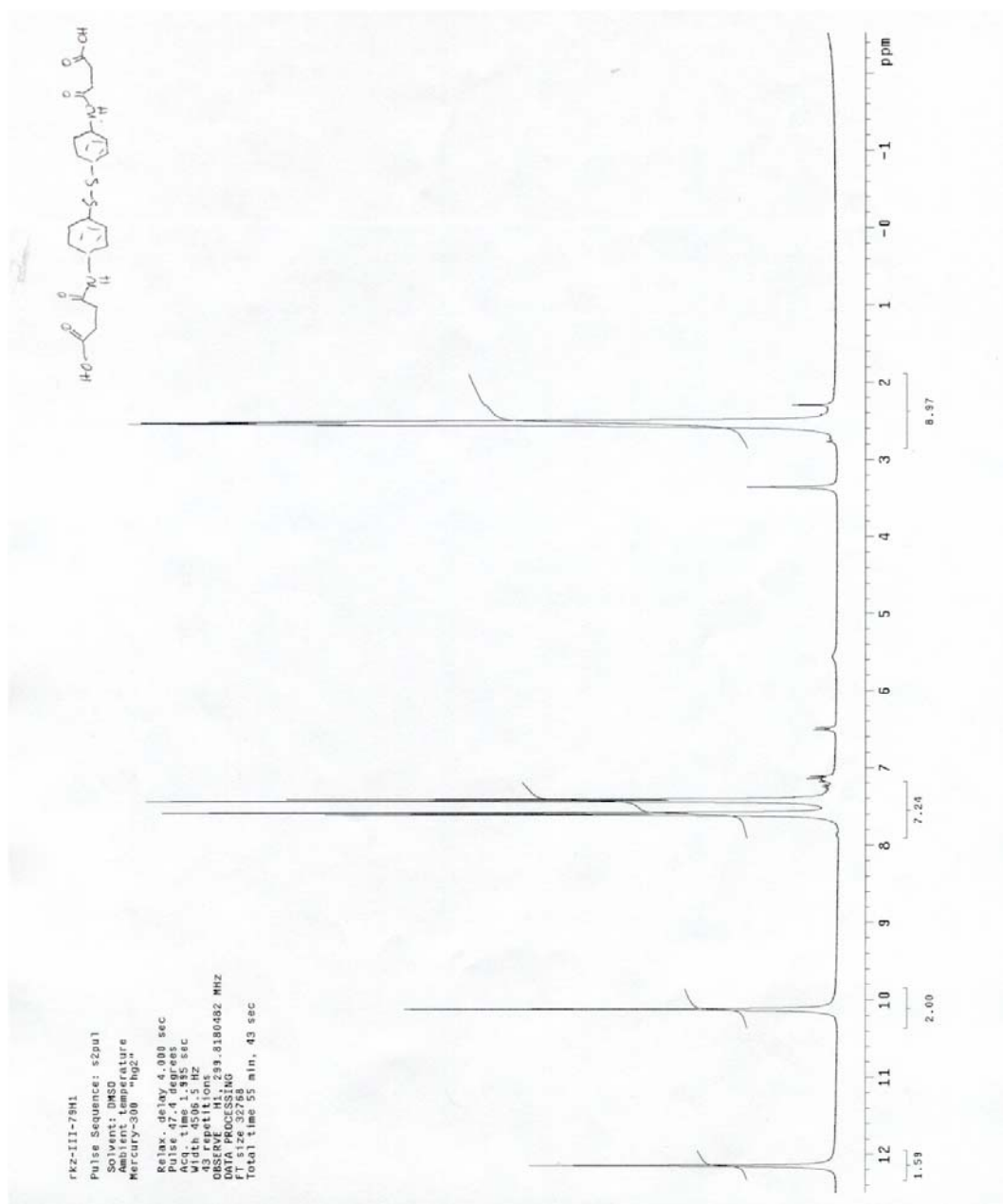
**Figure 5.9** <sup>1</sup>H NMR of carboxylic acid monomer.



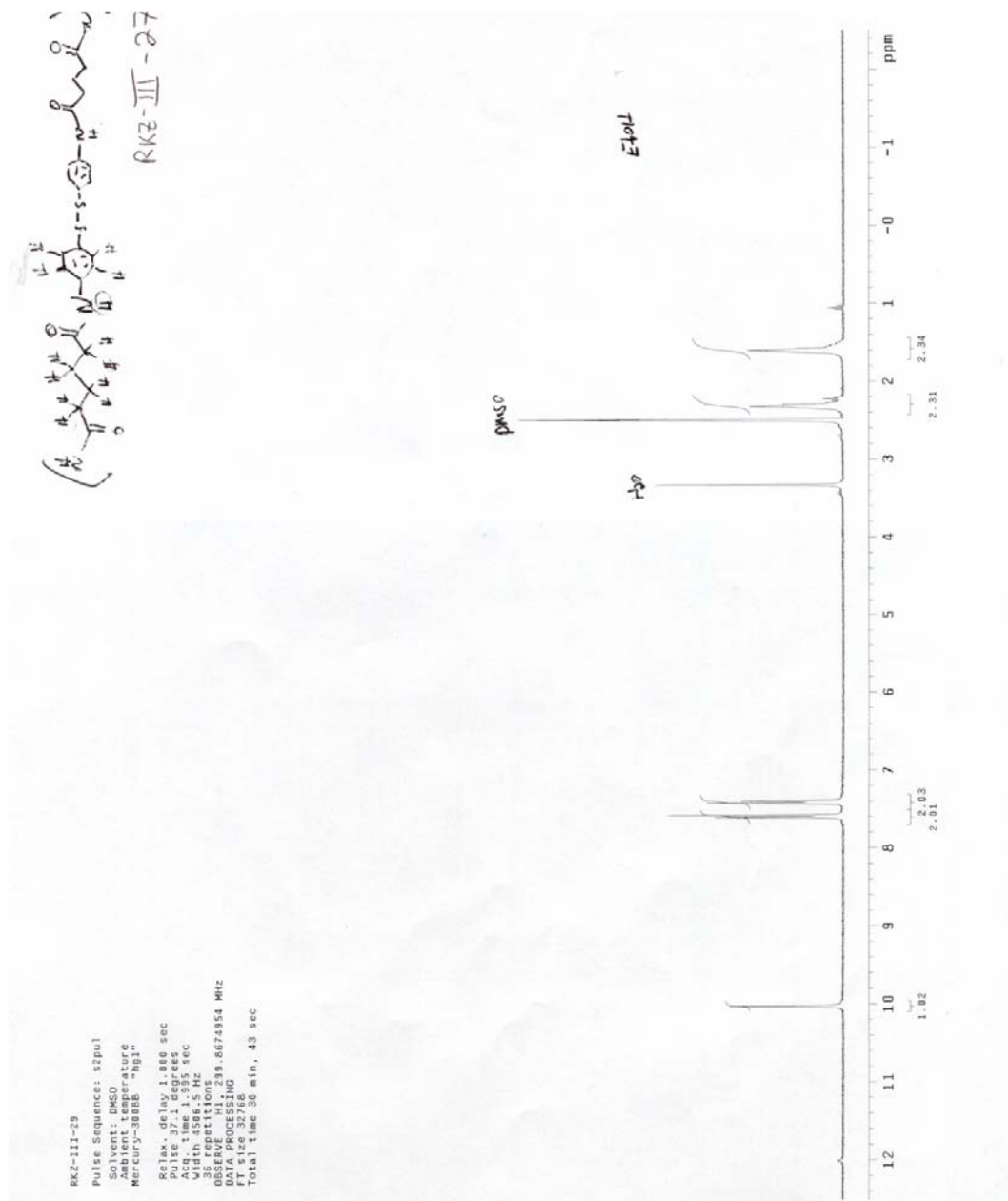
**Figure 5.10** <sup>1</sup>H NMR of olefin appended monomer.



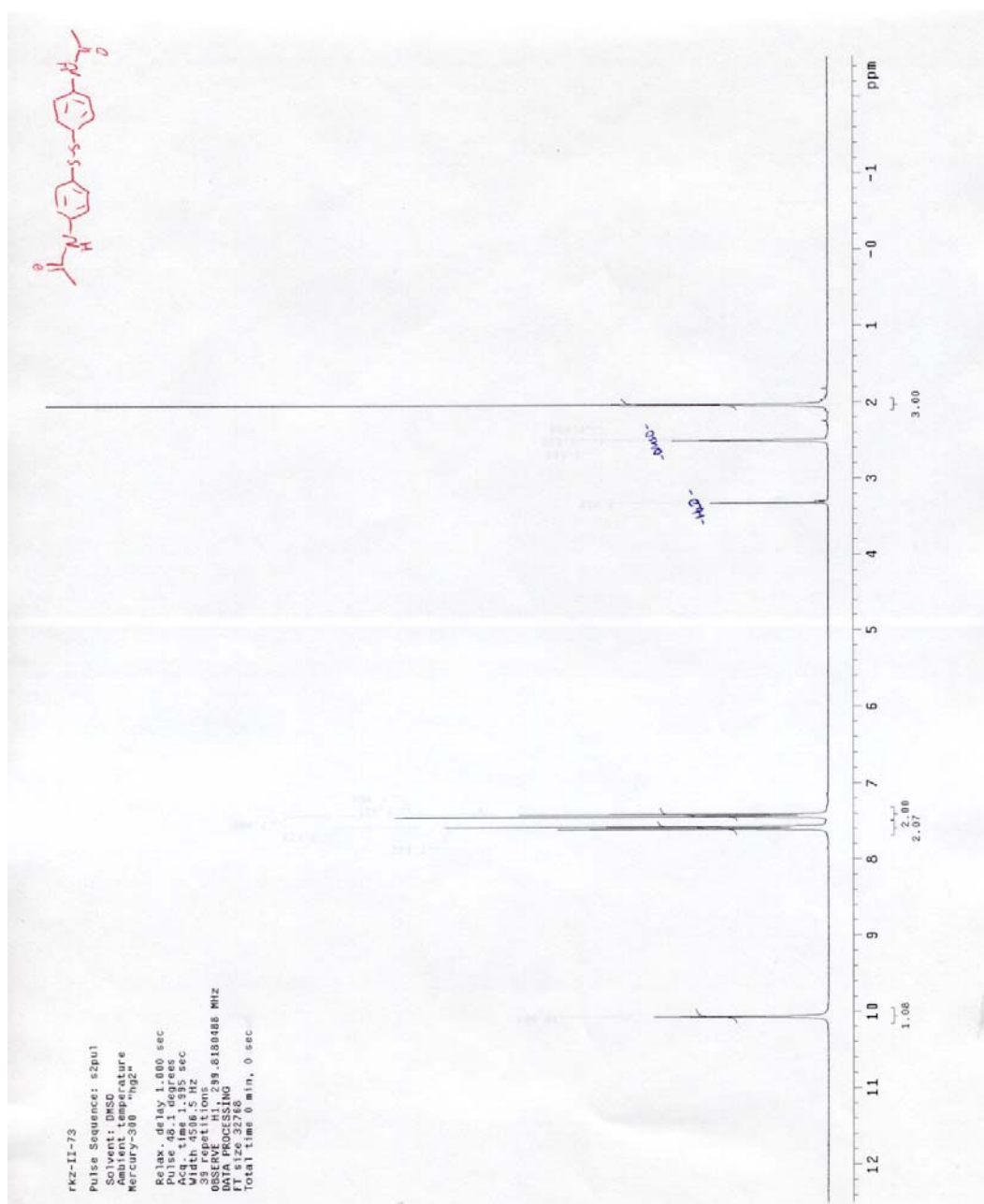
**Figure 5.11**  $^1\text{H}$  NMR of acrolein modified monomer.



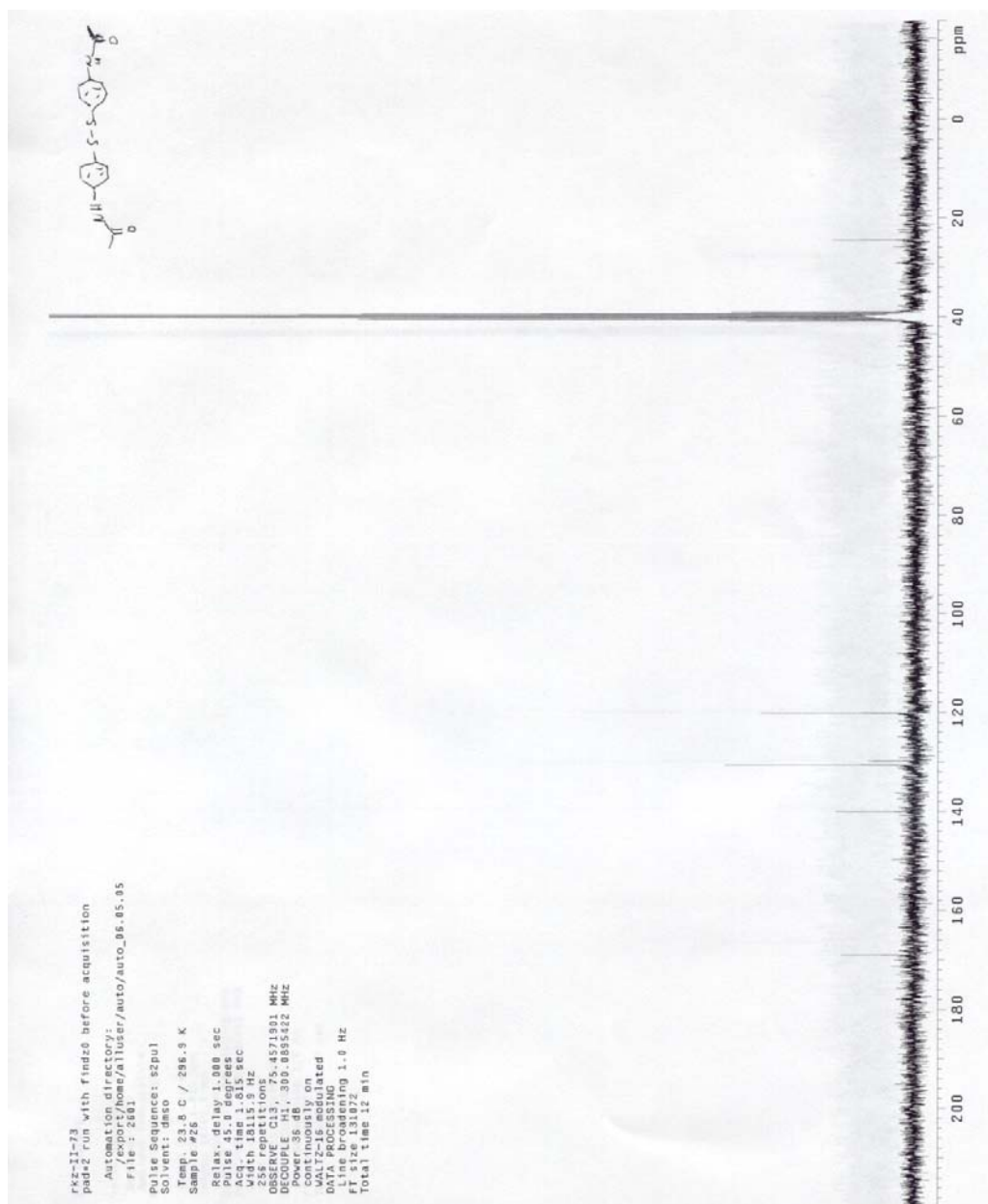
**Figure 5.12**  $^1\text{H}$  NMR of carboxyl appended monomer.



**Figure 5.13**  $^1\text{H}$  NMR of polymer 1.



**Figure 5.14** <sup>1</sup>H NMR of acetate protected monomer.



**Figure 5.15**  $^{13}\text{C}$  NMR of acetate protected monomer.

## 5.5 References

- [1] Hindeleh, A.M.; Hosemann, R.; Hinrichsen, G.; Springer, H. *Poly. Commun.* **1990**, *31*, 205-8.
- [2] Tanner, D.; Fitzgerald, J.A.; Phillips, B.R. *Progress in Rubber and Plastics Technology* **1989**, *5*, 229-251.
- [3] Milanesi, L.; Reid, G.D.; Beddard, G.S.; Hunter, C.A.; Waltho, J.P. *Chem. Eur. J.* **2004**, *10*, 1705-1710.



## **Chapter 6**

### **Conclusions**

## 6.1 Conclusions

A number of different materials have been synthesized and their properties investigated as described in the previous chapters. Chapter 2 provided an in depth examination of the effect of thiols on bisphenol A synthesis through careful homogeneous control experiments utilizing combinations of sulfonic acid and thiol catalysts. A significant increase in reaction rate and selectivity is observed when sulfonic acids are used in combination with thiols, and this trend is upheld when heterogeneous catalysts bearing sulfonic acid sites are used in combination with homogeneous thiols. Based on these findings, I prepared a number of heterogeneous catalysts incorporating thiols and sulfonic acids together through a co-condensation synthesis approach. These materials contained sulfonic acid and thiol sites randomly dispersed on the surface of the catalyst, with some sites presumably in close proximity to one another. Through immobilization of these functionalities concurrently on the surface, remarkable improvements in reaction rate and selectivity for bisphenol A were observed as a result of cooperative catalytic interactions between these sites, significantly improving upon the best homogeneous conditions attempted.

Chapter 3 is an extension of the concept of cooperative interactions between immobilized functional groups. In this work, I prepared catalysts containing incompatible functional groups simultaneously in the form of acidic and basic groups. Through a similar co-condensation approach, materials bearing sulfonic acids and primary amines together were prepared and used towards the aldol condensation between acetone and 4-nitrobenzaldehyde. Significant improvements in reactivity were observed compared to the individual functionalities used heterogeneously, and even more

importantly, when the acid and base were used together homogeneously no conversion was observed. Further improvements in reactivity were observed when the pK<sub>a</sub> of the acid component was carefully chosen, causing an effect on the equilibrium between quenched ion pair and free acid/base allowing for nearly quantitative conversion to the aldol product in the case of carboxylic acid.

Chapter 4 presented a general and simply implemented method for labeling cyclodextrin containing materials. Taking advantage of the reactivity of the primary alcohols of cyclodextrin, labeled ethylene oxide can be reacted with cyclodextrin in the gas phase in the absence of solvent to readily incorporate an isotopic or radioactive label into the material. This labeled material can then be easily quantified and traced when used in animal biodistribution studies. The nature of this method allows for general reactivity between any cyclodextrin containing material and ethylene oxide, and could be utilized in any material bearing nucleophilic sites.

A method for degrading polymers through a two-fold mechanism is illustrated in Chapter 5 that utilizes the homolytic cleavage of aromatic disulfides through irradiation. This two switch method allows for precise initiation of polymer degradation and prevents undesired degradation in the incidental exposure of the polymer to one switch independently. This method illustrates how an *in situ* oxidation can be carried out with peroxide upon irradiation of aromatic disulfides, leading to irreversible cleavage of this group. A number of different polymers are presented that incorporate this aromatic disulfide monomer into their synthesis.

**Appendix A**

**Progress toward the Total Synthesis of  
Nomofungin/Communesin B**

**(In collaboration with Jeremy May and Yeeman  
Ramtohl under Prof. Brian Stoltz)**

This chapter was reproduced in part with permission from May, et. al., *Tetrahedron Letters* 44, 1203-1205 (2003). Copyright 2003 Elsevier.

**A.1 Abstract**

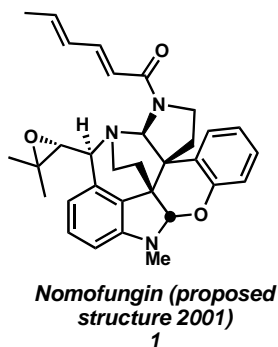
Progress toward the synthesis of the indole alkaloid natural product communesin B/nomofungin is presented herein. Identification of the recently isolated nomofungin as a previously identified natural product, communesin B, as well as evidence supporting this claim is also described. A synthetic approach utilizing an inverse-demand Diels-Alder reaction with an electron rich indole serving as a dienophile and an in situ generated ortho-quinone methide imine as a diene inspired from a proposed biosynthesis is also outlined. The first example of such a reaction as well as applications toward the synthesis of communesin B/nomofungin are also reported.

**Appendix A. Progress toward the Total Synthesis of  
Nomofungin/Communesin B (in collaboration with Jeremy May and Yeeman  
Ramtohl)**

**A.2 Introduction**

Recently the new indole alkaloid nomofungin (**1**), which bears a unique oxygen containing hemi-aminal linkage at C(6) (Figure A.1), was isolated from a fungus growing on a ficus tree in Hawaii.<sup>1</sup>

**Figure A.1**



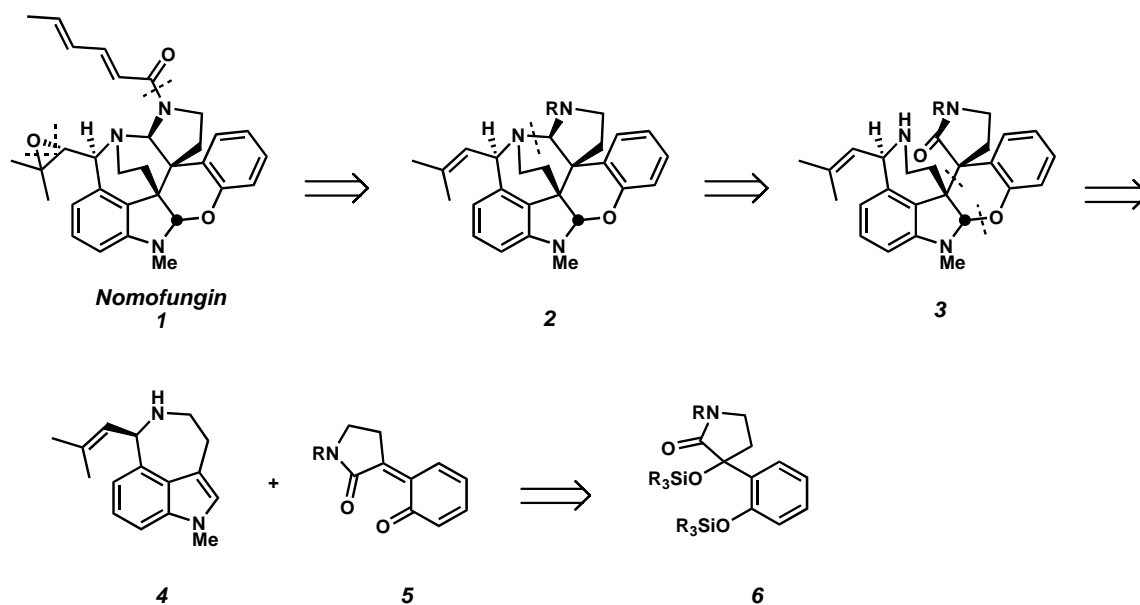
This new natural product disrupted microfilament formation in the cell, which is of biological importance because of the role of microfilaments in cellular reproduction. Microfilaments are strands of the protein actin and are known to be involved in cellular locomotion. More specifically, microfilaments are known to be involved in separation of chromosomes during the last stage of mitosis.<sup>2</sup> Disrupting microfilament formation interrupts cellular reproduction, and disruption of microfilaments has been postulated as a potential method for curbing reproduction of cancer cells.<sup>3</sup> The interesting structure and

potential applications in cancer treatment led us to develop an approach toward the synthesis of nomofungin.

### A.3 Results

When examining structure **1** we first attempted to hypothesize a reasonable biosynthesis to guide our synthetic planning. We were, however, unable to propose a biosynthetic strategy for generating this type of hemi-aminal linkage, and we searched for other synthetic methods to generate this structure. There has been work done in which ortho-quinone methides are generated in situ and are used for Diels-Alder reactions as dienes. It was through this approach that the key disconnection was made toward constructing the core of nomofungin, as shown in the retrosynthetic plan in Scheme A.1.

**Scheme A.1**



The efficiency of the Diels-Alder strategy could be appreciated by first removing the acyl group and the epoxide to reveal **2**, and then disconnecting the aminal linkage yielding structure **3**. A Diels-Alder disconnection reveals indole **4** and ortho-quinone methide diene **5**. This type of ortho-quinone methide has been generated by fluoride induced desilylation of silyl protected phenols such as **6** with an  $\alpha$ -leaving group.<sup>4</sup> Dienes similar to **5** were generated and then trapped immediately with an electron-rich dienophile to undergo an inverse demand Diels-Alder reaction, similar to the strategy shown above. This is where investigations toward the synthesis of nomofungin were initiated.

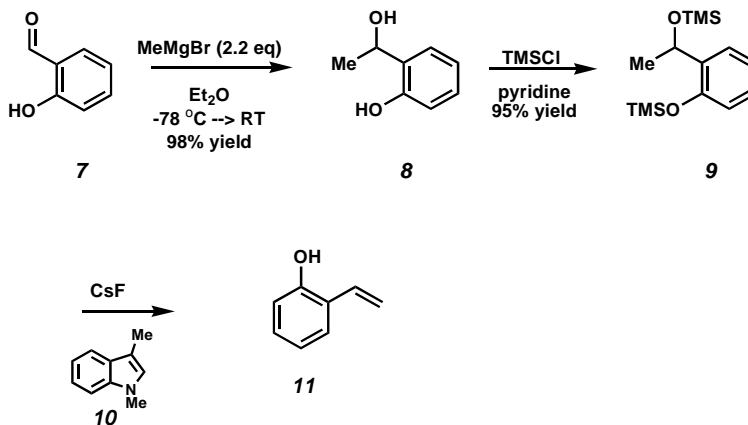
#### *Model Studies Toward Nomofungin*

Initial studies toward the feasibility of an inverse-demand Diels-Alder reaction using an ortho-quinone methide with an electron-rich indole as a dienophile started with readily available 1,3-dimethyl indole (**10**) as a model dienophile. The synthesis of the disilyl-protected phenol **9** was carried out by adding methyl Grignard to commercially available salicylaldehyde (**7**), followed by trimethylsilyl protection of both hydroxyls to yield **9** as shown in Scheme 2. Fluoride induced deprotection of **9** in the presence of 1,3-dimethyl indole (**10**) did not give rise to any of the desired Diels-Alder adduct; the only isolated product was deprotected styrene **11**. Numerous reaction conditions were screened including different fluoride sources, different silyl protecting groups, and substituting



halogens as a leaving group for the secondary alcohol at the  $\alpha$ -position, but no conditions afforded the Diels-Alder product.

**Scheme A.2**



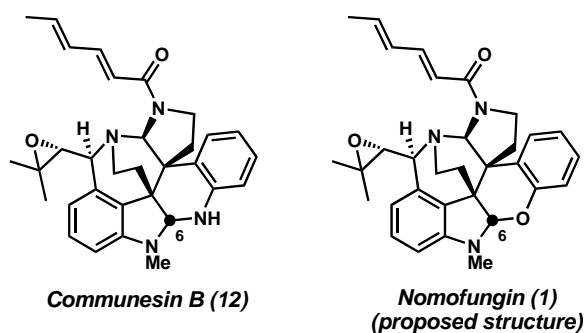
It was at this early stage in the project that an ambiguity in the structure of nomofungin became apparent.

### *Reassignment of the Structure of Nomofungin*

Difficulties in devising a reasonable biosynthetic proposal for synthesis of the oxygen containing hemi-aminal were not initially troubling. However, after closer examination, it was noted that another natural product, communesin B (**12**), and nomofungin had very similar structures.

Communesin B<sup>5</sup> (**12**), shown in Figure A.2, differed from the structure of nomofungin only in a substitution for the oxygen in the hemi-aminal with a nitrogen. We questioned whether or not the oxygen containing structure of nomofungin was reasonable. The reported NMR data for the two natural products were nearly identical in all respects. The two different structures would be expected to exhibit different <sup>1</sup>H and <sup>13</sup>C shifts at C(6) if they were, in fact, different at this position. Nomofungin was reported to have a <sup>1</sup>H chemical shift of 4.70 ppm and a <sup>13</sup>C chemical shift of 82.4 ppm at C(6).<sup>1</sup> Communesin B was reported to have a <sup>1</sup>H chemical shift of 4.69 ppm and a <sup>13</sup>C chemical shift of 82.4 ppm at C(6).<sup>3</sup> Based on these observations, it was clear that one of the isolationists had misidentified their natural product, and we reported that nomofungin and communesin B were indeed the same compound.<sup>6</sup> After we brought this discrepancy to their attention, the isolation chemists of nomofungin have since withdrawn their report.<sup>7</sup>

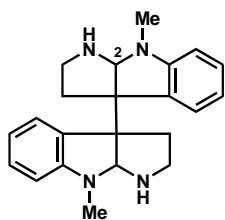
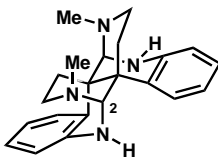
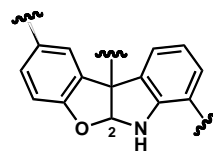
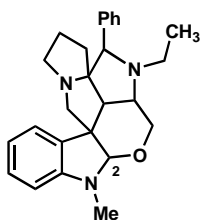
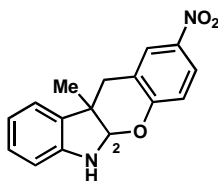
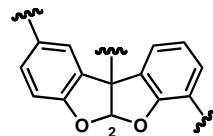
**Figure A.2**



Further progress toward the synthesis of the natural product required determination of the true structure, the hemi-aminal structure of nomofungin or the diaminal structure of communesin B.

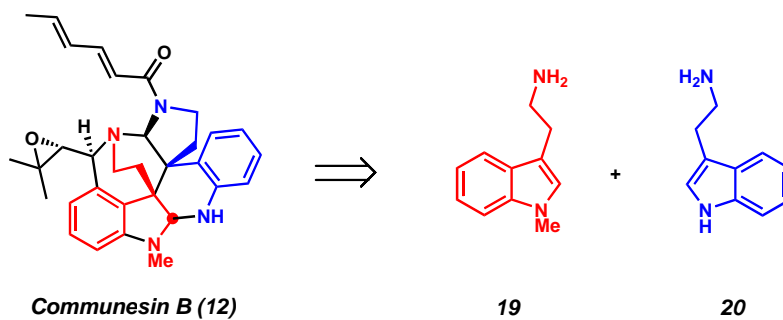
Looking at the literature to support either structure provided some evidence for one of these two structures.<sup>8</sup> Structures containing a diaminal linkage, such as alkaloids **13** and **14** in Figure A.3, typically had a <sup>1</sup>H chemical shift between 4.3 and 4.5 ppm for the hydrogen on the carbon between the two nitrogens. The <sup>13</sup>C chemical shift of this carbon between the nitrogens was typically between 70 and 85 ppm. Structures with oxygen containing hemi-aminal linkages tended to exhibit slightly larger <sup>1</sup>H chemical shifts. Compounds **16** and **17** illustrated that the chemical shift of these types of protons tend to fall between 5 and 5.5 ppm, while the carbon chemical shifts are closer to 100 ppm. The same trend of a decreased chemical shift for substitution of a nitrogen for an oxygen was also seen in the original and revised structures of Diazonamide A, compounds **15** and **18**, respectively. These data supported the conclusion that the actual structure of nomofungin/communesin B contains a diaminal moiety rather than the oxygen containing hemi-aminal. Further evidence for this conclusion comes from possible biosynthetic routes to the proposed diaminal structure.

Figure A.3

**(+)-Isochimonanthine****13**C-2  $^1\text{H}$  4.32 ppmC-2  $^{13}\text{C}$  83.7 ppm**(+)-Calycanthine****14**C-2  $^1\text{H}$  4.42 ppmC-2  $^{13}\text{C}$  71.0 ppm**Diazonamide A (revised structure)****15**C-2  $^1\text{H}$  6.34 ppmC-2  $^{13}\text{C}$  106.1 ppm**16**C-2  $^1\text{H}$  5.0 ppmC-2  $^{13}\text{C}$  97.2 ppm**17**C-2  $^1\text{H}$  5.44 ppmC-2  $^{13}\text{C}$  -----**Diazonamide A (original structure)****18**C-2  $^1\text{H}$  6.93 ppmC-2  $^{13}\text{C}$  98.0 ppm*Biosynthesis*

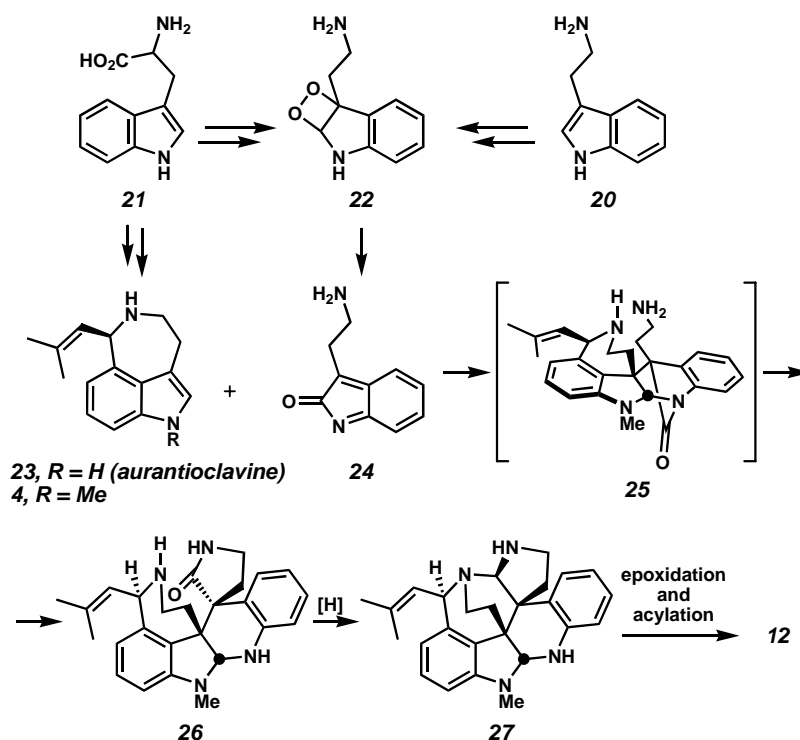
An examination of communesin B (**12**) reveals the underlying skeleton of two tryptamine/tryptophan subunits as shown in Scheme A.3. Since biosynthetically there is no benzofuran equivalent of indole, where the indole nitrogen is replaced with oxygen, this type of biosynthetic analysis is not possible for the original nomofungin structure (**1**).

## Scheme A.3



Scheme A.4 illustrates how communesin B could come about from a dimerization of tryptamine. Aurantioclavine (**23**) has been previously isolated and a biosynthesis from tryptophan has been proposed.<sup>9</sup> Oxidation of tryptamine could result in formation of an oxindole diene **24**. An inverse-demand Diels-Alder reaction between the electron-deficient diene **24** and electron-rich indole **4** could build up the core structure **25** of communesin B in one step.

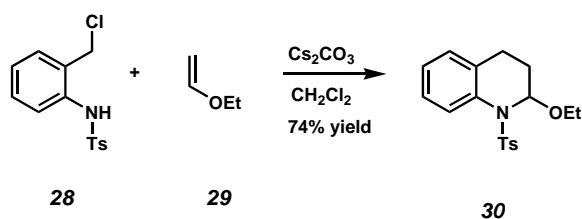
Scheme A.4



The Diels-Alder product **25** would contain a very strained bridging carbonyl moiety (analogous to the quinuclidone ring system) that could then be opened up by the free tryptamine side chain to form the necessary spirocycle in communesin B. A reduction to the diaminal, followed by further epoxidation and acylation would give rise to communesin B. This reasonable hypothesis for the biosynthesis of communesin B from the very common cellular building blocks tryptamine and tryptophan guided our planning for a synthesis in the lab, and it also provided further support for the diaminal structure of communesin B as the true structure. At this point, we commenced experiments in the laboratory to confirm the diaminal structure of the natural product.

*Model Study for Diels-Alder Reaction*

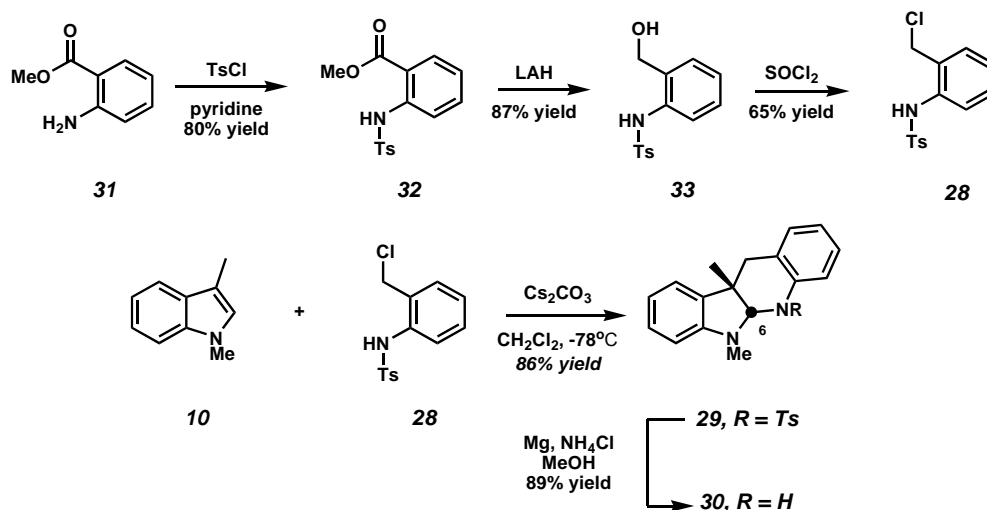
The first approach to elucidation of the true structure of nomofungin/communesin B involved building up a similar diaminal structure to compare NMR data with the natural product. This was an opportunity to test some of the hypotheses concerning an inverse-demand Diels-Alder reaction being used with an indole to build the core. Recently Steinberger and Corey<sup>10</sup> demonstrated that ortho-quinone methide imine type dienes generated *in situ* by base induced halogen elimination from an ortho-chloroaniline **28** underwent an inverse-demand Diels-Alder reaction with an electron-rich diene **29**, as shown in Scheme A.5.

**Scheme A.5**

Analogous to the proposed biosynthesis in Scheme A.4, it was desired to carry out an inverse-demand Diels-Alder reaction with an ortho-quinone methide imine diene using an electron-rich olefin as a dienophile. We chose the readily available 1,3-dimethyl indole (**10**) as our test olefin and the simple chloroaniline **28** used by Corey as the precursor to the diene, as these two components would give rise to an amination linkage similar to the core of communesin B. The synthesis of chloroaniline **28** is presented in Scheme A.6.

Starting from methylantranilate (**31**), sulfonamide protection of the aniline was carried out to give **32**, followed by an LAH reduction to primary alcohol **33**. Displacement of the alcohol using thionyl chloride provided the desired chloraniline **28**. Treating **28** with base in the presence of 1,3-dimethyl indole (**10**) did cause an immediate inverse-demand Diels-Alder reaction providing a single diastereomer **29** in 86% yield. Cleavage of the sulfonamide protecting group by exposure of tetracycle **29** to Mg, NH<sub>4</sub>Cl and MeOH afforded diaminal **30**.

Scheme A.6



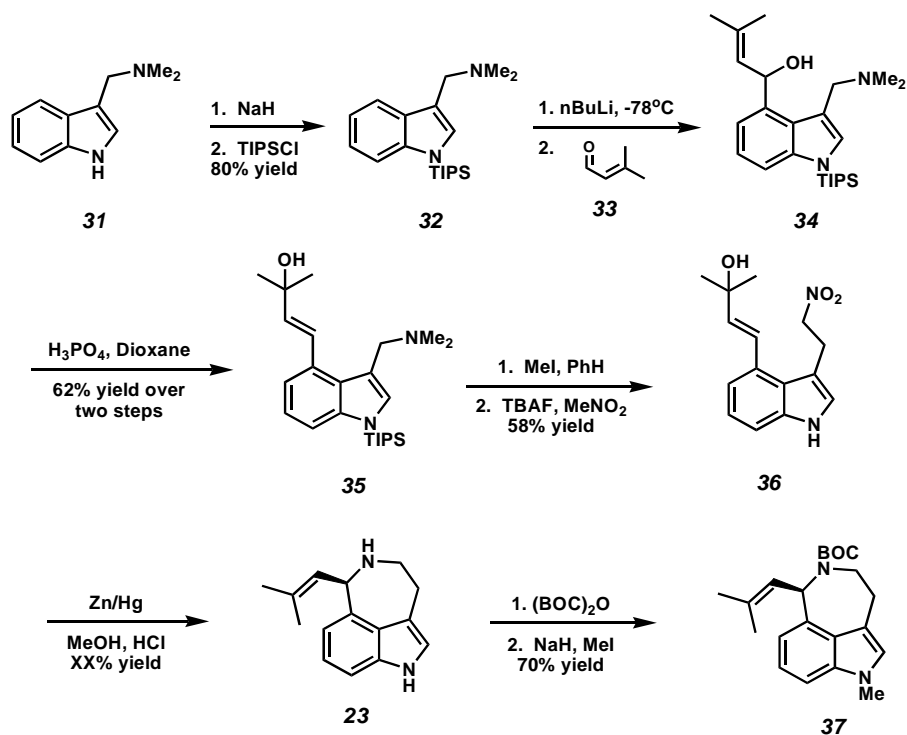
Interestingly, the  $^1\text{H}$  NMR chemical shift of the proton at C(6) of **30** is at 4.14 ppm and the  $^{13}\text{C}$  resonance is at 83.9 ppm. These values are in close agreement with the shifts reported for both communesin B and nomofungin of 4.69-4.70 ppm ( $^1\text{H}$ ) and 82.4 ppm ( $^{13}\text{C}$ ), strongly suggesting that the communesin structure is the appropriate representation for the natural product. This was also the first example of an inverse-demand Diels-



Alder reaction between an electron-rich indole and an electron-deficient ortho-quinone methide imine diene.

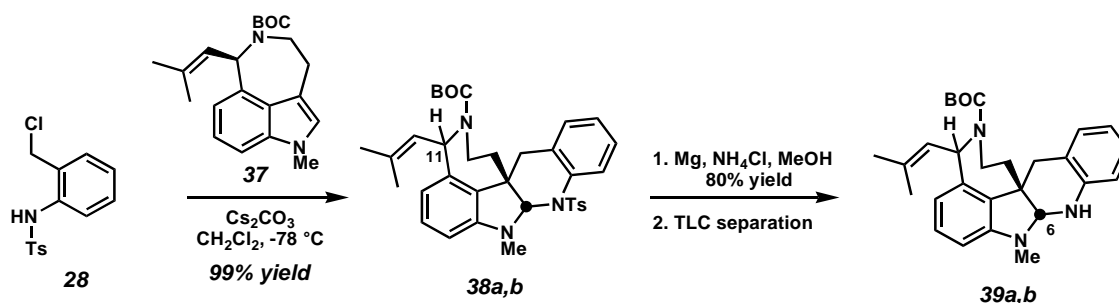
We next turned our attention to applying this reactivity toward building the core of communesin B. The indole necessary for the Diels-Alder in the proposed biosynthesis, aurantioclavine (**23**), was prepared by known methods (Scheme A.7),<sup>11</sup> and its *N*-BOC-*N*-methyl derivative **37** was tested for reactivity in the Diels-Alder reaction with chloroaniline **28** from above. Starting from commercially available gramine (**31**) the indole nitrogen was protected with a triisopropylsilyl group in good yield to sterically shield the indole C-2 position, as the next step in the sequence was a directed lithiation at C-4 followed by addition of commercially available aldehyde **33**. An acid catalyzed rearrangement then provided the tertiary alcohol **35** in good yield over the two steps. Quaternization of the amine in **35** with methyl iodide followed by a TBAF triggered deprotection/nitromethane addition sequence proceeded in good yield to give the nitro compound **36**. A reductive cyclization using a Zn/Hg amalgam gave the desired aurantioclavine (**23**) in moderate yields. Aurantioclavine could then be selectively BOC protected on the amine and then methylated at the indole nitrogen in 70% overall yield to give the desired *N*-BOC-*N*-methyl aurantioclavine (**37**).

Scheme A.7

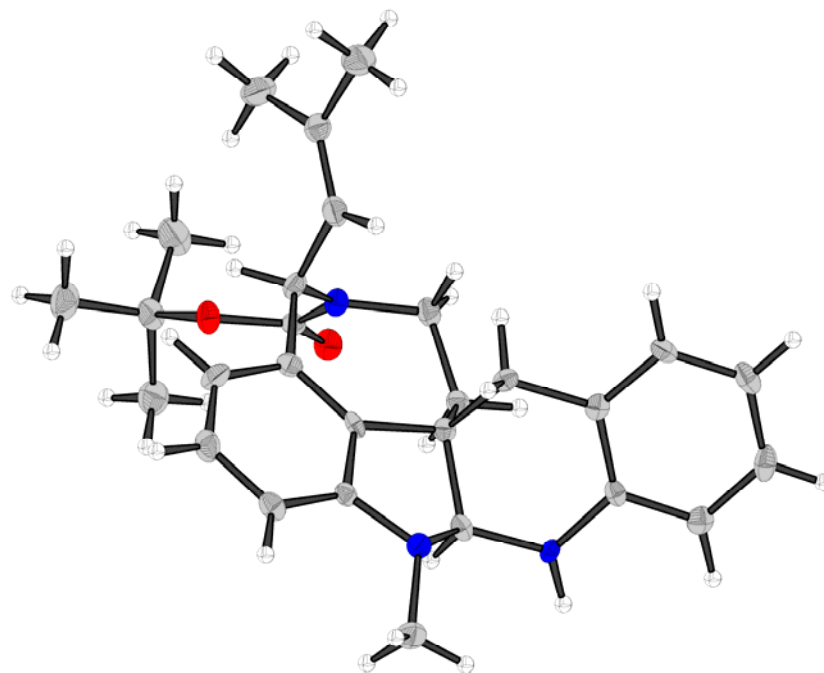


With the desired indole **37** in hand, the inverse-demand Diels-Alder reaction using this more functionalized indole was explored. As shown in Scheme A.8, rapid cycloaddition occurred upon treatment of **37** and **28** with  $\text{Cs}_2\text{CO}_3$  to give the desired Diels-Alder product **38** in excellent yield.

## Scheme A.8



Unfortunately, the cycloadduct was produced in a 2:1 mixture of diastereomers with respect to the methylpropenyl side chain at C(11). These diastereomers were inseparable at this stage, but removal of the sulfonamide protecting group with  $\text{Mg}$ ,  $\text{NH}_4\text{Cl}$  and  $\text{MeOH}$  allowed for TLC separation of the deprotected diastereomers. The  $^{13}\text{C}$  NMR shifts for C(6) of diastereomers **39a** and **39b** were at 84.8 and 83.9 ppm, again in full agreement with the data for communesin B and nomofungin, further supporting the diaminal structure. The remote stereocontrol that was desired by the methylpropenyl side chain was presumably counteracted by concomitant shielding of the bottom face of the indole by the BOC protecting group, as a crystal structure of minor diastereomer **39b** illustrated (Figure A.4). The Diels-Alder product **38** demonstrated the reactivity of aurantioclavine type indoles as competent dienophiles in inverse-demand Diels-Alder reactions and served as a proof of concept for their involvement in the biosynthesis of communesin B/nomofungin.

**Figure A.4. X-ray Crystal Structure of 39b**

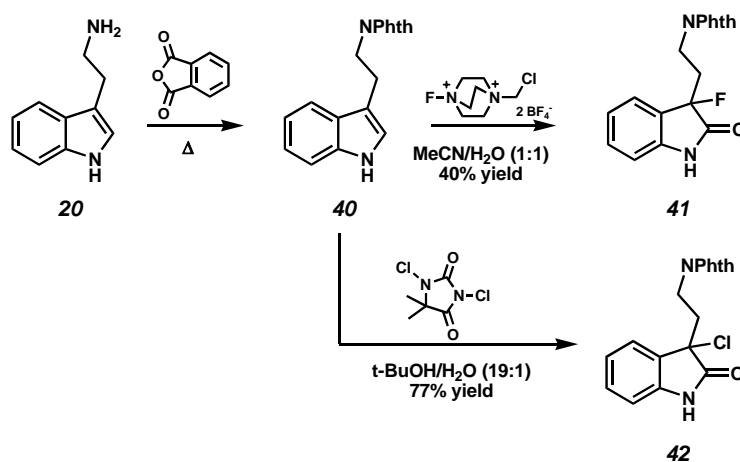
### *Biosynthetic Approach to Communesin B*

Having demonstrated the feasibility of using aurantioclavine (**23**) as a dienophile in the proposed Diels-Alder reaction, we next looked to demonstrate the feasibility of using oxindole-type dienes, like compound **24**, as dienes in inverse-demand Diels-Alder reactions. Inspired by the Corey approach of using a base-induced elimination of an  $\alpha$ -halogen, we looked to synthesizing  $\alpha$ -halogenated oxindoles from tryptamine.

Fluorooxindoles have been synthesized by treatment of indoles with a fluorinating reagent, Selectfluor, in the presence of water.<sup>12</sup> It was possible to treat *N*-phthalimide protected tryptamine **40** with Selectfluor and obtain the fluorinated oxindole product **41** in modest yield, as shown in Scheme A.9. A screen of various halogenating reagents also

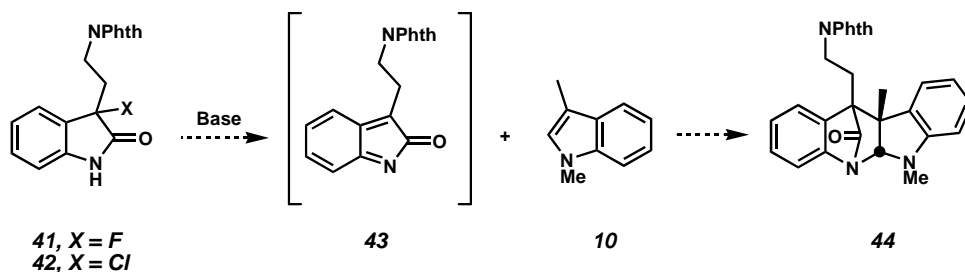
resulted in access to chlorooxindole **42** in good yield using 1,3-dichloro-5,5-dimethyl hydantoin in the presence of water.

**Scheme A.9**



With the desired oxindoles in hand, the biosynthetically proposed Diels-Alder reaction was attempted. As depicted in Scheme A.10, base induced elimination of the  $\alpha$ -halogen was attempted in order to form diene **43**, which would then be trapped by 1,3-dimethyl indole (**10**), an indole which we have shown to be a reactive dienophile in such Diels-Alder reactions.

Scheme A.10

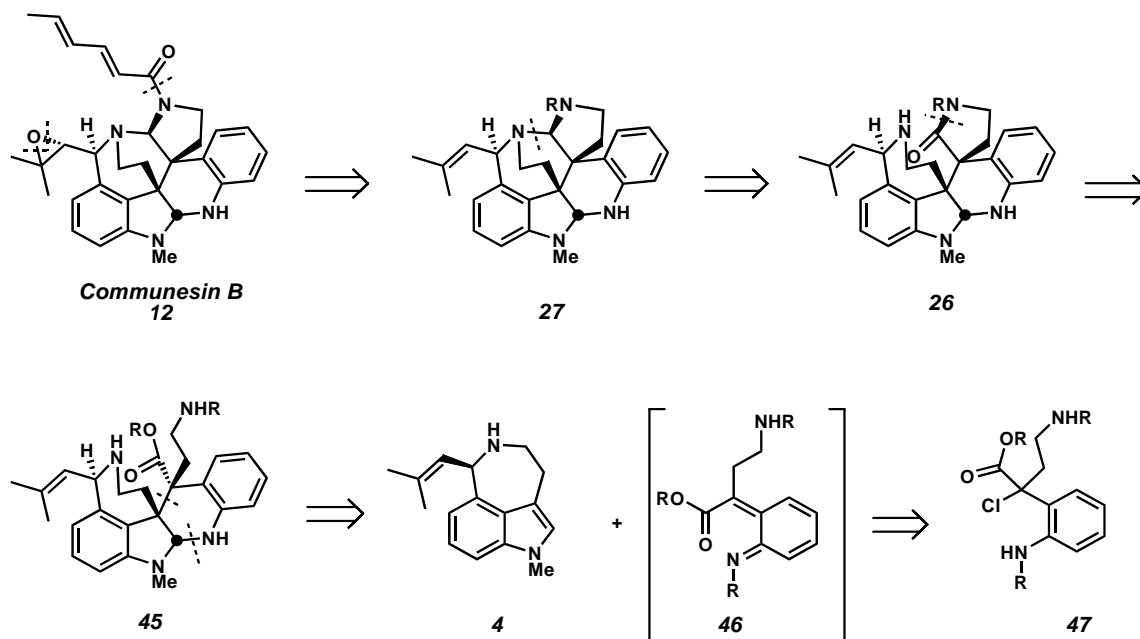


Unfortunately, under a variety of conditions there was no desired cycloaddition. An exhaustive screen of bases and inclusion of halogen scavengers in the reaction mixture did not result in the desired Diels-Alder reaction. This may be in part due to the energetic barrier in creating an anti-aromatic compound **43** from aromatic **41** or **42**, as such a barrier is expected to be large. Attempts at forming halogenated oxindoles with the tryptamine chain unprotected and monoprotected were unsuccessful. This inability to carry out the proposed biosynthetic route does not preclude this strategy as the true biosynthetic path to communesin B. This only shows that we were unable to replicate the necessary conditions in the laboratory to carry out the transformation. It is at this point that we decided to turn our attention toward the intermolecular inverse-demand Diels-Alder reactions using chloroaniline derivatives to synthesize communesin B/nomofungin, since we have shown these dienes to be reactive with indole dienophiles.

*New Retrosynthetic Approach*

A new approach toward communesin B was then envisioned that would take advantage of the above method used for generating ortho-quinone methide imines. After removing the epoxide and acyl appendage, and then disconnecting the uppermost diaminal linkage, our target structure remained **26**, an intermediate in our proposed biosynthesis (Scheme A.11). At this point, however, we envisioned opening the spirocyclic lactam in **26** to reveal a substituted quaternary carbon center in tetracycle **45** on the communesin B core, knowing that the unsubstituted core is accessible via Diels-Alder chemistry (see intermediates **39a, b**). A retro Diels-Alder disconnection then reveals *N*-methyl aurantioclavine (**4**) and diene **46** in which the desired substituents for the quaternary center are carried in on the terminal olefin of the diene. Analogous to our previous method of generating ortho-quinone methide imine dienes from  $\alpha$ -chloroanilines, we looked to make the disubstituted  $\alpha$ -chloroaniline **47** as a precursor to the ortho-quinone methide imine diene. The most important question concerning this route was whether or not the substituents on the diene would be too sterically encumbering to allow for formation of the diene or would prevent approach of the dieneophile to the diene for cycloaddition to occur. We looked to a simple model system to answer this question.

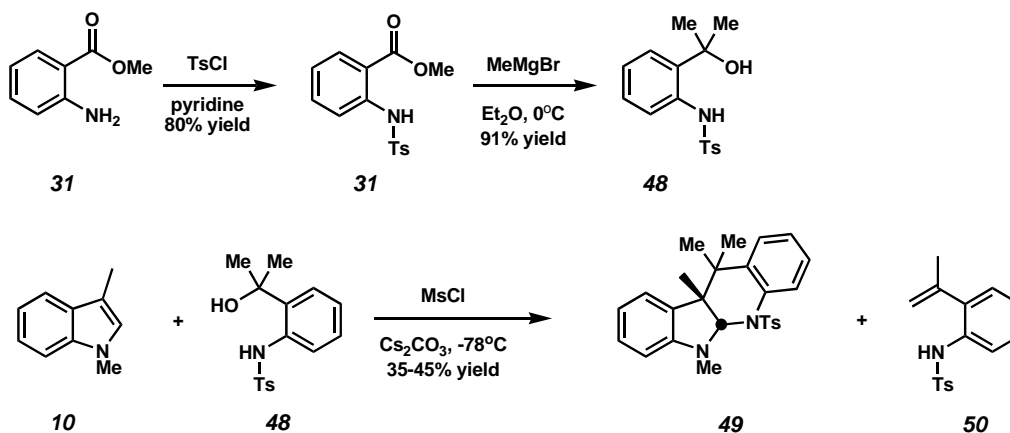
## Scheme A.11

*Substituted Dienes in Diels-Alder Reaction*

As a test to see if  $\alpha$ -substitution would be tolerated on the diene we looked to make the simple  $\alpha$ -dimethyl,  $\alpha$ -hydroxy substituted aniline **48** (Scheme A.12). We decided to make the hydroxyaniline rather than the chloroaniline for this study as we had recently developed better methods to carry out the Diels-Alder reactions directly from the alcohol using  $\text{MsCl}$  to convert the free alcohol into a leaving group to generate the diene. Making the chloride from the tertiary alcohol also proved to be troublesome as the elimination product **50** was the only product, and this was an indication that elimination might be a problem under the Diels-Alder reaction conditions.



Scheme A.12

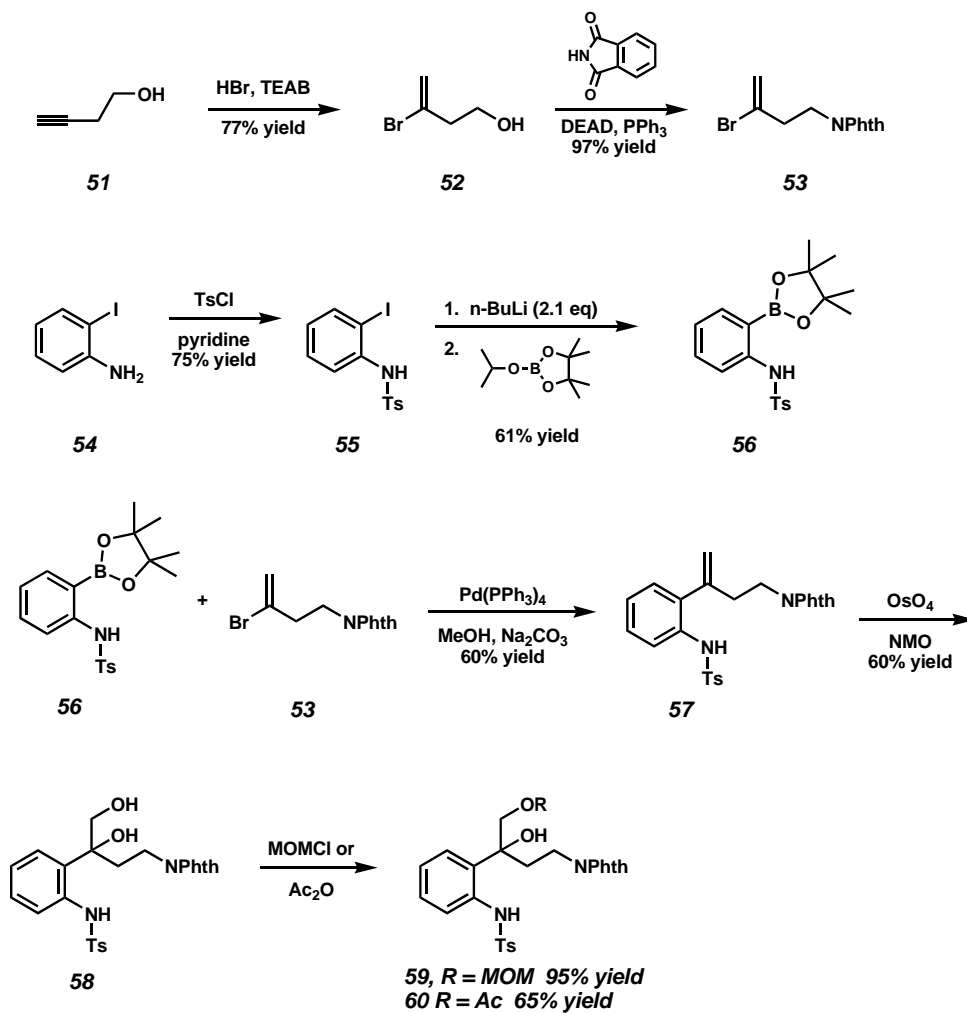


Starting with commercially available methylanthranilate (**31**) and putting on a sulfonamide protecting group followed by addition of two equivalents of methyl Grignard gave alcohol **48**. Attempting the Diels-Alder reaction with **48** using 1,3-dimethyl indole (**10**) as a dienophile under the  $\text{MsCl}$  induced diene generation conditions did give modest yields of the desired Diels-Alder adduct **49**. However, varying amounts of the elimination product **50** were obtained depending on the exact reaction conditions. If the reaction was not done at  $-78^\circ\text{C}$  and then slowly warmed to room temperature, elimination would become the major reaction pathway. This model system did serve to prove that it was feasible to carry out a Diels-Alder reaction with substitution on the diene with our simple indole dienophile. We then looked to synthesize and test the actual diene necessary to complete the synthesis of communesin B/nomofungin.

*Synthesis of Aniline 47 and Attempts at Diels-Alder Reaction*

The synthesis of aniline **47** was carried out as illustrated in Scheme A.13. Beginning with commercially available homo-propargyl alcohol (**51**), a regioselective bromination of the alkyne was carried out with HBr to give olefin **52** in good yield. A Mitsunobu reaction with phthalimide was then done to introduce the desired nitrogen substitution in **53**. This compound would be used as a coupling partner in a Suzuki coupling. The synthesis of the boronic ester **56** commenced with iodoaniline (**54**). A sulfonamide protecting group was placed on the aniline followed by a halogen-metal exchange to make boronic ester **56**. This compound was then subjected to Suzuki coupling conditions in the presence of vinyl bromide **53** to cleanly afford the coupled styrenyl aniline **57**. Treatment of **57** with catalytic osmium tetroxide afforded the dihydroxylated product **58**. Diol **58** could then be selectively protected on the primary alcohol with an acetate or a MOM protecting group to afford a reduced version of the desired  $\alpha$ -substituted aniline in which the ketone is masked as the protected primary alcohol.

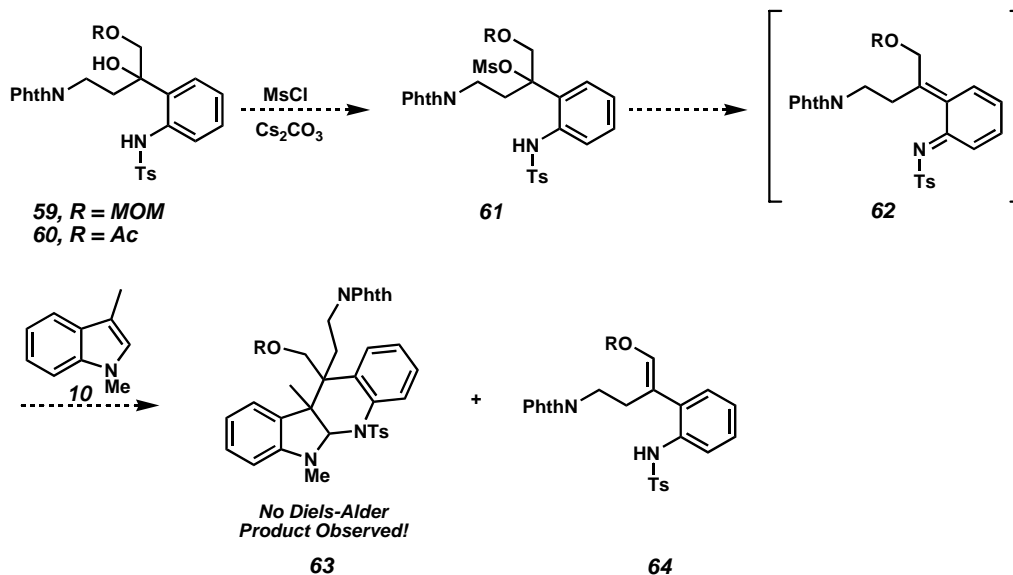
Scheme A.13



With compounds **59** and **60** in hand, we began screening for reactivity with the simple 1,3-dimethyl indole (**10**) dienophile (Scheme A.14). An exhaustive screen was conducted using all of the conditions that had been previously used in our studies, as well as numerous new sets of conditions, to effect the desired Diels-Alder reaction. Different additives were screened for generating the leaving group (MsCl, TFAA, Tf<sub>2</sub>O, SOCl<sub>2</sub>, Ac<sub>2</sub>O) as well as a variety of bases to induce elimination. All conditions screened

unfortunately provided no Diels-Alder product and only a few of the harshest conditions caused elimination of water to form trapped enol **64**.

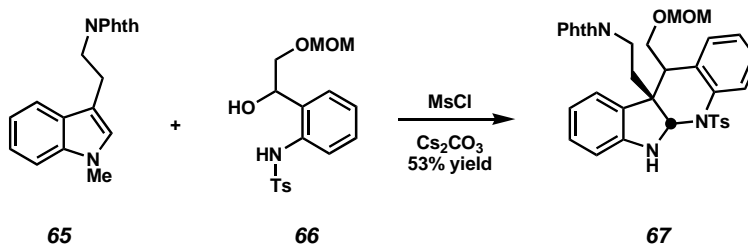
**Scheme A.14**



The bulky substituents on the diene **62** may prevent appropriate approach of the dienophile for reaction, or the elimination to form the diene may be unfavorable due to the steric congestion caused by the substituents on the diene. This was very discouraging and to date we still have been unable to carry out a Diels-Alder reaction with these elaborated disubstituted diene precursors. Attempts to carry out the Diels-Alder with one substituent on the diene rather than two were undertaken by Jeremy May. Dienes with one substituent were capable of cycloaddition with modest yields, but elaboration of these products to the core of communesin B were unsuccessful as well (Scheme A.15). These difficulties in setting the quaternary center with an intermolecular Diels-Alder

reaction caused us to revise our approach and consider intramolecular Diels-Alder reactions.

**Scheme A.15**

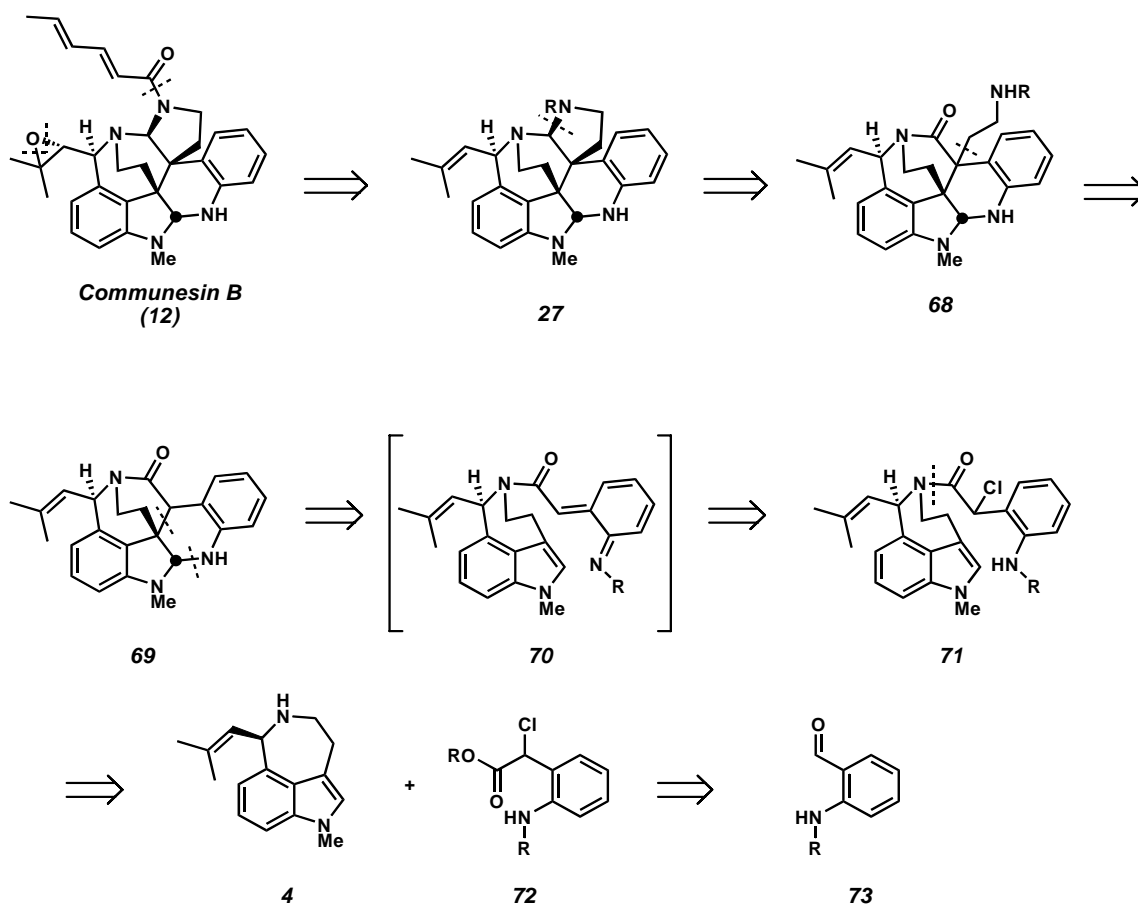


#### *Intramolecular Approach to Communesin B/Nomofungin*

Our new strategy toward communesin B began with similar disconnections as previous approaches, leading to structure **27**.

At this point, we envisioned installing the quaternary carbon center with a late stage addition of a nitroethylene type fragment to reveal **69** (Scheme A.16). This disconnection then allowed for us to look at Diels-Alder reactions with less substitution around the diene by installing this carbon-carbon bond after the cycloaddition. Taking **69** back through an intramolecular Diels-Alder cycloaddition reveals amide **71**, which could be made by adding *N*-methyl aurantioclavine (**4**) to acid **72**, which could arise from an ortho-substituted benzaldehyde derivative **73**.

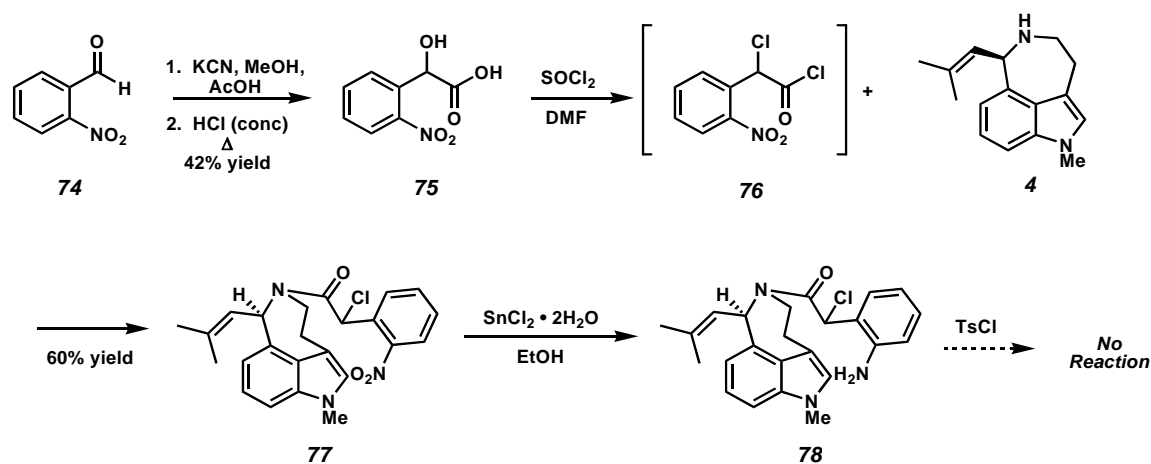
## Scheme A.16

Synthesis of Amide **71**

Our approach to the desired amide **71** began with commercially available *o*-nitrobenzaldehyde (**74**) as shown in Scheme A.17. Cyanohydrin formation was carried out by treating the aldehyde with potassium cyanide, followed by hydrolysis of the nitrile moiety to the nitromandelic acid **75**. It was not possible to carry the desired aniline moiety into formation of the cyanohydrin by starting with *o*-aminobenzaldehyde as the electron-donating amino group prevented cyanohydrin formation, thus necessitating

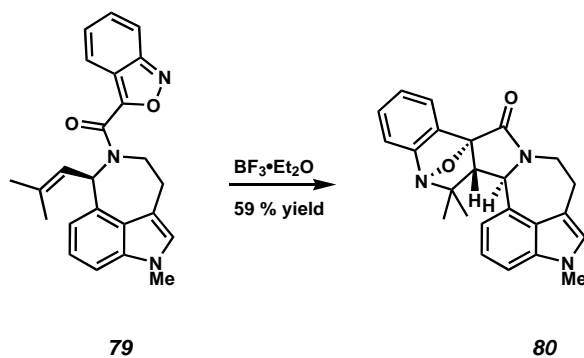
use of the nitrobenzaldehyde. Formation of the acid chloride, with simultaneous displacement of the secondary alcohol with a chloride, followed by treatment with *N*-methyl aurantioclavine (**4**) yielded the desired aurantioclavine coupled amide **77**. Reduction of the nitro compound **77** provided what appeared to be aniline **78** based on the  $^1\text{H}$  NMR shifts of the aromatic protons. However, attempted sulfonamide protection of this aniline proved difficult, indicating that the reduction of the nitro group to the aniline may not have occurred, and that **78** is potentially a half-reduction product such as the hydroxylamine. All other reduction conditions tried were either unreactive or gave the same product that was not readily protected with a sulfonamide. Efforts are ongoing to bring in the required aniline oxidation state before the coupling with *N*-methyl aurantioclavine as well as efforts toward fully reducing nitro compound **77**. Attempts to trigger a Diels-Alder reaction directly from **77** using reducing conditions as well as thermal and photolytic conditions did not afford the Diels-Alder adduct.

### Scheme A.17



*Synthesis of an Aurantioclavine Derivative*

Other studies toward intramolecular Diels-Alder reactions using *N*-methyl aurantioclavine brought about another difficulty. In work done by Jeremy May, the appended methylpropenyl side chain of aurantioclavine turned out to be more reactive as a dienophile with a benzisoxazol diene in the intramolecular Diels-Alder reaction (Scheme A.18). Treatment of amide **79** with  $\text{BF}_3 \cdot \text{Et}_2\text{O}$  at  $0^\circ\text{C}$  provided a rapid Diels-Alder reaction to afford the undesired Diels-Alder adduct **80** where the methylpropenyl olefin served as an electron rich dienophile.

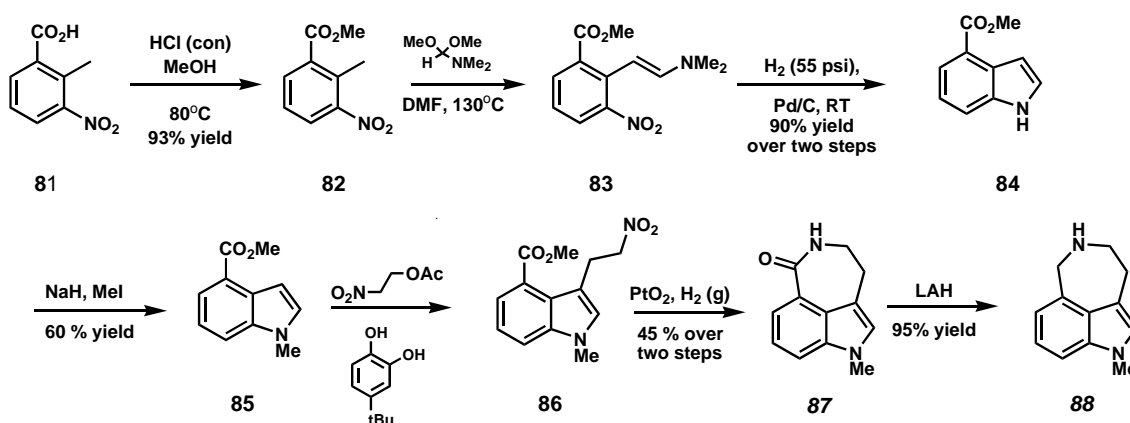
**Scheme A.18**

For this reason, we wanted to synthesize an aurantioclavine analog lacking this side chain. Synthesis of an analog of this type has been completed following precedent procedures<sup>13</sup> and is outlined in Scheme A.19. Beginning with commercially available 2-methyl-3-nitro benzoic acid (**81**), a Fischer esterification to ester **82** was carried out in good yield. A Batcho-Leimgruber indole synthesis sequence then provided indole **84** in



good yield over the two steps. Methyl protection of the indole followed by addition of 1-acetoxy-2-nitroethane yielded nitro indole **86**. Reductive cyclization over  $\text{PtO}_2$  under a hydrogen atmosphere yielded lactam **87**. LAH reduction provided the simplified aurantioclavine analog **88** in good yield. Studies toward using **88** in Diels-Alder cyclizations are underway.

### Scheme A.19

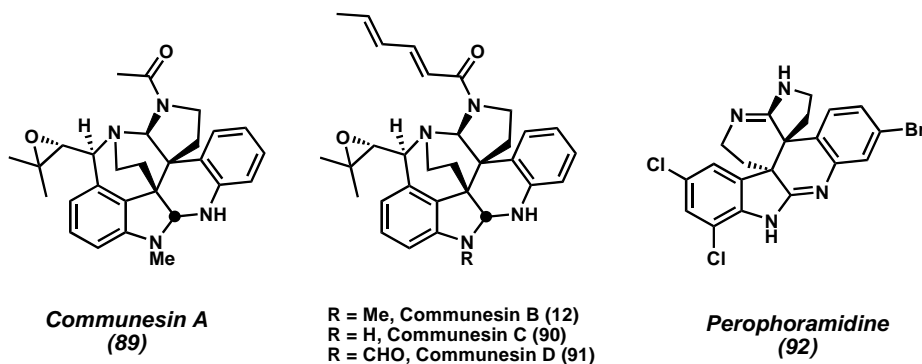


### A.4 Conclusion and Future Work

In summary, we have attempted to carry out a synthetic approach to the proposed structure of nomofungin. In the process, a structural misidentification has been recognized and we hypothesized that nomofungin was actually a previously isolated natural product, communesin B. A revised strategy was undertaken aimed at building up the core structure of communesin B/nomofungin. With hopes of gaining access to this core, we have initiated an in depth program aimed at using inverse-demand Diels-Alder reactions involving electron rich indoles as dienophiles and dienes containing

heteroatoms generated from aromatic systems by base induced elimination of an  $\alpha$ -leaving group. We have been the first to report the revised structure of nomofungin, a biosynthetically inspired approach to communesin B/nomofungin, as well as the first example of an indole being used as a dienophile in an inverse-demand Diels-Alder reaction with an ortho-quinone methide imine diene and the application of this chemistry toward constructing the core of communesin B/nomofungin. This approach works well for unsubstituted dienes, but it has proven ineffective when using highly substituted dienes necessary for building the elaborated core of communesin B/nomofungin. Efforts are ongoing to extend this reaction to more substituted dienes, as well as examining its utility in an intramolecular sense. We are also continuing work on elaborating the Diels-Alder products from simple dienes into the more functionalized core of communesin B/nomofungin. The methods developed toward communesin B/nomofungin will also be applied toward the synthesis of the remaining communesin family of natural products, communesins A, C, and D (Figure A.5), as well as other indole alkaloid natural products (e.g., perophoramidine).

**Figure A.5**



## A.5 Experimental Section

**Diels-Alder adduct 29.** To a cooled solution of 1,3 dimethyl indole (**10**, 23 mg, 0.16 mmol) and Cs<sub>2</sub>CO<sub>3</sub> (168 mg, 0.360 mmol) in 0.2 mL anhydrous CH<sub>2</sub>Cl<sub>2</sub> at -78°C was added choroaniline **28** (53 mg, 0.179 mmol) in 0.8 mL anhydrous CH<sub>2</sub>Cl<sub>2</sub> via syringe pump over 4 hours. The solution was then warmed to room temperature for 30 min, immediately filtered over a Celite plug rinsing with CH<sub>2</sub>Cl<sub>2</sub> (3 x 10 mL), concentrated in vacuo, and subjected to flash chromatography (6:1 hexane:EtOAc) to provide 54.7 mg of the Diels-Alder adduct **29** as a white solid (86%). **29**: <sup>1</sup>H NMR (300 MHz, CDCl<sub>3</sub>) δ 7.55 (dd, *J* = 7.9, 1.2 Hz, 1H), 7.48 (d, *J* = 8.5 Hz, 2H), 7.22 (d, *J* = 8.2 Hz, 2H), 7.11 (t, *J* = 7.6 Hz, 1H), 6.98 (td, *J* = 7.6, 4.4 Hz, 1H), 6.88 (dd, *J* = 7.6, 7.6 Hz, 1H), 6.76 (dd, *J* = 7.6, 7.6 Hz, 2H), 6.45 (dd, *J* = 7.3, 7.3 Hz, 1H), 6.14 (d, *J* = 7.9 Hz, 1H), 5.66 (s, 1H), 2.99 (s, 3H), 2.52 (d, *J* = 14.1 Hz, 1H), 2.42 (s, 3H), 1.62 (s, *J* = 14.1 Hz, 1H), 1.34 (s, 3H); <sup>13</sup>C NMR (75 MHz, CDCl<sub>3</sub>) δ 150.0, 143.8, 137.9, 135.3, 135.1, 132.8, 129.8, 128.4, 128.2, 128.0, 127.3, 127.2, 126.8, 121.6, 117.0, 104.5, 86.5, 51.0, 38.1, 29.9, 29.2, 21.8; IR (neat) 3052, 3028, 2951, 2920, 1608, 1494 cm<sup>-1</sup>; MS *m/z* calc'd for [C<sub>24</sub>H<sub>24</sub>N<sub>2</sub>O<sub>2</sub>S+H]<sup>+</sup>: 405.1637, found 405.1634.

**Detosylated Diels-Alder adduct 30:** To **29** (10.7 mg, 0.0265 mmol) in 2.7 mL MeOH at 20°C was added NH<sub>4</sub>Cl (50 mg, 0.954 mmol) and then Mg (50 mg, 2.067 mmol) that had been crushed and polished. After 2 hours, quenched reaction with NH<sub>4</sub>Cl (aq) and extracted with EtOAc, dried and concentrated in vacuo. Purified by flash chromatography on silica gel (hexanes:EtOAc, 9:1) to obtain **30** (88.5%). **30**: <sup>1</sup>H NMR

(300 MHz, CDCl<sub>3</sub>)  $\delta$  7.17-7.12 (comp. m, 2H), 7.06 (dd,  $J$  = 7.3, 7.9 Hz, 1H), 7.00 (d,  $J$  = 7.3 Hz, 1H), 6.79 (dd,  $J$  = 7.0, 7.6 Hz, 1H), 6.69 (dd,  $J$  = 7.3, 7.3 Hz, 1H), 6.64 (d,  $J$  = 7.9 Hz, 1H), 6.54 (d,  $J$  = 7.6 Hz, 1H), 4.65 (br. s, 1H), 4.14 (s, 1H), 2.81 (d,  $J$  = 15.2 Hz, 1H), 2.78 (s, 3H), 2.51 (d,  $J$  = 15.2 Hz, 1H), 1.24 (s, 3H); <sup>13</sup>C NMR (75 MHz, CDCl<sub>3</sub>)  $\delta$  149.2, 141.1, 137.2, 129.2, 127.9, 127.1, 121.5, 121.4, 118.8, 118.0, 113.5, 108.1, 83.9, 39.1, 37.7, 32.5, 21.7; IR (neat) 3404, 2956, 2851, 1609 cm<sup>-1</sup>; MS  $m/z$  calc'd for [C<sub>17</sub>H<sub>18</sub>N<sub>2</sub>+H]<sup>+</sup>: 250.1470, found 250.1461.

**Diels-Alder Adduct 38.** To a solution of *N*-Boc-*N*-methyl aurantioclavine **37** (19.3 mg, 0.0567 mmol) and Cs<sub>2</sub>CO<sub>3</sub> (62.1 mg, 0.187 mmol) in 0.3 mL anhydrous CH<sub>2</sub>Cl<sub>2</sub> at -78 °C was added chloroaniline **28** (24.5 mg, 0.068 mmol) in 0.3 mL anhydrous CH<sub>2</sub>Cl<sub>2</sub>. Stirred reaction at -78 °C for one hour and then allowed to room temperature. Quenched reaction with water, extracted with EtOAc (2 x 10 mL) and dried over Na<sub>2</sub>SO<sub>4</sub>. Purified by flash chromatography on silica gel (hexanes:EtOAc, 15:1 then 9:1) to obtain 30.1 mg **38** as a mixture of diastereomers (90%). These diastereomers were characterized in the following step after removal of the sulfonamide protecting group.

**Detosylated Diels Alder Adduct 39.** To **38** (30 mg, 0.050 mmol) in 5.0 mL MeOH was added NH<sub>4</sub>Cl (382 mg, 7.29 mmol) and then Mg (383 mg, 15.83 mmol) that had been crushed and polished. After 4 hours, quenched reaction with NH<sub>4</sub>Cl (aq) and extracted with EtOAc, dried and concentrated in vacuo. Purified by flash preparative chromatography on silica gel (hexanes:EtOAc, 4:1) to obtain two diastereomers **39a** and

**39b** (82%). **39a**:  $^1\text{H}$  NMR (300 MHz,  $\text{CDCl}_3$ , 50  $^\circ\text{C}$ )  $\delta$  7.10-7.05 (comp. m, 3H), 6.79 (dd,  $J = 7.1, 7.7$  Hz, 1H), 6.63 (d,  $J = 8.2$  Hz, 1H), 6.54 (br. s, 1H), 6.42 (d,  $J = 7.7$  Hz, 1H), 6.15 (br. d,  $J = 66.5$  Hz, 1H), 5.34 (br. s, 1H), 4.59 (br. s, 1H), 4.01 (br. s, 2H), 3.20-3.12 (m, 1H), 2.77 (app. s, 2H), 2.73 (s, 3H), 1.82 (s, 3H), 1.77 (s, 3H), 1.69-1.62 (comp. m, 3H), 1.53 (s, 9H);  $^{13}\text{C}$  NMR (75 MHz,  $\text{CDCl}_3$ , 50  $^\circ\text{C}$ )  $\delta$  155.1, 141.2, 139.6, 132.6, 129.8, 129.4, 128.0, 127.2, 124.4, 121.0, 118.0, 113.2, 106.7, 84.8, 80.0, 57.6, 56.4, 40.0, 33.2, 32.1, 29.0, 25.9, 18.7; IR (neat) 3371, 2975, 2245, 1672, 1600  $\text{cm}^{-1}$ ; MS  $m/z$  calc'd for  $[\text{C}_{28}\text{H}_{35}\text{N}_3\text{O}_2\text{-H}]^+$ : 444.2651, found 444.2640. **39b**:  $^1\text{H}$  NMR (300 MHz,  $\text{CDCl}_3$ , 50  $^\circ\text{C}$ )  $\delta$  7.25 (d,  $J = 4.0$  Hz, 1H), 7.09-7.01 (comp. m, 2H), 6.69 (dd,  $J = 6.0, 7.7$  Hz, 1H), 6.63 (d,  $J = 7.1$  Hz, 1H), 6.52 (br. s, 1H), 6.45 (d,  $J = 7.7$  Hz, 1H), 6.0 (d,  $J = 57.7$  Hz, 1H), 5.43 (br. s, 1H), 4.58 (br. s, 1H), 3.96 (s, 1H), 3.91-3.70 (m, 1H), 3.50-3.35 (m, 1H), 3.09-2.80 (comp. m, 2H), 2.74 (s, 3H), 1.84 (s, 3H), 1.77 (s, 3H), 1.57-1.29 (comp. m, 2H), 1.42 (s, 9H);  $^{13}\text{C}$  NMR (75 MHz,  $\text{CDCl}_3$ , 23  $^\circ\text{C}$ )  $\delta$  154.9, 150.3, 141.4, 141.2, 140.6, 138.5, 138.3, 132.6, 132.2, 129.8, 128.1, 127.8, 127.5, 124.3, 120.1, 119.9, 118.8, 117.9, 113.6, 113.5, 107.5, 83.9, 79.9, 79.5, 59.0, 57.7, 41.7, 41.5, 38.7, 38.1, 33.2, 33.1, 32.5, 32.4, 31.2, 28.7, 26.1, 18.6, 18.5; IR (neat) 3363, 2973, 2242, 1672, 1594  $\text{cm}^{-1}$ ; MS  $m/z$  calc'd for  $[\text{C}_{28}\text{H}_{35}\text{N}_2\text{O}_2]^+$ : 445.2729, found 445.2731.

## A.6 References

1. Ratnayake, A. S.; Yoshida, W. Y.; Mooberry, S. L.; Hemscheidt, T. K. "Nomofungin: A New Microfilament Disrupting Agent." *J. Org. Chem.*, **2001**, *66*, 8717-8721. This paper has been withdrawn by the author.
2. Voet, D.; Voet, J. G. *Biochemistry*, John Wiley & Sons. New York. 1995, pg. 1251-1254.
3. Jordan, M. A.; Wilson, L. "Microtubules and Actin Filaments: Dynamic Targets for Cancer Chemotherapy." *Curr. Opin. in Cell Biol.*, **1998**, *10*, 123-130.
4. Marino, J. P.; Dax, S. L. "An Efficient Desilylation Method for the Generation of o-Quinone Methides: Application to the Synthesis of (+)- and (-)-Hexahydrocannabinol." *J. Org. Chem.*, **1984**, *49*, 3671-3672.
5. Numata, A.; Takahashi, C.; Ito, Y.; Takada, T.; Kawai, K.; Usami, Y.; Matsumura, E.; Imachi, M.; Ito, T.; Hasegawa, T. "Communesins, Cytotoxic Metabolites of a Fungus Isolated from a Marine Alga." *Tetrahedron Lett.*, **1993**, *34*, 2355-2358.
6. May, J. A.; Zeidan, R. K.; Stoltz, B. M. "Biomimetic Approach to Communesin B (a.k.a. Nomofungin)." *Tetrahedron Lett.*, **2003**, *44*, 1203-1205.
7. Ratnayake, A. S.; Yoshida, W. Y.; Mooberry, S. L.; Hemscheidt, T. K. "Nomofungin: A New Microfilament Disrupting Agent. [Erratum for vol. 66, 2001]." *J. Org. Chem.*, **2003**, *68*, 1640.
8. For NMR data, see: (a) Jackson, A. H.; Smith, A. E. "Protonation of Tryptamine Derivatives in Acidic Media." *J. Chem. Soc.*, **1964**, 5510. (b) Dachriyanus; Sargent, M. V.; Wahyuni, F. S. "(+)-Isochimonanthine, a Pyrrolidinoindole Alkaloid from *Argostemina Yappii* King." *Aust. J. Chem.*, **2000**, *53*, 159-160. (c) Horne, S.; Taylor, N.; Collins, S.; Rodrigo, R. "Rapid Syntheses of some Indole Alkaloids of the Calabar Bean." *J. Chem. Soc., Perkin Trans. 1*, **1991**, 3047-3051. (d) Nyergers, M.; Rudas, M.; Bitter, I.; Toke, L. M. "1,3-Dipolar Cycloaddition Approach to Indolic aza-analogues of Cephalotaxine." *Tetrahedron*, **1997**, *53*, 3269-3280. (e) Spande, T. F.; Wilchek, M.; Witkop, B. "Reaction of Derivatives of Tryptophan, Tryptamine, and other Indoles with 20hydroxy-5-nitrobenzyl Bromide." *J. Am. Chem. Soc.*, **1968**, 3256-3258. (f) Chan, T.-L.; Schellenberg, K. A. "Studies on Presence and Role of Tryptophan in Pig Heart Mitochondrial Malate Dehydrogenase." *J. Biol. Chem.*, **1968**, *243*, 6284. (g) Decodts, G.; Wakselman, M.; Vilkas, M. "Alkylation of Indole Compounds by Hydroxymethylphenol, Aminomethylphenol, and Halomethylphenol." *Tetrahedron*, **1970**, *26*, 3313. (h) Britten, A. Z.; Bardsley, W. G.; Hill, C. M. "Furano-Indolines and Pyrano-Indolines - Model Compounds for Indole Alkaloid Studies." *Tetrahedron*, **1971**, 5631. (i) Lyle, F. R. US Patent 5 973 257, 1985; Chem. Abstr, **1985**, *65*, 2870. (j) Lindquist, N.; Fenical, W.; Van Duyne, G. D.; Clardy, J. "Isolation and Structure Determination of Diazonamides A and B, Unusual Cytotoxic Metabolites from the

Marine Ascidian *Diazona Chinensis*." *J. Am. Chem. Soc.*, **1991**, *113*, 2303-4. (k) Li, J.; Burgett, A. W. G.; Esser, L.; Ameczcua, C.; Harran, P. G. "Total Synthesis of Nominal Diazonamides - Part 2: On the True Structure and Origin of Natural Isolates." *Angew. Chem., Int. Ed.*, **2001**, *40*, 4770-4773. (l) Li, J.; Jeong, S.; Esser, L.; Harran, P. G. "Total Synthesis of Diazonamides - Part 1: Convergent Preparation of the Structure Proposed for (-)-Diazonamide A." *Angew. Chem., Int. Ed.*, **2001**, *40*, 4765-4769.

9. (a) Soloveva, T. F.; Kuvichkina, T. N.; Baskunov, B. P.; Kozlovskii, A. G. "Alkaloids from the Fungus *Penicillium Aurantio-Virens* Biourge and Some Aspects of Their Formation." *Microbiol.*, **1995**, *64*, 550-554. (b) Kozlovskii, A. G.; Soloveva, T. F.; Sakharovskii, V. G.; Adanin, V. M. "Biosynthesis of Unusual Ergot Alkaloids by Fungus *Penicillium Aurantio-Virens*." *Dokl. Akad. Nauk. SSSR*, **1981**, *260*, 230.

10. Steinhagen, H.; Corey, E. J. "A Convenient and Versatile Route to Hydroquinolines by Inter- and Intramolecular Aza-Diels-Alder Pathways." *Angew. Chem. Int. Ed.*, **1999**, *38*, 1928-1931.

11. (a) Yamada, F.; Makita, Y.; Suzuki, T.; Somei, M. "The Chemistry of Indoles. 26. A Total and Practical Synthesis of Ergot Alkaloid, (+/-) Aurantioclavine." *Chem. Pharm. Bull.*, **1985**, *33*, 2162-2163. (b) Somei, M.; Yamada, F. Jpn. Patent JP 85-47044 19850308, 1986; (c) Iwao, M.; Motoi, O. "Methodology for the Efficient Synthesis of 3,4-Differentially Substituted Indoles - Fluoride Ion-Induced Elimination-Addition Reaction of 1-Triisopropylsilyl Gramine Methiodides." *Tetrahedron Lett.*, **1995**, *36*, 5929-5932.

12. Takeuchi, Y.; Tarui, T.; Shibata, N. "A Novel and Efficient Synthesis of 3-Fluorooxindoles from Indoles Mediated by Selectfluor." *Org. Lett.*, **2000**, *2*, 639-642.

13. Crawley, S. L.; Funk, R. L. "A Synthetic Approach to Nomofungin/Communesin B." *Org. Lett.*, **2003**, *5*, 3169-3171.